DOCTOR THESIS

STUDY OF LOW-TEMPERATURE PLASMA STERILIZATION FOR MEDICAL APPLICATION

Lei XU

Graduate School of

Electronic Science and Technology

Shizuoka University

February, 2007

静 岡 大 学 博 士 論 文

STUDY OF LOW-TEMPERATURE PLASMA STERILIZATION FOR MEDICAL APPLICATION

医療用低温プラズマ滅菌に関する研究

徐　蕾

静 岡 大 学

大 学 院 電 子 科 学 研 究 科

ナノビジョン工学専攻

２００７年２月

Contents

Abstract

Recent demands for low-temperature sterilization in the medical and food industrial fields have prompted the development of various novel sterilization techniques, such as plasma sterilization and electron beam sterilization among others. Until now, dry heat or hot steam techniques such as the autoclave, ethylene oxide (EtO) gas sterilization and gamma-ray sterilization have mainly been used in sterilizing medical instruments. Dry heat or hot steam sterilization can be applied only to objects that can withstand high temperatures. In contrast, EtO gas sterilization can be used on heat-sensitive materials, but the EtO gas itself is toxic, carcinogenic and inflammable and poses a threat to the environment in the form of chlorofluorocarbons. Gamma-ray sterilization techniques can be used on medical instruments after covering them with plastic sheets or carton cases. However, this technique is expensive and there is a concern that the materials may be modified physically by the gamma-ray irradiation.

A recent development has been the application of plasma discharge to sterilization. Plasma sterilization methods have several advantages over conventional methods, including a low sterilization temperature (typically less than 70°C) and a short sterilization period of several minutes to one hour. By using higher microwave power, we can achieve the same sterilization in a shorter treatment time. However, the risk of heat damage caused by the surface contact between the plasma and the medical instrument becomes serious, especially for plastic materials. For this study, to achieve sterilization at a low temperature of less than 70°C, a pulse-modulated microwave system was used. The sterilization characteristics of *Geobacillus stearothermophilus* spores as biological indicator (BI) were studied. Mechanisms of plasma sterilization were studied in O_2, N_2 and N_2-O_2 plasmas. To expand the application of microwave plasma sterilization technique, a large-volume medical sterilizer using microwave plasma, which could achieve large sterilization volume and internal sterilization effect, was developed.

For plasma sterilization, the BIs used were *G. stearothermophilus* (ATCC No. 12980) spores with population of 10^6, which were spread on a small stainless steel disc and placed in Petri dishes set on a movable substrate stage about 15-23 cm below the quartz vacuum window in 40-cm-diameter surface-wave plasma (SWP) device. During plasma irradiation, the stage temperature was measured using thermo-label sheets attached to the Petri dish. After plasma irradiation, the spores were incubated in culture solution for seven days at an incubation temperature of 55-60 °C. Subsequently, it could be determined whether the spores had been killed or not because

the color of the culture solution changed from purple to yellow if the spores were still viable.

Sterilization of BI samples with 10^6 *G. stearothermophilus* spores was confirmed using continuous wave (CW) SWP in O_2, N_2 and N_2-O_2 mixture gas within 4 min. It was found that all the BI samples were sterilized by the pulse-modulated oxygen plasma when the total microwave on time was longer than 120 s, even when the on-duration per pulse was 10 μs. Based on the thermo-label measurements, it can be shown that the surface temperature of the Petri dish during total processing period, was always less than 70 °C. When the total microwave on time was much shorter than 120 s, we found that a longer on-duration per pulse was required for successful sterilization.

To study the mechanism of plasma sterilization, diagnoses of plasma using optical emission and mass spectrometry, and SEM analyses of shapes of spores after plasma treatments were applied. There exist UV emissions in N_2-O_2 mixture gas discharge plasma. Several strong lines at 282.0, 297.7, 313.6, 315.9, 337.1, 357.7 nm were originated from the second positive systems ($C^3\Pi_u \rightarrow B^3\Pi_g$) of N_2 molecules. Several UV emissions at 214.1, 226.9, 237.0, 247.9, 258.8 nm were considered originated from NO γ system ($A^2\Sigma^+ \rightarrow X^2\Pi$). They might play some role in sterilizing the spores in addition to N_2 positive system in the wavelength region of 300~400 nm and the etching process due to oxygen radicals.

In the new large-volume microwave plasma sterilizer, a discharge transition between SWP and volume-wave plasma (VWP) could be controlled. So far, we have demonstrated sterilization of the spores packaged in glassine pouch using SWP/VWP filled the new sterilizer with air-simulated N_2-O_2 gas mixture. We have confirmed that the wrapped 10^8 *Bacillus atrophaeus* spores and 10^7 *G. stearothermophilus* spores were sterilized by CW or time-modulated microwave excited O_2, N_2 and N_2-O_2 plasmas for net on time of roughly 20 min. When water vapor was added on different gas species plasma, it has been found a great improvement on sterilization effect, especially on internal sterilization of polyethylene (PE) film wrapped materials.

The possible sterilization mechanisms were studied and summarized as presented below. When microwave energy was induced to a chamber filled with oxygen, nitrogen and water vapor, microwave plasma was excited, then UV radiation, oxygen radicals and some strong oxidizer would be produced. Consequently, spores will be inactivated by UV radiation, be etched by oxygen radicals, be oxidized by some strong oxidizer. If spores were wrapped by PE film, oxygen radicals would loose energy while contacting PE film, therefore, oxygen radicals would be shut down by PE film.

1 Introduction

1.1 Plasma (physics)

1.1.1 Common plasmas

In physics and chemistry, a plasma is typically an ionized gas, and is usually considered to be a distinct phase of matter in contrast to solids, liquids and gases because of its unique properties. "Ionized" means that at least one electron has been dissociated from a proportion of the atoms or molecules. The free electric charges make the plasma electrically conductive so that it responds strongly to electromagnetic fields.

This fourth state of matter was first identified in a discharge tube (or Crookes tube), and so described by Sir W. Crookes in 1879 (he called it "radiant matter"). The nature of the Crookes tube "cathode ray" matter was subsequently identified by British physicist Sir J. J. Thomson in 1897, and dubbed "plasma" by I. Langmuir in 1928 [1].

Plasmas are the most common phase of matter. It has often been said that 99% of the matter in the universe is in the plasma state. This estimate may not be very accurate, but it is certainly a reasonable one in view of the fact that stellar interiors and atmospheres, gaseous nebulae, and much of the interstellar hydrogen are plasmas. In our own neighborhood, as soon as one leaves the earth's atmosphere, one encounters the plasma comprising the Van Allen radiation belts and the solar wind. On the other hand, in our everyday lives encounters with plasmas are limited to a few examples: the flash of a lightning bolt, the soft glow of the Aurora Borealis, the conducting gas inside a fluorescent tube or neon sign, and the slight amount of ionization in a rocket exhaust. It would seem that we live in the 1% of the universe in which plasmas do not occur naturally. [2]

1.1.2 Definition of plasma

Although a plasma is loosely described as an electrically neutral medium of positive and negative particles, a more rigorous definition requires three criteria to be satisfied:

1. **The plasma approximation**: Charged particles must be close enough together that each particles influences many nearby charged particles, rather than just the interacting with the closest particle (these collective effects are a distinguishing feature of a plasma). The plasma approximation is valid when the number of

electrons within the sphere of influence (called the *Debye sphere* whose radius is the *Debye length*, $\lambda_D \equiv \sqrt{\varepsilon_0 k T_e/(e^2 n_0)}$) of a particular particle is large.

2. **Bulk interactions**: The *Debye length* is short compared to the physical size of the plasma. This criterion means that interactions in the bulk of the plasma are more important than those at its edges, where boundary effects may take place.
3. **Plasma frequency**: The electron plasma frequency (measuring plasma oscillations of the electrons) is large compared to the electron-neutral collision frequency (measuring frequency of collisions between electrons and neutral particles). When this condition is valid, plasmas act to shield charges very rapidly (quasi-neutrality is another defining property of plasmas). [3]

Therefore, a useful definition is concluded as follows [2]: *A plasma is a quasi-neutral gas of charged and neutral particles which exhibits collective behavior*.

1.1.3 Areas of plasma technology

There are many areas of plasma technology, such as: plasma etching processing, thin film deposition; plasma-based lighting systems; plasma chemistry; plasma spray and bulk materials work; sources and display systems; environmental and medical applications; materials synthesis; and power systems, thrusters, etc. In this thesis, I concentrated on low-temperature plasma sterilization for medical application.

1.2 Definition of sterilization and disinfection

Sterilization is the elimination of all transmissible agents (such as bacteria, prions and viruses) from a surface, a piece of equipment, food or biological culture medium. It is different from disinfection, where only organisms that can cause disease are removed by a disinfectant. In general, any instrument that enters an already sterile part of the body should be sterilized. This includes equipment like scalpels, hypodermic needles and artificial pacemakers, etc. It is also essential in the manufacture of many sterile pharmaceuticals, medical instruments and food processing.

Disinfection is the destruction of pathogenic and other kinds of microorganisms by physical or chemical means. Disinfectants are chemical substances used to destroy viruses and microbes (germs), such as bacteria and fungi, as opposed to an antiseptic which can prevent the growth and reproduction of various microorganisms, but does not destroy them. The ideal disinfectant would offer complete sterilization, without

harming other forms of life, be inexpensive, and non-corrosive. Unfortunately ideal disinfectants do not exist. Many disinfectants are only able to partially sterilize. The most resistant pathogens are bacteria spores but some viruses and bacteria are also highly resistant to many disinfectants.

1.3 Conventional methods of sterilization

The agents that cause sterilization range from heat to lethal chemicals to physical processes [4]. The preferred principle for sterilization is through heat. There are also chemical methods of sterilization. [5]

1.3.1 Heat sterilization

This can be achieved by moist or dry heat. Moist heat generally used for sterilization is saturated steam. Pressurized steam has the advantage of sterilizing penetrable materials and exposed surfaces quickly. Dry heat requires high temperature and longer times, but will penetrate a wide range of materials.

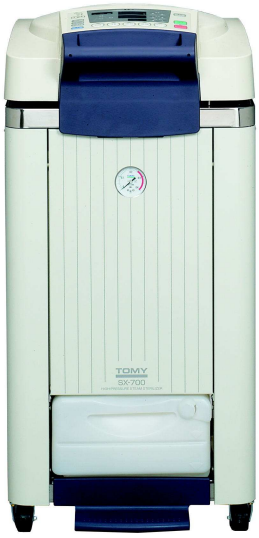

Fig. 1.1 Photograph of an autoclave, TOMY SX-700.

Sterilization by steam is only applicable if damage by heat and moisture is not a problem. A widely-used method for moist heat sterilization is the **autoclave**. A medical autoclave is a device that uses steam to sterilize equipment and other objects. This means that all bacteria, viruses, fungi, and spores are inactivated. However, in 2003 scientists discovered a single-celled organism, Strain 121, which can survive at a scorching 130 °C higher than the traditional autoclave temperatures. Prions (A prion – short for proteinaceous infectious particle – is a type of infectious agent made only of protein.) also may not be destroyed by autoclaving. Autoclaves work by allowing steam to enter, then maintaining pressure at 103 kPa (15 psi). This causes the steam to reach 121 °C, and this is maintained for at least 15 minutes. The steam and pressure transfer sufficient heat into organisms to kill them. Autoclaves are found in many medical settings and other places that need to ensure sterility of an object. In our laboratory, we have a top loading autoclave (TOMY SX-700, **Fig. 1.1**) to sterilize failed samples of sterilization

experiments before discard. Autoclaves that first happened with hypodermic needles were once more common, but many procedures today use single-use items rather than sterilized, reusable items. For instance, many surgical instruments (forceps, needle holders, scalpel handles, etc.) are commonly single-use items rather than reusable. Because damp heat is used, heat-labile products (such as some plastics) cannot be sterilized this way or they will melt. Some paper or other products that may be damaged by the steam must also be sterilized another way. In stovetop autoclaves, items should always be separated to allow the steam to penetrate the load evenly.

Examples of sterilization by **dry heat** are infrared radiation and incineration. The penetration of the heat caused by the infrared radiation at the surface of the material is by means of conduction. On the other hand, incineration is a very effective sterilization method, but destructive to the medium. If hot air is used, it is estimated that at a temperature of 170 °C, it takes approximately 60 min to get complete sterilization [4]. Dry heat has the advantage that it can be used on powders and other heat-stable items that are adversely affected by steam (for instance, it does not cause rusting of steel objects), however, the disadvantage is that it can only be applied to instruments that can withstand the high temperatures.

Other heat methods include flaming, boiling and tindalization.

Flaming is done to loops and straight-wires in microbiology laboratories. Leaving the loop in a Bunsen burner flame until it glows red ensures that any infectious agent gets inactivated. This is commonly used for small metal or glass objects, but not for large objects.

Boiling in water for 15 minutes will kill most bacteria and viruses, but boiling is ineffective against prions and many bacterial spores; therefore boiling is unsuitable for sterilization. However, since boiling does kill most bacteria and viruses, it is useful if no better method is available. Boiling is a simple and familiar enough process, and is an option available to most anyone most anywhere, requiring only water, enough heat, and a container that can withstand the heat; however, boiling can be hazardous and cumbersome.

Tindalization is a cumbersome process designed to reduce the level of activity of sporolating bacteria that are left by a simple boiling-in-water method. The process involves boiling for 20 minutes, cooling, incubating for a day, boiling for 20 minutes, cooling, incubating for a day, boiling for 20 minutes, cooling, incubating for a day, and finally boiling for 20 minutes again. The three incubation periods are to allow spores formed by bacteria in the previous boiling period to produce the heat-sensitive bacterial stage, which are killed by the next boiling step. Tindalization is also ineffective

against prions.

1.3.2 Chemical sterilization

Chemicals are also used for sterilization. Although heating provides the most effective way to rid an object of all transmissible agents, it is not always appropriate, because it destroys objects such as most fiber optics, most electrics, and some plastics.

Ethylene oxide gas (EOG) kills bacteria (and their endospores), mold, and fungi, and can therefore be commonly used to sterilize substances, which would be damaged by sterilizing techniques such as pasteurization that rely on heat (temperature > 60 °C), such as plastics, optics and electrics. Ethylene oxide treatment (**Fig. 1.2**) is generally carried out between 30 °C and 60 °C with relative humidity above 30% and a gas concentration between 200 mg/l and 800 mg/l for at least 3 hours. Ethylene oxide penetrates very well, moving through paper, cloth, and some plastic films and is highly effective. However, it is highly flammable, and requires a long time to sterilize than any heat treatment. The process also requires one or more weeks for aeration post sterilization to remove toxic residues and poses environmental risks. Ethylene oxide is widely used and sterilizes around 50% of all disposable medical supplies such as bandages, sutures and surgical implements. The way by which ethylene oxide reacts with bacteria is a process referred to as alkylation [4]. Alkylation is the replacement of a hydrogen atom by an alkyl group. In a bacterial cell this substitution is lethal.

Fig. 1.2 Photograph of a commercial EOG sterilizer (3M) used in the hospital (by courtesy of Hamamatsu University School of Medicine).

Ozone is used in industrial setting to sterilize water and air, as well as a disinfectant for surfaces. It has the benefit of being able to oxidize most organic matter. On the other hand, it is a toxic and unstable gas that must be produced on-site, so it is not practical to use in many settings. The effectiveness of ozone as a bactericidal is due to its interference with cellular respiration.

Bleach is another accepted liquid sterilizing agent. Household bleach, also used in hospitals and biological research laboratories, consists of 5.25% sodium hypochlorite. At this concentration it is most stable for storage, but not most active. According to the Beth Israel Deaconess Medical Center Biosafety Manual (2004 edition), in most cases, it should be diluted to 1/10 of its storage concentration immediately before use; however, it should be diluted only to 1/5 of the storage concentration to kill *Mycobacterium tuberculosis*. This dilution factor must take into account the volume of any liquid waste that it is being used to sterilize. Bleach will kill many organisms immediately, but should be allowed to incubate for 20 minutes for full sterilization. Bleach will kill many spores, but is ineffective against certain extremely resistant spores. It is highly corrosive, even causing rust of stainless steel surgical implements.

Glutaraldehyde and **formaldehyde** solutions (also used as fixatives) are additional accepted liquid sterilizing agents, provided that the immersion time is long enough – it can take up to 12 hours for glutaraldehyde to kill all spores, and even longer for formaldehyde. (This assumes that a liquid not containing large solid particles is being sterilized. Sterilization of large blocks of tissue can take much longer, due to the time required for the fixative to penetrate.) Glutaraldehyde and formaldehyde are volatile, and toxic by both skin contact and inhalation. Glutaraldehyde has quite a short shelf life (<2 weeks), and is expensive. Formaldehyde is less expensive and has a much longer shelf life if some methanol is added to inhibit polymerization to paraformaldehyde, but is much more volatile. Formaldehyde is also used as a gaseous sterilizing agent; in this case, it is prepared on-site by depolymerization of solid paraformaldehyde.

Fig. 1.3 Photograph of Sterrad® 100S (cited from website of STERRAD®, Johnson & Johnson).

Ortho-phthalaldehyde (OPA) is a sterilizing chemical which received Food and Drug Administration (FDA) clearance in late 1999. Typically used in a 0.55% solution, OPA shows better myco-bactericidal activity than glutaraldehyde. It also is effective against glutaraldehyde-resistant spores. OPA has superior stability, is less volatile, and does not irritate skin or eyes, and it acts more quickly than glutaraldehyde. On the other hand, it is more expensive, and will stain proteins (including skin) gray in color.

Another chemical sterilizing agent is **hydrogen peroxide**. It is relatively non-toxic once diluted to low concentrations (although a dangerous oxidizer at high concentrations), and leaves no residue. The Sterrad® 100S (**Fig. 1.3**) and other Sterrad® sterilization chambers combine hydrogen

peroxide gas with an RF discharge plasma [4] to sterilize heat-sensitive equipment such as rigid endoscopes. The Sterrad® 100S sterilizes in 55 minutes and also penetrates some lumen devices. The most recent Sterrad® model, Sterrad® NX, can sterilize most hospital loads in as little as 20 minutes and has greatly expanded lumen claims compared to earlier models. However, the Sterrad® has limitations with processing certain materials such as paper and long thin lumens, and currently this equipment is assumed to effectively sterilize due to the high concentration of hydrogen peroxide rather than to the plasma component.

Endoclens is another new liquid chemical sterilization system providing chemical sterilization of flexible endoscopes. It mixes two chemicals (hydrogen peroxide and formic acid) together to make its antiseptic as needed. The machine has two independent asynchronous bays, and cleans (in warm detergent with pulsed air), sterilizes and dries the endoscopes automatically. All air and water inlets are filtered, and the machine handles temperature, timing and chemical concentration. The total time for the whole process is 30 minutes, and a hard-copy report of the cycle is printed (as well as being stored electronically). Studies with synthetic soil containing bacterial spores showed this machine achieved sterilization effectively.

The **Dry Sterilization Process, DSP**, is a process originally designed for the sterilization of plastic bottles in the beverage industry. It uses hydrogen peroxide with a concentration of 30-35% and runs under vacuum conditions. Using the common reference germs for hydrogen peroxide sterilization processes, endospores of different strains of *Bacillus atrophaeus* and *Geobacillus stearothermophilus*, the Dry Sterilization Process achieves a germ reduction capability of the sterilization process is 10^6-10^8. The complete cycle time of the process is 6 seconds. The surface temperature of the sterilized items is only slightly increased during the process by 10 °C-15 °C. Particularly due to the high germ reduction and the slight temperature increase the Dry Sterilization Process is also useful for medical and pharmaceutical applications. However, the disadvantage is the concentration of hydrogen peroxide is a little higher.

1.3.3 Radiation sterilization

Methods exist to sterilize using radiation such as X-rays, gamma rays, or subatomic particles. **Gamma rays** are very penetrating, but as a result require bulky shielding for the safety of the operators of the gamma irradiation facility; they also require storage of a radioisotope, which continuously emits gamma rays (it cannot be turned off, and therefore always presents a hazard in the area of the facility). **X-rays** are less

penetrating and tend to require longer exposure times, but require less shielding, and are generated by an X-ray machine that can be turned off for servicing. Subatomic particles may be more or less penetrating, and may be generated by a radioisotope or a device, depending upon the type of particle. Even though, α-particle and protons could be used, electrons are the usual choice in this method. Since β-particles from radioactive sources cannot penetrate too far, accelerated electrons are used. **Electron beam irradiation** is presently an active research area for the treatment of infectious medical waste. Irradiation with X-rays or gamma rays does not make materials radioactive. Irradiation with particles may make materials radioactive, depending upon the type of particles and their energy, and the type of target material: neutrons and very high-energy particles can make materials radioactive, but have good penetration, whereas lower energy particles (other than neutrons) cannot make materials radioactive, but have poorer penetration.

Fig. 1.4 Photograph of a commercial UV germicidal lamp (cited from the Wikimedia Commons).

Ultraviolet radiation (UV, from a germicidal lamp as shown in **Fig. 1.4**) can also be used for irradiation, but only on surfaces and some transparent objects (note that many objects that are transparent to visible light actually absorb UV). It provides some degree of protection from infection with pathogenic microorganisms. Ultraviolet radiation is most effective against bacteria in the 230 nm-240 nm range. It is not ionizing. Its lethality comes from exciting large molecules the size of proteins. It appears that UV induces changes in the cellular nucleic acids structure. It is also suggested that UV irradiation of the cellular DNA results in the formation of photoproducts, which may have a detrimental effect on the DNA structure. It is routinely used to sterilize the interiors of biological safety cabinets between uses, but is ineffective in shaded areas, including areas under dirt (which may become polymerized after prolonged irradiation, so that it is very difficult to remove). It also damages many plastics, as can be seen if one forgets a polystyrene foam object in the cabinet with the germicidal lamp turned on overnight. In practice, the UV radiation is

produced by low-pressure mercury vapor lamp made of quartz tubes. They emit 95% of their total radiation at 253.7 nm.

1.4 Conventional methods of disinfection

Disinfectants are antimicrobial agents that are applied to non-living objects to destroy microorganisms, the process of which is known as **disinfection**. Disinfectants should generally be distinguished from *antibiotics* that destroy microorganisms within the body, and from *antiseptics*, which destroy microorganisms on living tissue. *Sanitisers* are high level disinfectants that kill over 99.9% of a target microorganism in applicable situations. Not all disinfectants and sanitisers can sterilize (the complete elimination of all microorganisms), and those that can depend entirely on their mode of application. Bacterial endospores are most resistant to disinfectants, however some viruses and bacteria also posess some tolerance.

From the next section, types of disinfectants will be introduced. [6]

1.4.1 Alcohols

Alcohols, usually ethanol or isopropanol, are wiped over benches and skin and allowed to evaporate for quick disinfection. They have wide microbiocidal activity, are non corrosive, but can be a fire hazard. They also have limited residual activity due to evaporation, and have a limited activity in the presence of organic material. Alcohols are more effective combined with water — 70% alcohol is more effective than 95% alcohol. Alcohol is not effective against fungal or bacterial spores.

1.4.2 Aldehydes

Aldehydes, such as glutaraldehyde, have a wide microbiocidal activity and are sporocidal and fungicidal. They are partly inactivated by organic matter and have slight residual activity.

1.4.3 Halogens

Chloramine is used in drinking water treatment instead of chlorine because it produces less disinfection byproducts.

Chlorine is used to disinfect swimming pools, and is added in small quantities to

drinking water to reduce waterborne diseases.

Hypochlorites (Sodium hypochlorite), often in the form of common household bleach, are used in the home to disinfect drains, and toilets. Other hypochlorites such as calcium hypochlorite are also used, especially as a swimming pool additive. Hypochlorite gives off free chlorine and it is the chlorine that is the true disinfectant. Hypobromite solutions are also sometimes used.

Iodine is usually dissolved in an organic solvent or as Lugol's iodine solution. It is used in the poultry industry. It is added to the birds' drinking water. Although no longer recommended because it increases scar tissue formation and increases healing time, tincture of iodine has also been used as an antiseptic for skin cuts and scrapes.

1.4.4 Oxidizing agents

Oxidizing agents act by oxidizing the cell membrane of microorganisms, which results in a loss of structure and leads to cell lysis and death.

Chlorine dioxide is used as an advanced disinfectant for drinking water to reduce waterborne diseases. In certain parts of the world, it has largely replaced chlorine because it forms fewer byproducts. Sodium chlorite, sodium chlorate, and potassium chlorate are used as precursors for generating chlorine dioxide.

Hydrogen peroxide is used in hospitals to disinfect surfaces. It is sometimes mixed with colloidal silver. It is often preferred because it causes far fewer allergic reactions than alternative disinfectants. Also used in the food packaging industry to disinfect foil containers. A 3% solution is also used as an antiseptic. When hydrogen peroxide comes into contact with the catalase enzyme in cells it is broken down into water and a hydroxyl free radical. It is the damage caused by the oxygen free radical that kills bacteria. However, as recent studies have show hydrogen peroxide to be toxic to growing cells as well as bacteria, its use as an antiseptic is no longer recommended.

Ozone is a gas that can be added to water for sanitation.

Peracetic acid is a disinfectant produced by reacting hydrogen peroxide with acetic acid. It is broadly effective against microorganisms and is not deactivated by catalase and peroxidase, the enzymes which break down hydrogen peroxide. It also breaks down to food safe and environmentally friendly residues (acetic acid and hydrogen peroxide), and therefore can be used in non-rinse applications. It can be used over a wide temperature range (0-40°C), wide pH range (3.0-7.5), in clean-in-place (CIP) processes, in hard water conditions, and is not affected by protein residues.

Potassium permanganate ($KMnO_4$) is a red crystalline powder that colours everything it touches, and is used to disinfect aquariums. It is also used widely in community swimming pools to disinfect ones feet before entering the pool. Typically, a large shallow basin of $KMnO_4$/water solution is kept near the pool ladder. Participants are required to step in the basin and then go into the pool. Additionally, it is widely used to disinfect community water ponds and wells in tropical countries, as well as to disinfect the mouth before pulling out teeth. It can be applied to wounds in dilute solution; potassium permanganate is a very useful disinfectant.

1.4.5 Phenolics

Phenolics are the active ingredient in most bottles of "household disinfectant". They are also found in some mouthwashes and in disinfectant soap and handwashes. Phenol is probably the oldest known disinfectant as it was first used by Lister, when it was called carbolic acid. It is rather corrosive to the skin and sometimes toxic to sensitive people, so the somewhat less corrosive phenolic *o*-phenylphenol is often used in favour. Hexachlorophene is a phenolic which was once used as a germicidal additive to some household products but was banned due to suspected harmful effects.

1.4.6 Quaternary ammonium compounds

Quaternary ammonium compounds (Quats), such as benzalkonium chloride, are a large group of related compounds. Some have been used as a low level disinfectant. They are effective against bacteria, but not against some species of Pseudomonas bacteria or bacterial spores. Quats are biocides which also kill algae and are used as an additive in large-scale industrial water systems to minimize undesired biological growth. Quaternary ammonium compounds can be effective disinfectants against enveloped viruses.

1.4.7 Other

Dettol is used to disinfect surfaces at home. It kills the majority of bacteria. It is one of the few disinfectants useful against viruses.

Virkon is a wide-spectrum disinfectant used in labs. It kills bacteria, viruses, and fungi. It is used as a 1% solution in water, and keeps for one week once it is made up. It is expensive, but very effective, its pink colour fades as it is used up so it is possible

to see at a glance if it is still fresh.

High-intensity ultraviolet light can be used for disinfecting smooth surfaces such as dental tools, but not porous materials that are opaque to the light such as wood or foam. Ultraviolet light fixtures are often present in microbiology labs, and are activated only when there are no occupants in a room (e.g., at night).

1.5 Low-temperature plasma sterilization

Conventional methods of sterilizing medical instruments have been mainly performed using a dry-heat or hot-steam autoclave for heat-resistant materials, and ethylene-oxide gas for heat-sensitive materials. However, as described in the previous two sections, we found several drawbacks of the conventional methods of sterilization or disinfection. Recently, a low-temperature plasma sterilization technique has been developed using low-pressure or atmospheric pressure plasma discharges. The plasma sterilization method has a number of advantages compared with the conventional methods. One of the advantages is to be able to perform sterilization at a relatively low temperature less than 70 °C, and in a relatively short period, for instance, from several min to several tens of min. This technique is particularly useful in surface sterilization of medical instruments and medical and food packaging materials.

M. Laroussi presented a brief review of notable recent efforts on the inactivation of bacteria by low-pressure plasmas [7]. Low-pressure plasmas have been considered for biological sterilization for some time. Some of the systems developed in the 1970s and 1980s were not really ‘‘plasma-based’’ sterilization systems. This is due to the use of gas mixtures that contain components with germicidal properties (such as H_2O_2 and aldehydes) before the plasma is ignited. [8, 9] These are more correctly termed as ‘‘plasma-assisted’’ sterilization systems. Plasma-based sterilization uses gases that posses no germicidal property on their own. They become biocidal only when a plasma is ignited. Example of such gases or mixtures of gases are air, helium/air or helium/ O_2, and N_2/ O_2. In this section, only plasma-based systems will be reviewed. Most recently, many studies on the effects of low-pressure plasma on biological matter in plasma-based systems were conducted for various gas mixtures. Examples are low-pressure oxygen plasmas and O_2/N_2 plasmas. [10–12] These studies were motivated by specific objectives such as the decontamination of interplanetary space probes and the sterilization of medical tools. RF and microwave driven low-pressure plasmas were mostly used in these studies.

Recently Bol’shakov et al. published a detailed study of the effects of radio

frequency (RF) oxygen plasma at reduced pressure on bacteria. [10] The study was carried out for two modes of operation, the inductively coupled mode and the capacitively coupled mode. The inductive mode was found to offer a better efficiency in destroying biological matter. This was due to higher electron and ion densities in this mode, which resulted in an enhancement of electron-impact processes. [10] High densities of atomic oxygen and perhaps O_2* in synergy with UV photons induced chemical degradation of the biological materials followed by volatilization of the decomposition products (CO_2, CO, N_2, etc.). Plasmid DNA degradation was evaluated for both the inductive mode and the capacitive mode. It was found that at the same power the inductively coupled plasma destroyed over 70% of supercoiled DNA in 5 s while only 50% was destroyed by the capacitively coupled plasma.[10] Characterization of the decomposition of the byproducts was carried out during plasma exposure by emission spectroscopy. CO, N_2, N_2^+, OH, Na, K, etc. were amongst the detected species. CN, CH, and NO were not detected indicating that their concentrations were below 1 ppm.[10]

Moreau et al. [11] and Moisan et al. [12] carried out detailed studies on the effects of low pressure N_2/O_2 plasma on various bacteria. The biological samples were placed in the flowing after-glow of a plasma generated by a surfatron source. [13] The surfatron source was driven by microwave power with a frequency of 915 or 2450 MHz. In their studies Moisan et al. [12] characterized the inactivation kinetics and correlated that with the physics and chemistry of the afterglow. Since this study was focused on the inactivation kinetics, brief introduction to some basic definitions are listed as below:

One kinetics measurement parameter, which has been used extensively by researchers studying sterilization by plasma, is what is referred to as the ‘‘D’’ value (Decimal value). The D-value is the time required to reduce an original concentration of microorganisms by 90%. The D-value is therefore expressed in the unit of time. Since survivor curves are plotted on semi-logarithmic scales, the D-value is determined as the time for a one $\log_{10}$ reduction.

In their early studies on the inactivation of *Bacillus subtilis* spores by low-pressure plasmas, Moisan et al. [12] reported that survivor curves (colony forming units, CFUs, versus treatment time) exhibited three inactivation phases. **Figure 1.5** shows a typical example of such survivor curves. [14] Moisan et al. [15] claimed that the first phase, which exhibited the shortest D-value, was mainly due to the action of UV radiation on isolated spores or on the first layer of stacked spores. The second phase, which had the slowest kinetics, was attributed to a slow erosion process by active species (such as atomic oxygen, O). Finally the third phase was initiated after spores and debris had

been cleared during phase 2, hence allowing UV to hit the genetic material of the still living spores. The D-value of this phase was observed to be close to the D-value of the first phase. However, in a more recent study, the same research group examined the inactivation process of *B. subtilis* spores exposed to the flowing afterglows of an N_2/O_2 mixture and of pure argon, and reported that UV radiation, not the radicals, played the dominant role. The survivor curves were biphasic and consistent with UV inactivation. The second phase represented spores that were shielded by others and that needed more irradiation time to accumulate a lethal UV dose. This observation was further supported by the fact that at low UV intensity a lag time existed before inactivation. This was due to the requirement that a minimum UV dose had to be achieved before irreversible damage to the DNA strands occurred. Since in pure argon, which would not contain oxygen radicals, inactivation was achieved for similar lengths of time, it was concluded that the role of oxygen in the N_2/O_2 plasma was mainly to provide oxygen atoms to form NO, which was the main source of the UV photons.

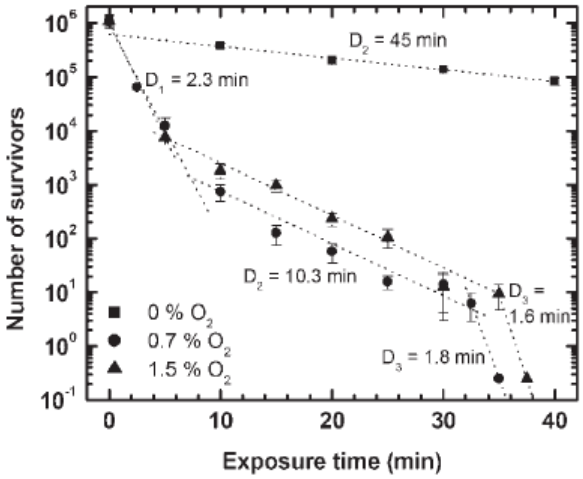

Fig. 1.5 Survival curves for *B. subtilis* spores exposed to a N_2/O_2 discharge afterglow. Gas pressure in the sterilization chamber is 5 torr. Gas flow is one standard l/min plus *x*% of added O_2 and discharge field frequency is 2450 MHz. [14, 15]

Switching the focus to high-pressure plasmas, M. Laroussi discussed the fundamental properties of non-equilibrium atmospheric pressure plasmas [7]. In addition to their practical side, design simplicity, and low operational cost, non-equilibrium atmospheric pressure plasmas exhibit unique features, which have provided the base for numerous applications. In these plasmas the electron energies are much higher than that of the heavy species, i.e. ions and neutrals. The energetic electrons collide with the background atoms and molecules causing enhanced level of dissociation, excitation and ionization. The attractive feature is the fact that these

reactions occur without a substantial increase in the operating gas temperature. Because the ions and the neutrals remain relatively cold, the plasma causes no or just minimal thermal damage to articles it may come in contact with. This characteristic opened up the possibility to use these plasmas for the treatment of heat-sensitive materials including biological tissues.

Several methods have been developed in the last two decades that allowed researchers to easily generate non-equilibrium plasmas at ‘‘high-pressures’’, up to one atmosphere. [16, 17] One requirement is common to all the methods: the inhibition of the glow-to-arc transition. Dielectric barrier discharges (DBDs) achieve this requirement by covering at least one of two electrodes (separated by a gas gap) with a dielectric sheet. [18] In this case, the discharge current is self-limited by charge build-up on the dielectric surface. DBDs are generally driven by sine-wave high voltages with frequencies in the kHz range. This frequency range has recently been extended all the way down to DC by replacing the dielectric barrier by a resistive layer, which plays the role of a distributed ballast, thus limiting the discharge current. [19] Plasma discharges with metallic bare electrodes driven by RF voltages in the MHz range were also developed. [20] In this case a gas composed mainly of a noble gas (such as He) is flown at a rate of few liters/min in the gap between the electrodes.

As for the sterilization application, Boudam et al. from Moisan’s group made a review of the literature on atmospheric pressure discharges used for microorganism inactivation. Their research results show, in particular, that UV photons can be the dominant species in the inactivation process, while a majority of researchers have come to the conclusion that, at atmospheric pressure, chemically reactive species such as free radicals, metastable atoms and molecules always control the inactivation process. [21]

1.6 Scope of the work

Our group [22-30] has started investigating low-temperature surface sterilization with a low-pressure large-area planar surface-wave plasma (SWP) source using oxygen discharge since 2002. From then on, the biological indicator (BI) samples of *G. stearothermophilus* with population of 1.5×10^6 spores were successfully sterilized by 750 W continuous microwave (CW) excited oxygen plasma irradiation for 3 min or longer, and the sterilization mechanism in the oxygen plasma was concluded that it might be due to a chemical etching reaction from the reactive oxygen radicals [22, 23].

The present work consists of three parts of low-temperature plasma sterilization experiments. The first part is to find out the discharge conditions for CW and

pulse-modulated SWPs in low-temperature sterilization, and to study the mechanisms of plasma sterilization with different gas species using a low-pressure SWP source [22-25]. Description of the SWP source will be presented in chapter 2. Low-temperature sterilization experiments with the SWP source will be presented in chapter 5.

The second part is to achieve and improve internal sterilization effect using a new large-area low-pressure planar microwave source, in which both SWP and volume-wave plasma (VWP) can be produced [27, 28, 30]. Description of the new VWP source will be presented in chapter 3. Low-temperature sterilization experiments with the VWP source will be presented in chapter 6.

The last part presented in chapter 7 is about atmospheric pressure plasma sterilization with some previous works and a recent result.

References

[1] I. Langmuir: Proc. Nat. Acad. Sci. U.S. **14**, 628 (1928).

[2] F. F. Chen: Introduction to Plasma Physics, (New York, NY: Plenum Press) chapter **1**, pp. 1-3 (1974).

[3] Plasma (physics)-Wikipedia, the free encyclopedia.

[4] P. T. Jacobs and S. M. Lin: Disinfection, Sterilization and Preservation 5th edn., ed. S. S. Block, (Philadelphia, PA: Lippincott Williams & Wilkins) (2000).

[5] Sterilization (microbiology)-Wikipedia, the free encyclopedia.

[6] Disinfectant-Wikipedia, the free encyclopedia.

[7] M. Laroussi: Plasma Process. Polym. **2**, 391-400 (2005).

[8] US 4207286 (1980), Biophysics Research & Consulting Corp., inv.: R. M. Boucher.

[9] US 4643876 (1987), Surgikos Inc., invs.: P. T. Jacobs, S. M. Lin.

[10] A. A. Bol'shakov, B. A. Cruden, R. Mogul, M. V. V. S. Rao, A. P. Sharma, B. N. Khare, M. Meyyappan: AIAA J. **42**, 823 (2004).

[11] S. Moreau, M. Moisan, J. Barbeau, J. Pelletier, A. Ricard: J. Appl. Phys. **88**, 1166 (2000).

[12] M. Moisan, J. Barbeau, S. Moreau, J. Pelletier, M. Tabrizian, L'H. Yahia: Int. J. Pharm. **226**, 1 (2001).

[13] M. Moisan, Z. Zakrzewski: J. Phys. D: Appl. Phys. **24**, 1025 (1991).

[14] N. Philip, B. Saoudi, M. C. Crevier, M. Moisan, J. Barbeau and J. Pelletier: IEEE Trans. Plasma Sci. **30**, 1429 (2002).

[15] M. Moisan, B. Saoudi, M. C. Crevier, N. Philip, E. Fafard, J. Barbeau and J.

Pelletier: Conf. Proc. Of 5th Int. Workshop Microwave Discharges: Fundamentals and Applications (Greifswald, Germany), pp.210-221 (2003).
[16] E. E. Kunhardt: IEEE Trans. Plasma Sci. **28**, 189 (2000).
[17] U. Kogelschatz: IEEE Trans. Plasma Sci. **30**, 1400 (2002).
[18] S. Kanazawa, M. Kogoma, T. Moriwaki, S. Okazaki: J. Phys. D: Appl. Phys. **21**, 838 (1988).
[19] M. Laroussi, I. Alexeff, J. P. Richardson, F. F. Dyer: IEEE Trans. Plasma Sci. **30**, 158 (2002).
[20] A. Scutze, J. Y. Jeong, S. E. Babyan, J. Park, G. S. Selwyn, R. F. Hicks: IEEE Trans. Plasma Sci. **26**, 1685 (1998).
[21] M. K. Boudam, M. Moisan, B. Saoudi, C. Popovici, N. Gherardi and F. Massines: J. Phys. D: Appl. Phys. **39**, 3494-3507 (2006).
[22] M. Nagatsu, F. Terashita, Y. Koide: Jpn. J. Appl. Phys. **42**, L856-L859 (2003).
[23] M. Nagatsu, F. Terashita, H. Nonaka, L. Xu, T. Nagata, Y. Koide: Appl. Phys. Lett. **86**, 211502 (2005).
[24] L. Xu, F. Terashita, H. Nonaka, A. Ogino, T. Nagata, Y. Koide, S. Nanko, I. Kurawaki and M. Nagatsu: J. Phys. D: Appl. Phys. **39**, 148-152 (2006).
[25] L. Xu, H. Nonaka, H. Y. Zhou, A. Ogino, T. Nagata, Y. Koide, S. Nanko, I. Kurawaki and M. Nagatsu: accepted by J. Phys. D: Appl. Phys. **40**, 803-808 (2007).
[26] M. Nagatsu, F. Terashita, L. Xu, H. Nonaka, K. Ninomiya, T. Nagata, Y. Koide, S. Nanko and I. Kurawaki: Abstracts and full-papers CD of 17th Int. Symp. Plasma Chemistry (Toronto, Canada), pp. 1100-1101 (2005).
[27] M. Nagatsu, L. Xu, H. Nonaka, K. Ninomiya, A. Ogino, T. Nagata, Y. Koide, S. Nanko and I. Kurawaki: Proc. Inter-Academia 2005, (Wuppertal, Germany), Vol. 1, pp. 217-225 (2005).
[28] M. Nagatsu, L. Xu, H. Nonaka, , H. Y. Zhou, A. Ogino, T. Nagata, Y. Koide, S. Nanko and I. Kurawaki: Proc. 6th Int. Conf. Reactive Plasma & 23rd Symp. Plasma Processing (Matsushima, Japan), pp. 557-558 (2005).
[29] H. Nonaka, T. Yamashita, L. Xu, A. Ogino, T. Nagata, Y. Koide, S. Nanko, I. Kurawaki and M. Nagatsu: Proc. 6th Int. Conf. Reactive Plasma & 23rd Symp. Plasma Processing (Matsushima, Japan), pp. 561-562 (2005).
[30] L. Xu, H. Y. Zhou, A. Ogino, Y. Koide and M. Nagatsu: Conf. Proc. 6th Int. Workshop Microwave Discharges: Fundamentals and Applications (Zvenigorod, Russia), pp. 321-326 (2006).

2 Surface-wave plasma source

2.1 Introduction to surface-wave plasma

Surface waves are electromagnetic waves along the interface of two different media with phase velocity less than the speed of light. Since the wave propagation involves the motion of free charged particles, they can propagate only at the interface of two media with opposite signs of dielectric permittivity, such as plasma and dielectric. Plasmas that are excited by propagation of electromagnetic surface waves carrying sufficient power flux are called surface-wave-sustained plasmas, usually as *surface-wave plasma (SWP)*. The surface wave mode allows to generate uniform high-frequency-excited plasmas in volumes whose lateral dimensions extends over several wavelengths of the electromagnetic wave, for example, microwaves of 2.45 GHz in vacuum the wavelength amounts to 12.2 cm. SWP sources can be divided into two groups depending upon whether the plasma generates part of its own waveguide by ionization or not.

The propagation of a non-ionizing electromagnetic surface wave along the interface between plasma and its surrounding dielectric media was first studied by Trivelpiece and Gould in 1959 [1]. Their study was focused on low amplitude electromagnetic waves propagating along the positive plasma column of a DC discharge in a cylindrical dielectric tube. It seems that Bulkin et al. [2] were the first to observe a discharge sustained by a surface wave when they reported the existence of a wave with a longitudinal electric field component along a pulsed discharge sustained in a waveguide. Tuma [3], who employed a surface-wave discharge to excite a laser medium, was probably the first to clearly identify its nature that surface waves propagating at the plasma-dielectric boundary could be absorbed in the plasma, thus sustaining the discharge.

In the 1970s and 1980s, the experimental works concerning surface-wave plasma were limited to cylindrical dielectric tubes [4-12]. Moisan et al. [4, 5] developed a first series of simple, compact and highly efficient surface-wave launchers, based on coaxial and waveguide components that were particularly suitable for the microwave generation of long plasma columns. However, the thin dielectric tube structure is difficult to generate large-diameter plasma. Since Komachi and Kobayashi [13] reported a new method for generating large area microwave plasma using traveling waves in an open dielectric waveguide in 1989, the concept of the large-area SWP source has emerged. According to the shape of the plasma-dielectric interface where surface waves are

guided, the large-area SWP sources can be divided into two groups: planar large-area SWP sources and tubular large-area SWP sources.

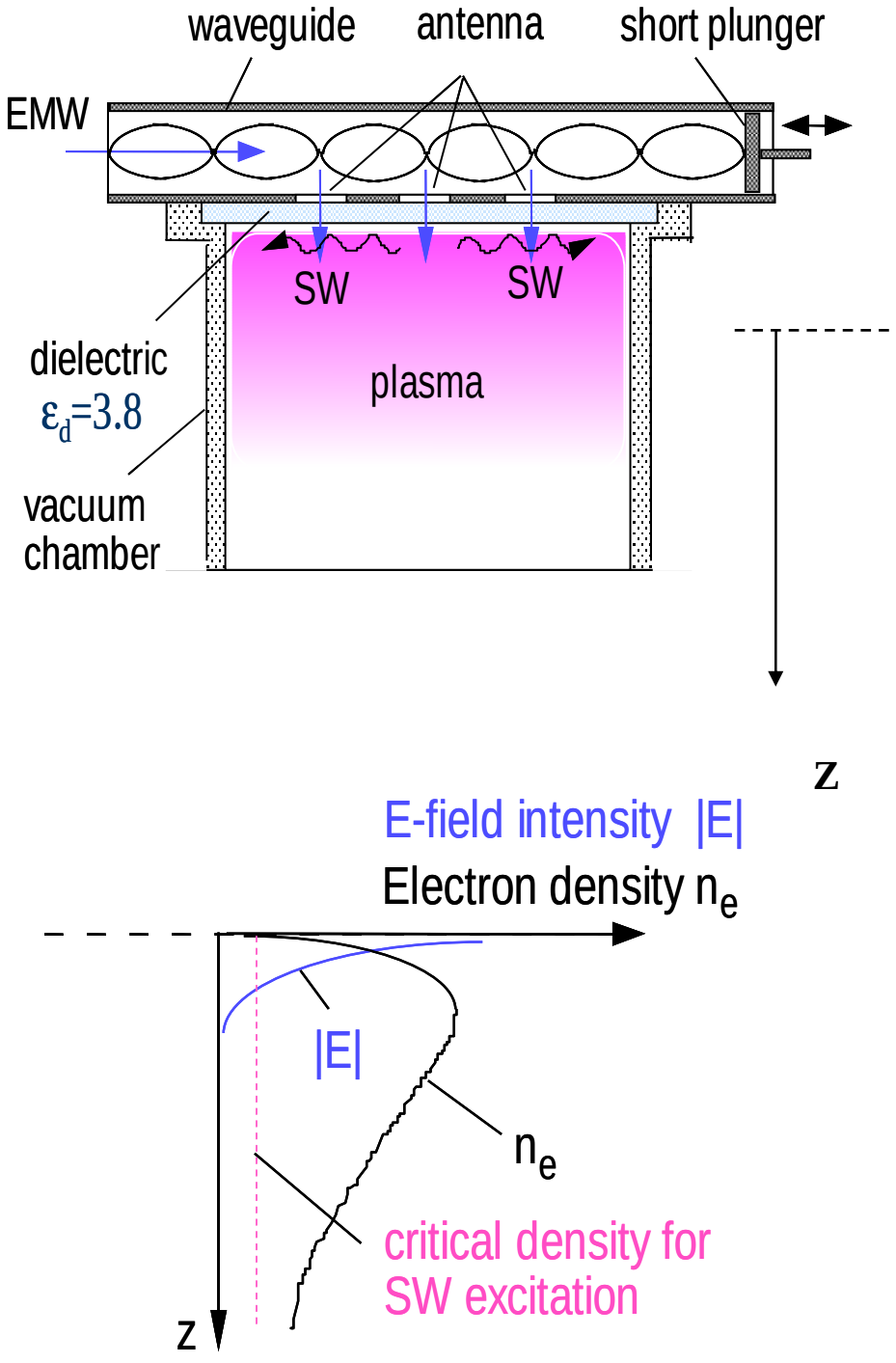

Fig. 2.1 Illustration of the surface-wave plasma.

Nagatsu et al. [14-26] reported the first slot antennae type planar SWP source in 1996. The 2.45 GHz microwave was fed from a rectangular waveguide through a pair of slot antennae contacting to a quartz window (diameter = 240 mm, thickness = 17 mm). The slots were half a wavelength in free space long, inclined in opposite directions, and a detailed study of the discharge production using other types of slot antennae is also available [25]. **Figure 2.1** shows the illustration of the SWP produced by slot antennae structure. The discharge was sustained by standing surface waves resulting in mode jumps and hysteresis, which has been explained by resonance surface-wave eigenmodes in the dielectric plate [15-17] also including the antennae configuration [24]. Plasma densities in order of 10^{12} cm^{-3} over a wide pressure range in various gases were achieved. The operation of the source without dielectric window, relying only on the underdense plasma layer at the metal-plasma boundary as the waveguiding interface, has also been reported [19].

2.2 Experimental setup

Figure 2.2 shows the SWP device in our laboratory. A schematic drawing of the experimental setup is shown in **Fig. 2.3**. The SWP was produced in a 40-cm-diameter, cylindrical vacuum chamber by introducing a 2.45 GHz microwave through a quartz window via slot antennae. A rectangular quartz window (18-mm thick quartz plate with dielectric constant $\varepsilon_d = 3.8$) with inner dimensions of 109 mm × 380 mm is used as vacuum sealing on the top metal plate. There is a water cooling system equipped around the quartz plate. Five transverse slots are cut vertically to the waveguide axis with a spacing of one-half of the waveguide wavelength, and four pairs of longitudinal slots are also cut between the transverse slots, as shown in the bottom schematic of **Fig. 2.3**. The width and length of each slot are 10 mm and $\lambda/2$ = 61 mm, where λ is a free-space wavelength. [27] For each antenna, the plunger was tuned to achieve minimum power reflectivity.

The microwave power is fed into the chamber from a rectangular waveguide. The rectangular waveguide line is equipped with E-H tuner (Nissin, MT-20), a water-cooled isolator (Nissin, IS-30J), two directional couplers (Nissin, PM-60) with power detector enabling the monitoring of the incident and reflected power respectively, and a pulse monitor coupler. The E-H tuner was used to minimize the reflected power, keeping the short plunger at optimum position. The whole system is powered by a stabilized 2.45 GHz magnetron generator (Nissin, MPS-30D) with the output power in the range from 0.2 to 3 kW. With the pulse unit (Nissin, MGP-30) and a function generator (Kenwood,

FG-272), the pulse-modulated plasma discharges could be operated using the microwave system with a modulation frequency of DC to 80 kHz. The microwave pulses were monitored by the incident power detector mounted on the waveguide just after the isolator. Typical rise and fall times, defined as a 10 to 90 % interval, were roughly 0.3 μs and 3 μs respectively, and maximum instantaneous power was 4 kW.

The top metal plate, bottom flange and the sidewall of the chamber are equipped with altogether 17 ports for pumping, leaking, pressure gauge, viewing, gas- and instrumentation-feedthroughs. The ports for pumping, pressure gauge and viewing are shielded against the radiation by a fine stainless steel mesh. There are two sidewall ports in a distance of 14 cm from the top metal plate, one set with glass window called Optopass Port (QYP-150-UV) is not only the main viewing port used to observe the inside of vacuum chamber, but also capable of transmitting light whose wavelength is greater than 150 nm through it from inside the chamber. The other one connected with quadrupole mass spectrometer is used for mass spectrum diagnosis. One horizontal port in the sidewall in a distance of 20 cm from the top plate and one vertical port on the bottom flange are used for the probe diagnostics. A Langmuir probe with a platinum wire tip was used to measure the spatial distribution of the basic plasma parameters, such as electron density, temperature and ion saturation currents. Axial distributions of the microwave electric field intensity at 2.45 GHz were also measured using the same Langmuir probe scannable in the z direction. The intensity of the 2.45 GHz microwave, picked up by the short wire tip of the probe, was directly measured using a spectrum analyzer (Tektronix, 491).

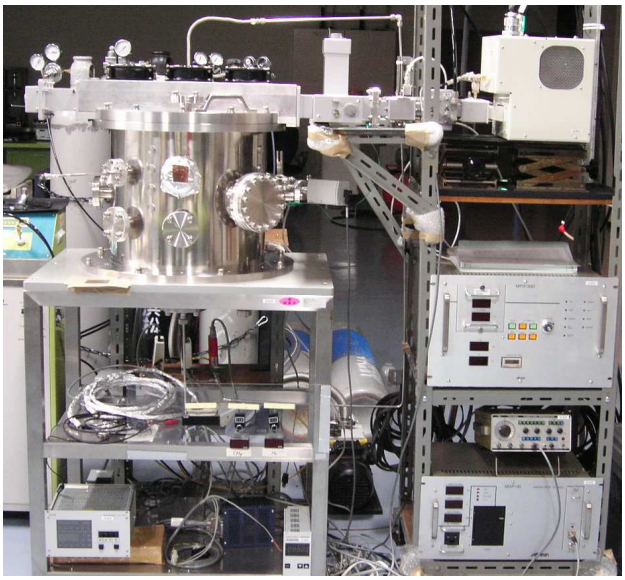

Fig. 2.2 Photograph of the surface-wave plasma device.

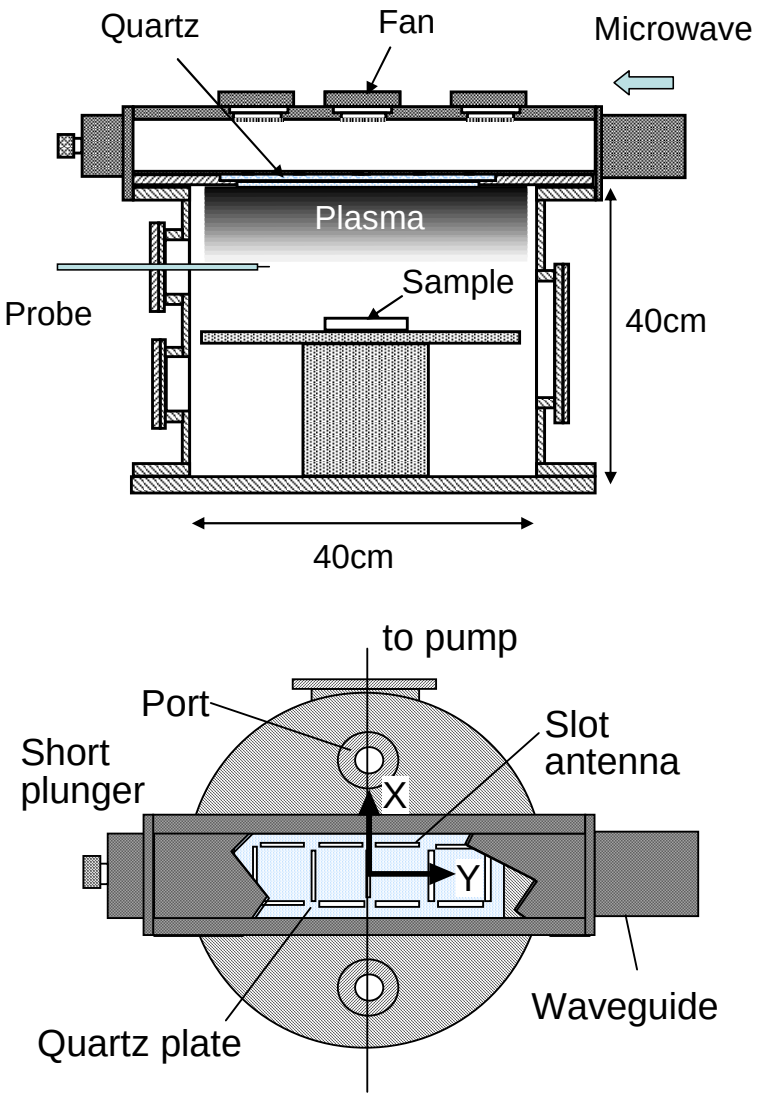

Fig. 2.3 Schematic of the surface-wave plasma source. [27]

The vacuum chamber is evacuated by a turbomolecular pump (Pfeiffer Vacuum, TMU 260 SG) with pumping speed of 210 l/s and a single-stage rotary vane pump (Pfeiffer Vacuum, DUO 10) with pumping speed of 10 m^3/h as the backing pump. The two pumps are operated by a display and operating unit (Pfeiffer Vacuum, TCP 380). The base pressure of the whole vacuum system can be evacuated to the order of 10^{-6} Torr. The working pressure during the experiment is controlled by a bleed valve and measured by a pressure gauge set (Pfeiffer Vacuum, SingleGauge meter + Compact process ion gauge sensor). The working gas, such as oxygen, nitrogen or argon, is introduced into the chamber from one top flange port and controlled by a mass flow meter.

2.3 Surface-wave plasma characteristics

In order to excite the pure surface mode [21], the plasma density should be higher than the critical density $n_{crit} = (1 + \varepsilon_d)n_c$, where n_c is the cutoff density $n_c = \varepsilon_0 m_e \omega_p^2/e^2$ (the electron plasma frequency ω_p = the wave frequency ω) and ε_d is the dielectric constant of the window, thus $n_{crit} = 3.6\times10^{11}$ cm^{-3}. Furthermore, as shown in **Fig. 2.1**, the electric fields of the launched electromagnetic wave should locally distribute near the quartz-plasma interface and exponentially decay with a characteristic length, which roughly equals the skin depth, c/ω_p, inside the plasma.

A Langmuir probe with a 0.7-mm-diameter, 8-mm-long platinum wire tip was used to measure the spatial distribution of the basic plasma parameters, such as ion saturation currents, and electron density in continuous microwave excited SWP. Axial distributions of the microwave electric field intensity were also measured using the same Langmuir probe, by measuring the electric field amplitudes at 2.45 GHz directly using a spectrum analyzer.

Since the SWP device presented in this thesis was made in Nagoya University before being displaced to Shizuoka University, the measurement of continuous microwave excited SWP characteristics was carried out in Nagoya University [28]. While, the measurement of pulse-modulated microwave excited SWP characteristics using a Langmuir probe with a 0.6-mm-diameter, 2-mm-long platinum wire tip was carried out during my doctoral course in Shizuoka University [29].

2.3.1 Characteristics of continuous SWP

First, the characteristics of the SWP in the case of low-pressure Ar gas are presented. **Figure 2.4** shows the *z*-axial distribution of ion saturation current and microwave electric field intensity in Ar plasma where the gas pressure was 20 mTorr, Ar gas flow rate was 71.4 sccm and the net microwave power was 700 W. The downside of quartz plate is defined as $z = 0$ throughout this thesis. By scanning the Langmuir probe in the *z* direction, the axial distribution of the ion saturation current was measured and found to achieve its maximum in the vicinity of $z = 40$ mm. This is due to the equilibrium between the plasma generation at the quartz-plasma interface and the plasma disappearance by diffusion process. Moreover, the electric field intensity of the 2.45 GHz wave is strongly damped and vanishes at $z > 20$ mm. The decay length of the electric field is typically of the order of 5-10 mm. This means the electric field, only existing at quartz-plasma interface, will not affect the plasma processing below.

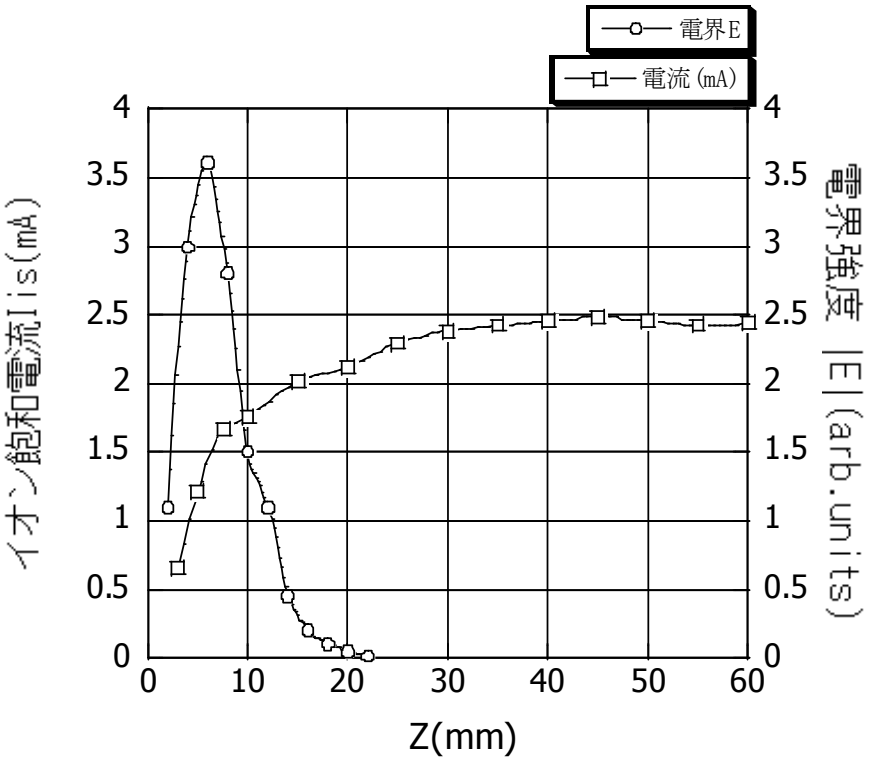

Fig. 2.4 Axial distributions of ion saturation current and microwave electric field intensity in Ar plasma. [28]

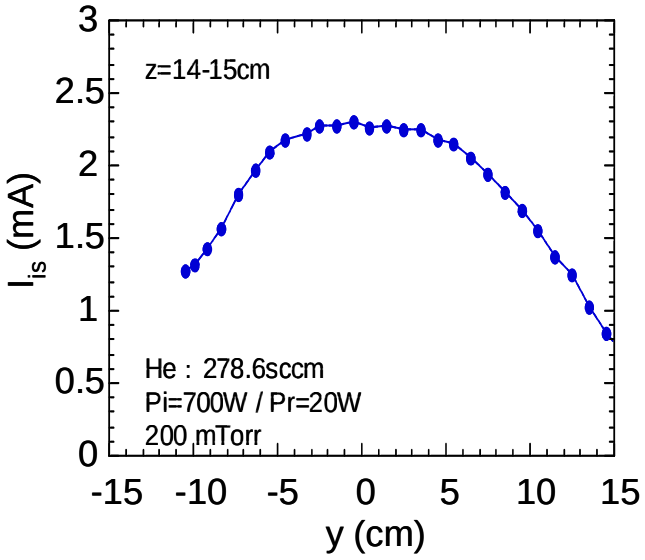

Fig. 2.5 Horizontal distribution of ion saturation current at z = 14~15 cm in He plasma. [28]

Next, the characteristic of the SWP in the case of low-pressure He gas is presented. **Figure 2.5** shows the horizontal distribution of plasma density profile in He plasma where the gas pressure was 200 mTorr, He gas flow rate was 278.6 sccm and net microwave power was 680 W. We find that uniform plasma within ±5% can be obtained in the vicinity of the center over about 10 cm on *y*-axial direction.

2.3.2 Characteristics of pulse-modulated SWP

Finally, the characteristics of pulse-modulated SWP in the case of low-pressure oxygen gas are presented. The waveforms of plasma densities of oxygen SWPs driven by pulse-modulated microwaves are shown. **Figure 2.6** shows typical waveforms of ion saturation currents under discharge conditions where the gas pressure was 60 mTorr and the duty ratio was 50% at modulation frequencies of 50 kHz and 25 kHz. A Langmuir probe was placed at z = 55 mm below the quartz window, and it was found that the plasma density saturated about 10 μs after the microwave onset. After the microwave pulse turn-off, ion saturation currents decayed with a time constant of about 30 μs. It was expected that oxygen with metastable states, such as O*(^{1}D) or O_2*($^1\Delta_g$), which are considered to play an important role in sterilization, would exist for a short time until they were released from surface attachment after the microwave was turned off.

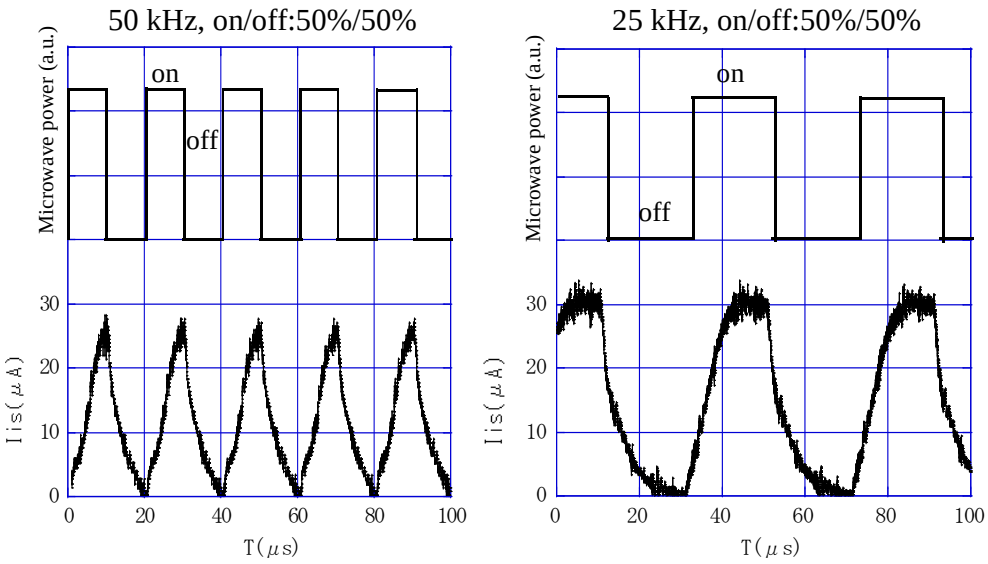

Fig. 2.6 Typical waveforms of ion saturation currents together with the pulse signals; modulation frequencies of (a) 50 kHz and (b) 25 kHz.

In order to study the discharge condition required for sterilization, the instantaneous power of the microwave pulses was varied. **Figure 2.7** shows the relationship between ion saturation current and instantaneous power, with the probe set at z = 55 mm and r = 100 mm and at a gas pressure of 60 mTorr. It can be seen that the ion density increases almost linearly with instantaneous power, apart from a change in gradient at around 1200~1300 W. This could be due to a slight change in the plasma density profile over the chamber cross section.

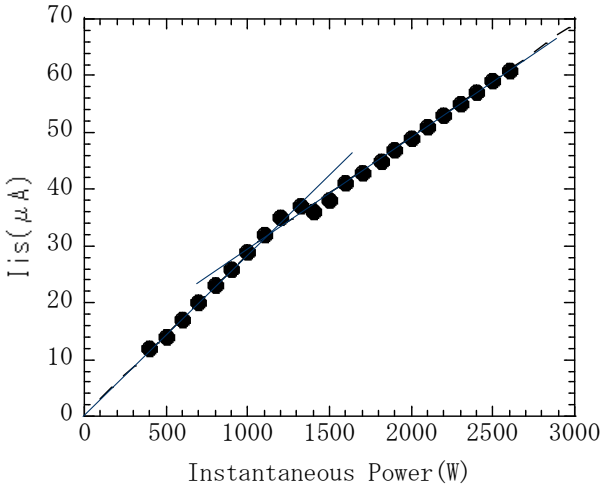

Fig. 2.7 Relationship between ion saturation current measured at z = 55 mm and incident microwave power.

References

[1] A. W. Trivelpiece and R. W. Gould: J. Appl. Phys. **30**, 1784 (1959).

[2] P. S. Bulkin, V. N. Ponomariev and G. S. Solntsev: Sov. Phys.-Tech. Phys. **8**, 911 (1964).

[3] D. T. Tuma: Rev. Sci. Instrum. **41**, 1519 (1970).

[4] M. Moisan, C. Beaudry and P. Leprince: Phys. Lett. **50A**, 125 (1974).

[5] M. Moisan, C. Beaudry and P. Leprince: IEEE Trans. Plasma Sci. **PS-3**, 55 (1975).

[6] M. Moisan, Z. Zakrzewski, R. Pantel and P. Leprince: IEEE Trans. Plasma Sci. **PS-12**, 203 (1984).

[7] M. Moisan and Z. Zakrzewski: Rev. Sci. Instrum. **58**, 1895 (1987).

[8] C. Boisse-Laporte, A. Granier, E. Dervisevic, P. Leprince and J. Marec: J. Phys. D: Appl. Phys. **20**, 197 (1987).

[9] A. Gamero, J. Cotrino, A. Sola and V. Colomer: J. Phys. D: Appl. Phys. **21**, 1275 (1988).
[10] C. M. Ferreira: J. Phys. D: Appl. Phys. **14**, 1811 (1981).
[11] Yu. M. Aliev, A. G. Boev and A. P. Shivarova: Phys. Lett. **92**, 235 (1982).
[12] I. Zhelyazkov and E. Benova: J. Appl. Phys. **66**, 1641 (1989).
[13] K. Komachi and S. Kobayashi: J. Microwave Power Electromagn. Energy **24**, 140 (1989).
[14] M. Nagatsu, G. Xu, M. Yamage, M. Kanoh and H. Sugai: Jpn. J. Appl. Phys. **35**, L341 (1996).
[15] I. Ghanashev, M. Nagatsu and H. Sugai: Jpn. J. Appl. Phys. **36**, 337 (1997).
[16] I. Ghanashev, M. Nagatsu, G. Xu and H. Sugai: Jpn. J. Appl. Phys. **36**, 4704 (1997).
[17] I. Ghanashev, M. Nagatsu and H. Sugai: Trans. Inst. Electr. Eng. Jpn. **EP-97**, 45 (1997).
[18] S. Morita, M. Nagatsu, I. Ghanashev, N. Toyoda and H. Sugai: Jpn. J. Appl. Phys. **37**, 468 (1997).
[19] M. Nagatsu, G. Xu, I. Ghanashev, M. Kanoh and H. Sugai: Plasma Sources Sci. Technol. **6**, 427 (1997).
[20] M. Nagatsu, I. Ghanashev, S. Morita and H. Sugai: Jpn. J. Appl. Phys. **37**, 2406 (1997).
[21] H. Sugai, I. Ghanashev and M. Nagatsu: Plasma Sources Sci. Technol. **7**, 192 (1998).
[22] I. Ghanashev, H. Sugai, S. Morita and N. Toyoda: Plasma Sources Sci. Technol. **8**, 363 (1999).
[23] I. Ghanashev, S. Morita, N. Toyoda, M. Nagatsu and H. Sugai: Jpn. J. Appl. Phys. **38**, 4313 (1999).
[24] I. Ghanashev and H. Sugai: Physics of Plasma **7**, 3051 (2000).
[25] M. Nagatsu, S. Morita, I. Ghanashev, A. Ito, N. Toyoda and H. Sugai: J. Phys. D: Appl. Phys. **33**, 1143 (2000).
[26] H. Sugai, I. Ghanashev and K. Mizuno: Appl. Phys. Lett. **77**, 3523 (2000).
[27] M. Nagatsu, T. Sano, N. Takada, W. X. Guang, T. Hirao, and H. Sugai: Jpn. J. Appl. Phys. **39**, L929, (2000).
[28] 佐野 徹「修士学位論文：大面積表面波プラズマCVDによるアモルファスカーボン膜生成とその膜特性」(2001).
[29] L. Xu, F. Terashita, H. Nonaka, A. Ogino, T. Nagata, Y. Koide, S. Nanko, I. Kurawaki and M. Nagatsu: J. Phys. D: Appl. Phys. **39**, 148-152 (2006).

3 Volume-wave plasma source

3.1 Introduction to volume-wave plasma

Sugai et al. [1] briefly recalled the main facts about microwave propagation in non-magnetized plasmas. They presented in the case of real bounded plasmas new phenomena occur. Suppose that microwaves are incident (e.g. axially) on a finite bounded plasma (e.g. cylindrical plasma column). In the low density (underdense) case (**Fig. 3.1(a)**) the waves penetrate into the plasma as *volume waves* (and give rise to volume resonances if the plasma dimensions are comparable to the wavelength determined from equation $\omega^2 = \omega_p^2 + c^2k^2$, where k is the wave vector, c is the speed of light in free space and $\omega_p = e(n_e/\varepsilon_0 m_e)^{1/2}$). In an overdense plasma such propagation is not possible, but an electromagnetic *surface wave* (a wave decaying exponentially away from the guiding structure [2]) can propagate along a dielectric-plasma interface (**Fig. 3.1(b)**), penetrating into the plasma at a few skindepths. This situation is eventually possible also along a plasma-metal boundary, because one can regard the low-density plasma sheet along the metal wall as a dielectric facing the overdense bulk plasma.

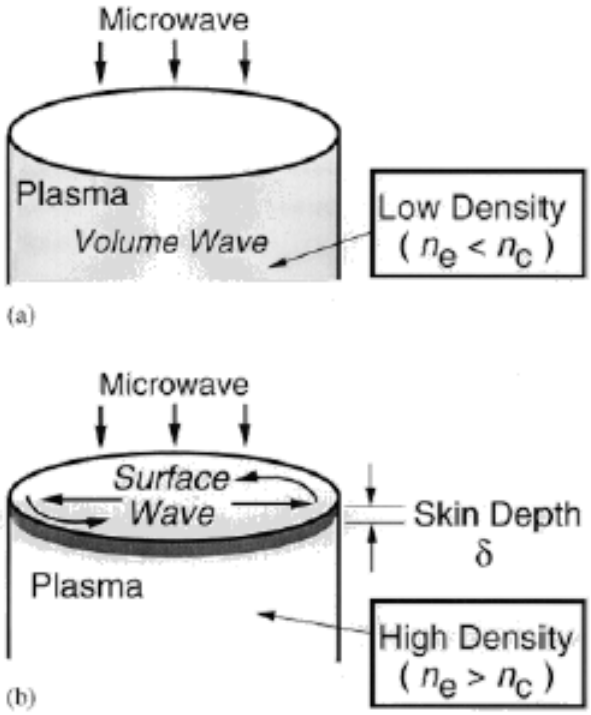

Fig. 3.1 Electromagnetic wave propagation in finite (a) underdense and (b) overdense plasmas. [1]

The planar-type overdense microwave plasmas produced without magnetic fields as so called surface-wave plasma (SWP) have been described in chapter 2. It has a number of advantages in producing high-density ($n_e > 10^{11}$ cm^{-3}), large-area ($L > 40$ cm) plasmas at pressures ranging from a low pressure of ~mTorr to a moderate pressure of ~10Torr [3-5]. However, a big issue in enlarging the plasma device is on the dielectric window needed for vacuum sealing. To hold a huge mechanical force, typically 10 tons/m^2 of dielectric window, one needs a very expensive, thick dielectric plate. [6] Recently, Nagatsu [7] has proposed a patent structure that using slot antennae (which are directly formed by punching the wall of a waveguide line) combining a planar cylindrical cavity resonator above the quartz plate plane, where only seven pieces of small-size quartz window are used instead of the general one cross-section-size piece of quartz plate as vacuum window. Moreover, with this structure, both *surface-wave plasma* (SWP) mode and *volume-wave plasma* (VWP) mode can be controlled by the electron density change, which in turn, is caused by the pressure change. Since the electron density can be controlled not only by changing the pressure, but, even more straightforwardly, by changing the power fed to the chamber, one should also observe similar mode changes when changing incident power at a fixed pressure. [8] The cutoff density was calculated as 7.4×10^{10} cm^{-3} corresponding to the microwave frequency of 2.45 GHz. [9] In the present work, we call the microwave device that can produce volume-wave plasma as volume-wave plasma source.

Figure 3.2 shows the illustration of the SWP and VWP produced by slot antennae structure. The SWP and VWP can be applied to etching, plasma CVD or plasma sterilization.

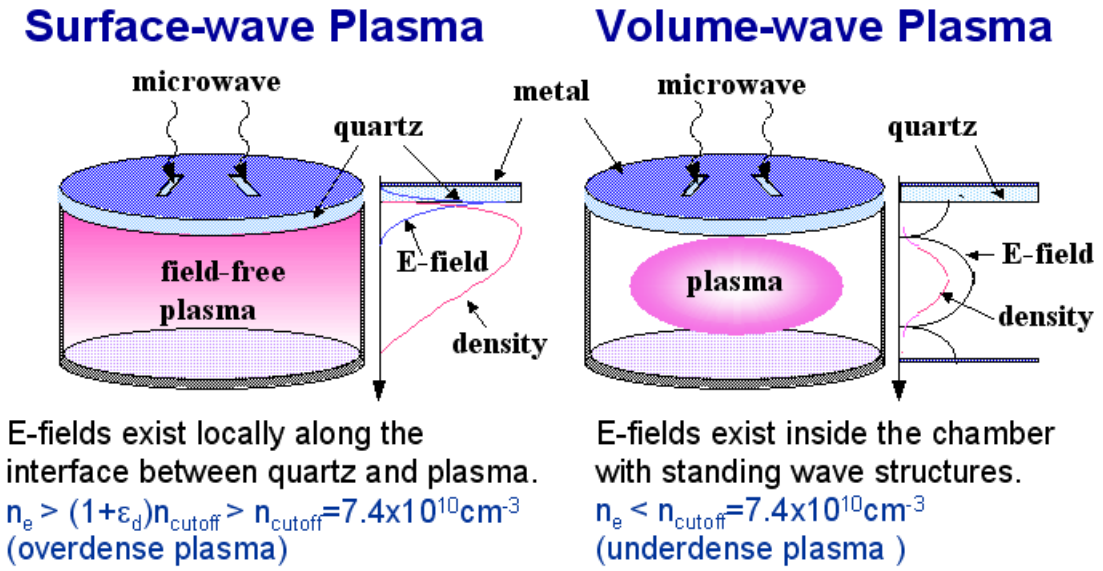

Fig. 3.2 Illustration of the surface-wave plasma and volume-wave plasma.

3.2 Experimental setup

Figure 3.3 shows the VWP device in our laboratory. A schematic drawing of the experimental setup is shown in **Fig. 3.4**. The 2.45 GHz microwave, guided by a rectangular waveguide, was fed into a vacuum chamber filled with discharge gas, through slot antennae cut in the broad face of each waveguide [10]. It has similar slot antennae and waveguide line as described in chapter 2 for the SWP device. The slot antennae were directly formed by punching the base plane of the waveguide. A planar cylindrical cavity resonator was combined just below the slot antennae plane and above the quartz plate plane, where only seven pieces of small-size quartz window were used instead of the general one cross-section-size piece of quartz plate as vacuum window (**Fig 3.5**).

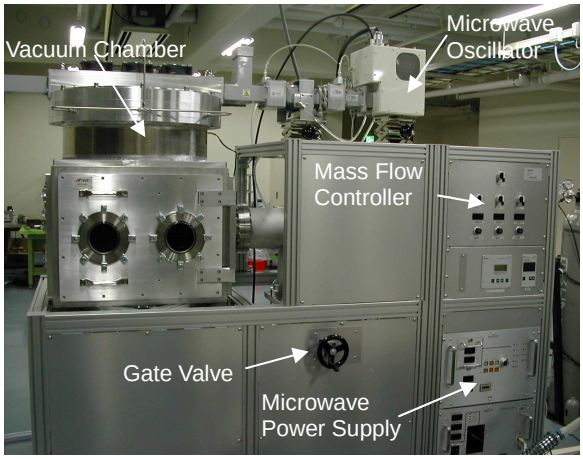

Fig. 3.3 Photograph of the volume-wave plasma device.

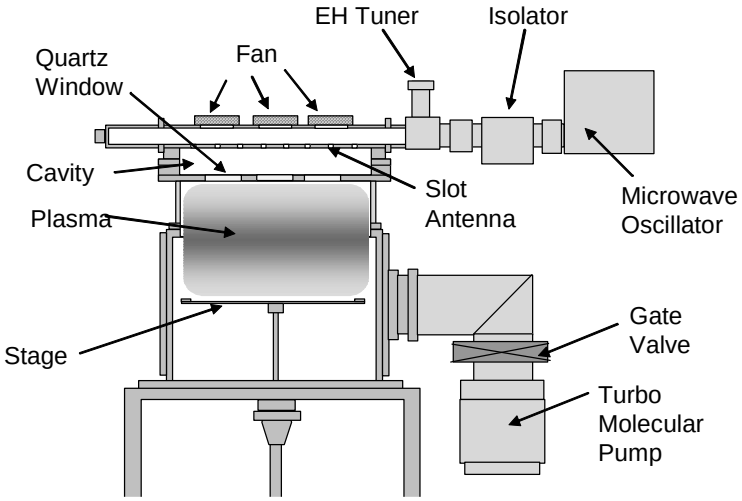

Fig. 3.4 Schematic drawing of the volume-wave plasma source.

The vacuum chamber consisted of an upper section with a cylindrical structure of 55 cm in diameter and of 21 cm in height for plasma source and a lower section with a square cross section of 63 × 63 cm^2 and of 48 cm in height for sample treatment. It is evacuated by a turbomolecular pump (Pfeiffer Vacuum, TMU 1001P) with pumping speed of 920 l/s and a single-stage rotary vane pump (Pfeiffer Vacuum, DUO 20) with pumping speed of 20 m^3/h as the backing pump. The two pumps are operated by a display and operating unit (Pfeiffer Vacuum, DCU 600). Base pressure of the whole vacuum system can be evacuated to the order of 10^{-5} Torr. Working pressure during the experiment is controlled by a gate valve and measured by a pressure gauge set (Pfeiffer Vacuum, SingleGauge meter + Compact process ion gauge sensor). The working gas, such as oxygen, nitrogen or argon, is introduced into the chamber from four inlets just below the quartz plate plane and controlled by a mass flow meter. The projected microwave power could be varied from 0.2 to 3 kW and the time-modulated plasma discharges could be operated using the microwave system with a remote-control on/off timer module.

There are total 8 ports on sidewalls of the lower section of the chamber, 2 viewing-windows on the convenient front-loading door and 3 ports on the bottom plane. The 3 ports on the bottom plane are for leaking, pressure gauge and a magnetic-force-holding moveable stage, respectively. The ports on left sidewall of the lower section of the chamber in a distance of 35 cm from the quartz plate plane can be connected with quadrupole mass spectrometer, Langmuir probe and matrass with pure water. A Langmuir probe with a platinum wire tip was used to measure the spatial distribution of ion saturation currents. Distributions of the microwave electric field intensity at 2.45 GHz were also measured using the same Langmuir probe. The intensity of the 2.45 GHz microwave, picked up by the short wire tip of the probe, was directly measured using a spectrum analyzer (Tektronix, 491).

Fig. 3.5 Photograph of the seven small quartz windows.

3.3 Characteristics of surface-wave plasma and volume-wave plasma

Profile of plasma produced in the large-volume discharge chamber has been investigated [11]. A Langmuir single probe placed at 35 cm below the quartz window was used to measure spatial distribution of ion saturation current by scanning probe through the chamber. When the microwave power was 0.75 kW at pressure of 30 mTorr, plasma density profile measured in $Ar/N_2/O_2$ gas mixture was plotted in **Fig. 3.6**. It was found that the value of ion saturation current kept more than half of maximum value broadened over 50 cm diameter. We also measured the relationship between ion saturation current and incident microwave power in $Ar/N_2/O_2$ plasma. When the microwave power was varied from 0.56 kW to 1.4 kW, **Fig. 3.7** showed ion saturation current in SWP increased almost linear with incident power without any density jump.

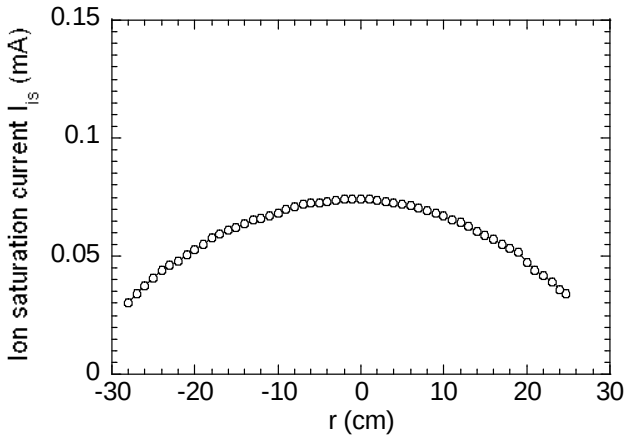

Fig. 3.6 Spatial distribution of ion saturation currents in SWP mode with $Ar/N_2/O_2$ gas mixture.

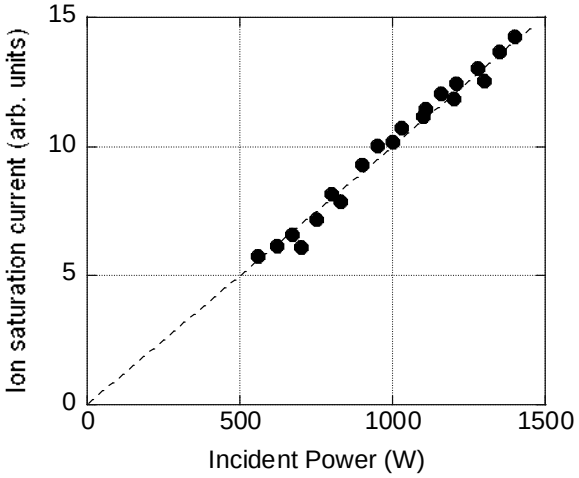

Fig. 3.7 Ion saturation currents versus microwave incident power in SWP mode.

For the measurement of electric field intensity, the picked-up microwave signals at 2.45 GHz were directly measured using a spectrum analyzer with a platinum wire tip of Langmuir probe. By varying discharge pressure and incident microwave power, discharge transition between SWP mode and VWP mode was observed in Ar plasma, O_2, N_2, air-simulated plasma, as shown in **Fig. 3.8(a)** and **(b)**, respectively. In Ar and air-simulated N_2-O_2 gas mixture, when the SWP was excited, bright plasma discharge was observed just below the quartz window, as shown in **Fig. 3.9(a)** and **Fig. 3.10(a)**, respectively. In previous SWP experiments, it has been found that the electron densities near quartz window were higher than the critical density for SW excitation, and diffused and decayed in the downstream region. When the VWP was excited, underdense plasma discharge entirely spread in the chamber, as shown in **Fig. 3.9(b)** in Ar and **Fig. 3.10(b)** in air-simulated N_2-O_2 gas mixture.

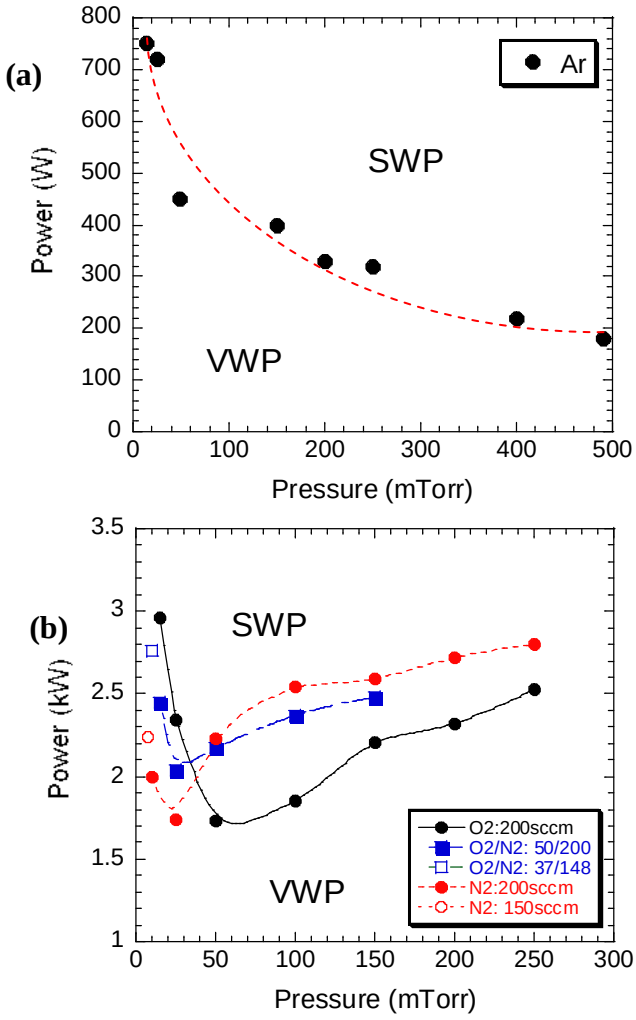

Fig. 3.8 Discharge transition between SWP mode and VWP mode in (a) Ar and (b) in O_2, N_2, and air-simulated N_2-O_2 gas mixture.

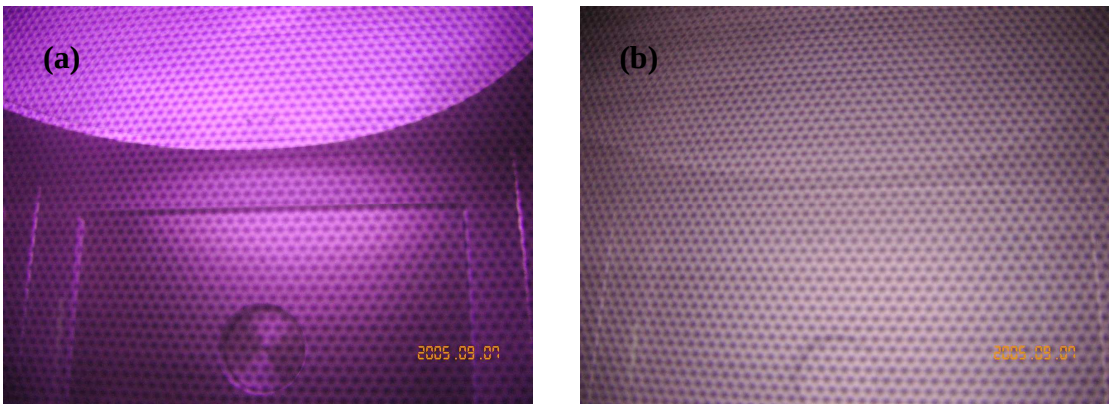

Fig. 3.9 Photograph of Ar discharge in (a) SWP mode and (b) VWP mode.

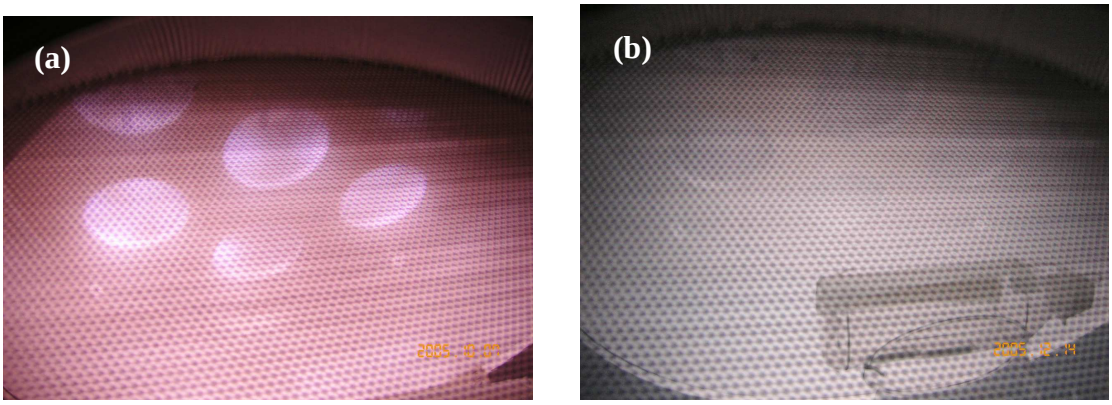

Fig. 3.10 Photograph of air-simulated N_2-O_2 gas mixture discharge in (a) SWP mode and (b) VWP mode.

References

[1] H. Sugai, I. Ghanashev and M. Nagatsu: Plasma Sources Sci. Technol. **7**, 192-205 (1998).

[2] R. E. Collin: Field Theory of Guided Waves (New York: McGraw-Hill) **ch. 11** (1960).

[3] E. Bluem, S. Bechu, C. Boisse-Laporte, P. Leprince and J. Marec: J. Phys. D: Appl. Phys. **28**, 1529 (1995).

[4] M. Nagatsu, G. Xu, M. Yamage, M. Kanoh and H. Sugai: Jpn. J. Appl. Phys. **35**, L341 (1996).

[5] I. Odrobina, J. Kudera and M. Kando: Plasma Sources Sci. Technol. **7**, 238 (1998).

[6] M. Nagatsu, K. Naito, A. Ogino, and K. Ninomiya: Appl. Phys. Lett. **87**, 161501 (2005).

[7] 永津雅章（発明者）、“マイクロ波プラズマ発生装置”、国立大学法人静岡大

学（出願者）、特願 2006-083677 (2006).
[8] I. Ghanashev, M. Nagatsu, G. Xu and H. Sugai: Jpn. J. Appl. Phys. **36**, 4704-4710 (1997).
[9] A. Ogino, K. Naito, F. Terashita, S. Nanko, and M. Nagatsu: Jpn. J. Appl. Phys. **44**, L352 (2005).
[10] M. Nagatsu, T. Sano, N. Takada, W. X. Guang, T. Hirao and H. Sugai: Jpn. J. Appl. Phys. **39**, L929, (2000).
[11] L. Xu, H. Y. Zhou, A. Ogino, Y. Koide and M. Nagatsu: Conf. Proc. 6th Int. Workshop on Microwave Discharges: Fundamentals and Applications (Zvenigorod, Russia), pp. 321-326 (2006).

4 Confirmation of sterilization

4.1 Introduction

Basic knowledge of plasma physics is well known for the researchers studying plasma science and plasma applications. However, the basic knowledge of sterilization is only well known for microbiologists and experts in medical and food packaging industries. To make all the present work be well understood, it is necessary to introduce the information on the biological indicators used in the present sterilization experiments, the method how to confirm sterilization result and agar-plate based colony-count method to know how much the bacteria have been inactivated, however, have still not been sterilized.

First, biological indicators with different kinds of microbe will be presented in section 4.2. Next, a quick method of confirming sterilization result by tryptic soy broth will be presented in section 4.3. Finally, the agar-plate based colony-count method will be presented in section 4.4.

4.2 Biological indicator

Sterilization is the act or process, physical or chemical, that destroys or eliminates all forms of life, especially microorganisms. This term is absolute, i.e. a substance cannot be partially sterile [1]. Due to the difficulty in confirming sterility, a more practical definition of sterility has been adopted, defining sterility as the process by which living organisms are removed or killed to an extent that they are no longer detectable in standard culture media in which they have previously been found to proliferate [1]. In practice, assurance of a low probability of any living microorganisms remaining is used as a measure of sterility. Sterility of a particular item can only be confirmed by destructive testing of the item, which is not practical for most purposes. [2]

Sterilization monitoring improves the assurance that medical devices have been adequately sterilized. Biological monitoring is accepted as the most effective method. Biological indicators function by introducing highly resistant bacterial spores into the sterilization cycle. If these spores are destroyed, it is assumed that any contaminating organisms in the load have also been killed, as these organisms have lower resistance than the spores, and are present in lower numbers [3].

Biological indicators (BIs) consist of an inoculated carrier contained within its

primary pack ready for use, and providing a defined resistance to the specified sterilization process. An inoculated carrier is a carrier on which a defined number of test organisms have been deposited (Association for the Advancement of Medical Instrumentation; AAMI ST59). In the present work, industrial use standard BIs manufactured by Raven biological laboratories, Inc. [4] were used.

4.2.1 Carriers

Discs have advantages over spore strips due to their size. Different materials may be compatible only with specific modes of sterilization. Discs can be used to monitor various sterilization methods and can be inoculated with any organism Raven Labs manufacture. Several types and sizes of discs are available including: paper, borosilicate paper, and stainless steel. In our experiments, we chose the stainless steel disc and called it **SUS** type.

Steel discs are representative of materials found in an isolator, and are compatible with vapor hydrogen peroxide. The polished stainless steel is strongly recommended to eliminate crevices in the carrier which can lead to tailing. The oblong disc is inoculated with *Geobacillus stearothermophilus* or *Bacillus atrophaeus* with mean strip recovery of 1.5×, 2.5× and 3.0×10^6 CFU/8mm×12mm stainless steel disc (CFU: colony forming units). Discs are packaged in a Tyvek®/poly pouch and may be exposed in the pouch or an off-center hole in the disc allows them to be removed from their package and suspended throughout the isolator to insure proper flow as shown in **Fig. 4.1(a)** and **(b)**.

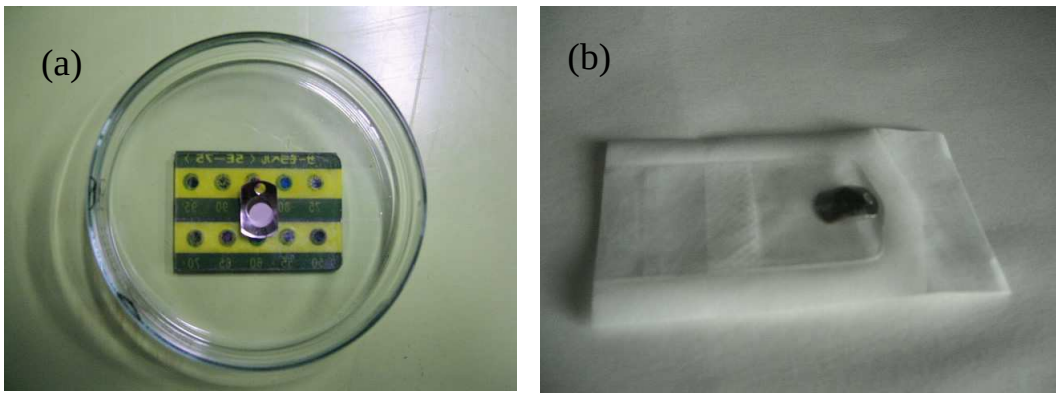

Fig. 4.1 Photograph of disc-type-carrier BIs in case of (a) being removed from package and (b) being packaged in a Tyvek®/poly pouch.

Paper strips are in Schleicher & Schuell filter paper – size 6.4 mm × 38.1mm – packaged in a peel open glassine paper pouch as shown in **Fig. 4.2(a)**. Glassine paper is permeable to sterilant but resistant to moisture and air at ambient temperature/pressure. This allows the user to transport the strip within the glassine from the sterilizer to a laminar flow hood, where it can be transferred into recovery medium such as the tryptic soy broth presented in next section.

Steri-chart is a set of strips with 5 different populations, all made from the same spore batch for use in cycle development as shown in **Fig. 4.2(b)**. Expose the five test strips to determine what level of sterility is being delivered by a particular cycle. A control strip is also included. Available with *G. stearothermophilus* (log 3, 4, 5, 6, & 7 test strips and a log 5 control) or *B. atrophaeus* (log 4, 5, 6, 7, & 8 test strips and a log 6 control).

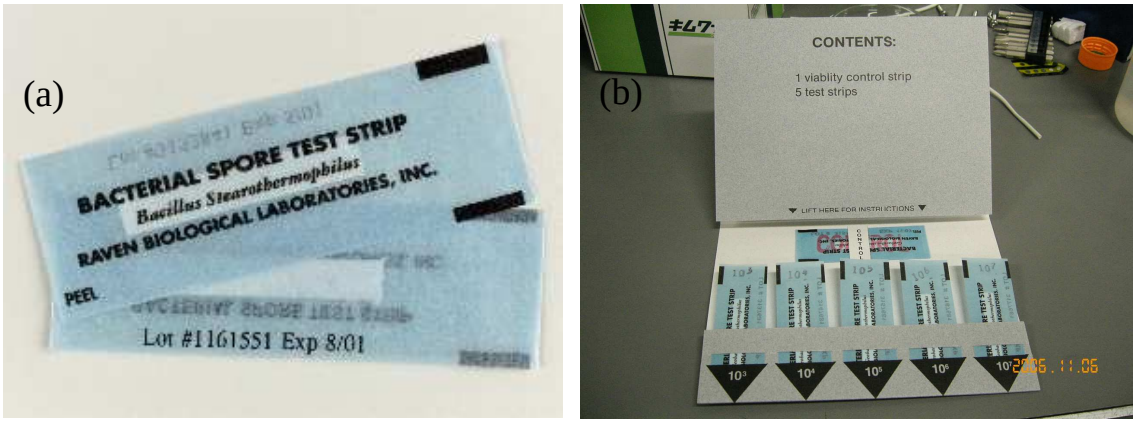

Fig. 4.2 Photograph of paper-strip-type-carrier BIs in case of (a) being packaged in glassine paper pouch and (b) Steri-chart.

4.2.2 Species

Raven Labs manufactures many species of non-pathogenic spore-forming bacteria. Most are used for various types of sterilization, though some have other uses. Following is a brief description of the most common uses:

Bacillus atrophaeus (previously *Bacillus. subtilis* variety niger, ATCC No. 9372) is Gram-positive, catalase-positive bacterium and has proven highly amenable to genetic manipulation, and has therefore become widely adopted as a model organism for laboratory studies. In terms of popularity as a laboratory model organism *B. subtilis* is often used as the Gram-positive equivalent of *Escherichia coli*, an extensively studied Gram-negative rod. It is used in steam sterilization procedures below 121°C. Some

pharmaceutical products are sterilized at 106° to 115°C for longer times because they are heat labile and would be damaged at 121°C or higher temperatures. This species has been used as a challenge to the lower temperatures in steam, where *G. stearothermophilus* would be too great a challenge. In using a lesser challenge it is necessary to have an extremely high level of control over the manufacturing process, environment, and bioburden of components. This organism is certified with a Steam D and z-value so its resistance at the lower temperatures can be determined.

Geobacillus stearothermophilus (ATCC No. 12980) has been used for steam and other types of sterilization by several BI manufacturers. In particular, it has been used to validate VHP sterilization of barrier isolators and clean areas in pharmaceutical production. To be able to provide a comparable product Raven Labs also offer *G. stearothermophilus* and test it in H_2O_2 vapor. This product is typically inoculated onto steel carriers so it is compatible with the H_2O_2 process. This organism is certified with an H_2O_2 D-value.

As described in above text, the industrial use BIs with species of *B. atrophaeus* and *G. stearothermophilus* spores are not specially used for the type of sterilization using plasma. However, these two species of non-pathogenic spore-forming bacteria can be considered as the representatives of highly resistant bacterial spores. Therefore, the biological indicators as steel discs or paper strips inoculated with *G. stearothermophilus* or *B. atrophaeus* are also useful in the plasma sterilization experiments.

The term *spore* may refer to the dormant stage of some bacteria or archaea, however these are more correctly known as endospores. An *endospore* is a dormant, tough, non-reproductive structure produced by a small number of bacteria from the Firmicute family. The primary function of most endospores is to ensure the survival of a bacterium through periods of environmental stress. They are therefore resistant to ultraviolet and gamma radiation, desiccation, lysozyme, temperature, starvation, and chemical disinfectants. So, sterilization of bacteria in spore status shows higher sterilizing performance than sterilization of common bacteria.

Most of the BIs used in the present work have been bought from Raven Labs. However, we occasionally ask our cooperating microbiology laboratory directly make BIs as steel discs or agar-plate inoculated with *Escherichia coli* not in spore status just to simulate the contaminated environment like our living environment. *E. coli* is a bacillus normally found in the human gastrointestinal tract and existing as numerous strains, some of which are responsible for diarrhea diseases.

4.3 Procedure for use

Raven Labs [4] manufactures prepared culture media specially formulated for use with their spore products. Soybean Casein Digest Broth is the recommended media (USP 24) for use with Biological Indicators. Raven's Tryptic Soy Broth is manufactured and tested to meet USP and NCCLS sterility and growth promotion guidelines. The general procedure for use is:

Spore carrier may be removed or left in primary packaging. Place carrier into test environment. Within completion of the sterilization cycle, aseptically transfer the spore carrier from the test unit into sterile Tryptic Soy Broth. An acid indicator may be used to facilitate detection of growth. Incubate at 55°-60°C for *G. stearothermophilus*, 30°-35°C for *B. atrophaeus*, for seven days. Check daily for growth and record growth as a failed sterilization cycle. If the spores were destroyed, the medium will remain a purple color. If sterilization processing was unsuccessful the spores will metabolize, causing a yellow color change after several days of incubation as shown in **Fig. 4.3(a)**.

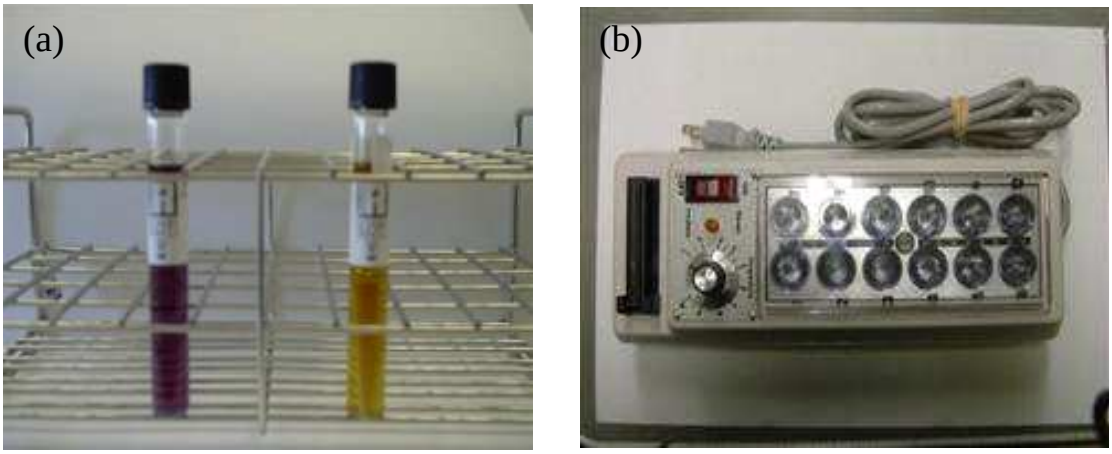

Fig. 4.3 Photograph of (a) culture tubes with Tryptic soy broth and (b) Dry bath incubator.

Raven Labs offer a Dry Bath Incubator as shown in **Fig. 4.3(b)** having features as:

- Ambient to 60°C temperature range (+/- 2°C)
- Removable, clear polycarbonate 12-well rack allows full viewing of all units at a glance for media tubes; Rack inserts into an aluminum block which maintains temperature stability
- Racks and/or blocks available for use with any Raven product
- Available in 35°C, or 55°C or a variable temperature model

4.4 Agar-plate based colony-count method

For the purpose of colony-count method, the following definition and principle should be known. Definition of colony count (culturable microorganisms): All aerobic bacteria, yeasts and moulds capable of forming colonies in or on the medium specified, under the test conditions described. Principle of colony count: Measured volumes of the sample or dilutions of the sample are mixed with molten yeast extract agar in sterile Petri dishes, and incubated under the conditions specified.

Figure 4.4 shows the steps of colony-count by spread plate method. Each of the remainder BI samples was put in 1.5 ml Brain-Heart Infusion (BHI) solution apart to obtain the original solution. Then, 0.1 ml pick-up from the original solution was diluted by adding 0.9 ml BHI solution to obtain the tenfold dilution. Also, 0.1 ml pick-up from the tenfold dilution was diluted by adding 0.9 ml BHI solution to obtain the hundredfold dilution. Later, 0.1 ml pick-up from the original solution, the tenfold dilution and the hundredfold dilution respectively was spread uniformly on the surface of a BHI agar plate. Having incubated inverted at 55 or 37°C for one day, the number of colonies formed by viable bacteria was counted. To avoid error, the average of the respectively counted number of colony forming units (CFU) from the above three solutions was used.

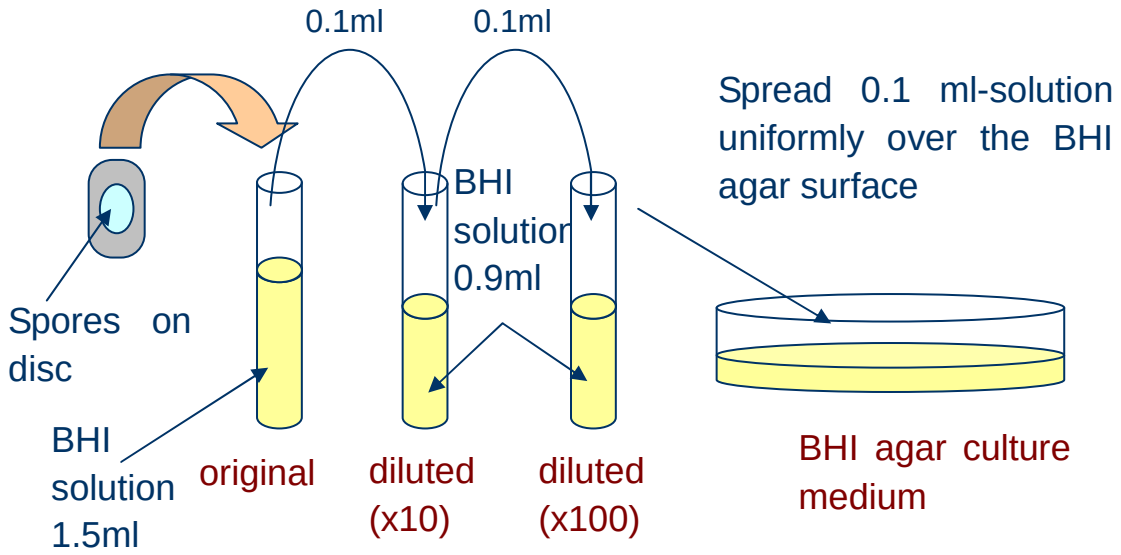

Fig. 4.4 Illustration of the steps of colony-count by spread plate method.

The number of colonies formed by viable bacteria on agar-plate (**Fig. 4.5**) is counted to know the number of CFU in the dilutions of the sample, therefore, the number of survived CFU in the sample after inactivation processing can be calculated. Decimal

reduction value (D value) is defined as the time to take a reduction of spore population by one order. The survivor data obtained by colony-count method can be plotted in a semi-logarithmic data graph. Since the plotted data roughly lie on a straight line, from the slope of the line, D value can be easily calculated.

4.5 Summary

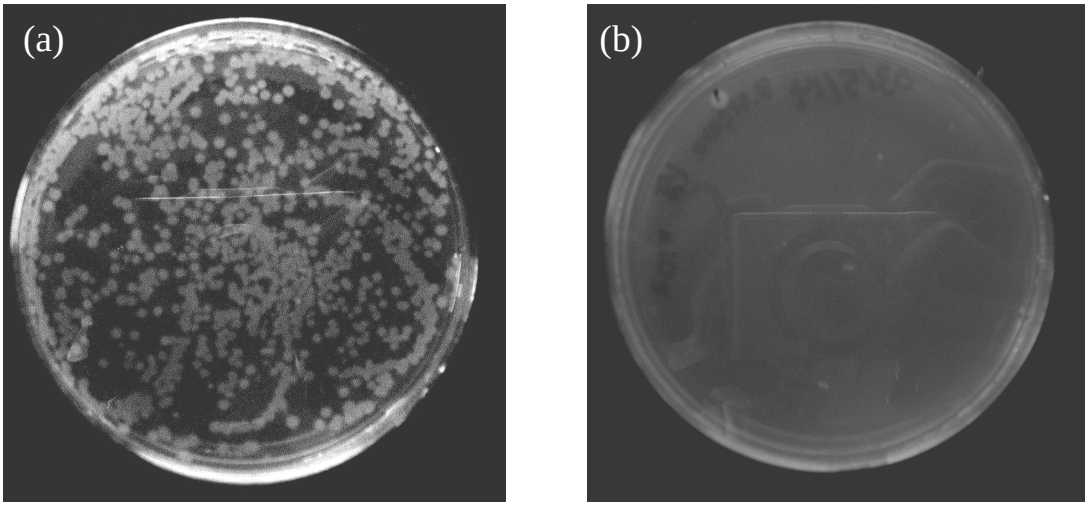

Fig. 4.5 Photographs of colonies formed on agar-plate in case of (a) after 1 min O_2 plasma irradiation and (b) after 4 min O_2 plasma irradiation.

Information on the biological indicators, the general procedure for use and the agar-plate based colony-count method have been presented in this chapter.

Thank Prof. Koide, Prof. Nagata and Mr. Uchijima for helping and instructing me how to do agar-plate based colony-count method at the microbiology laboratory of Hamamatsu University School of Medicine.

References

[1] L. J. Joslyn: Sterilization by heat. In Disinfection, Sterilization and Preservation 4th edn., ed. S. S. Block, (Philadelphia, PA: Lippincott Williams & Wilkins) pp. 495-526 (1991).

[2] H. Albert, D. J. Davies, L. P. Woodson and C. J. Soper: J. Appl. Mirobiol. **85**, 865-874 (1998).

[3] I. J. Pflug and T. E. Odlaug: J. Parenteral Sci. Technol. **40**, 242-248 (1986).

[4] Homepage of Raven Biological Laboratories Inc.

5 Low-temperature sterilization with surface-wave plasma source

5.1 Introduction

A recent approach of realizing low-temperature plasma sterilization is the utilization of microwave plasma. Examples include downstream plasma produced by microwave excitation [1-4], Duo-Plasmaline, Plasmodul and Planatron systems [5, 6], microwave-induced plasmas [7, 8], moving atmospheric microwave plasmas [9], and surface-wave plasmas [10-14]. It is also important to clarify the mechanism of plasma sterilization. Up to now, a number of studies have been devoted to make the sterilization mechanisms clear. Moisan et al. reported that UV emission was a main factor of sterilizing event in the sterilization experiments using afterglow of O_2 and N_2 mixture plasma [1-4]. They reported multi-slope characteristics of survival curves, where first, spores on the first layer were killed by UV emission, second the erosion process due to oxygen radicals occurred at slow D-value, and finally remaining survived spores were sterilized by UV emission. Typically, it took roughly 40 min to realize sterilization of 10^6 *Bacillus subtilis* spores under the optimum condition that the oxygen gas was added to nitrogen gas by 2 %. The effect of gas composition on spore mortality has been investigated by Lerouge et al. using gases such as pure O_2, O_2/CF_4, O_2/H_2, and O_2/Ar [10]. They used discontinuous microwave discharges of 30 s pulses followed by 30 s pauses. The results of scanning electron microscopy (SEM) analysis of the *Bacillus subtilis* spores showed a significant reduction in the sizes of spores by the O_2/CF_4 plasmas irradiations. It was deduced that the sterilization of the microorganism might be related to an etching process by the reactive plasma.

By using higher microwave power, we can achieve the same sterilization in a shorter treatment time. However, the risk of heat damage caused by the surface contact between the plasma and the medical instrument becomes serious, especially for plastic materials. For this study, to achieve sterilization at a low temperature of less than 70 °C, a pulse-modulated microwave system was used.

First, the preliminary experiments that tested sterilization effect with different gas species plasmas will be introduced. Next, the discharge conditions for continuous wave (CW) and pulse-modulated oxygen-discharge SWPs in sterilization of 1.5×10^6 and 3×10^6 *G. stearothermophilus* spores as a BI were studied. It was confirmed that using pulse-modulated SWPs serves to reduce the temperature of objects by roughly 10 °C, compared with that of CW SWPs. Last, some analyses of SWPs with N_2-O_2 mixture gas were carried out to make clear the mechanisms of plasma sterilization.

5.2 Experimental setup

For plasma sterilization, the BI samples used were placed in Petri dishes set on a movable substrate stage with a diameter of 20 cm, about z = 15-23 cm below the quartz vacuum window as shown in **Fig. 5.1**. During plasma irradiation, the stage temperature was monitored using a thermocouple (Custom, CT-700S Digital thermometer; Sensor: Type K -50 ~ +1200 °C) attached to the rear surface of the metal stage plate or indicated by thermo-label sheets (Nichiyu, Thermo Label 5E-50, 5E-75, 5E-100) attached to the Petri dish and covered by a piece of thin glass as shown in **Fig. 5.2**. The thin glass was used to avoid any direct contact between the plasma and the thermo-label sheet. The morphology of the spores after the plasma irradiation has been analyzed with the scanning electron microscope (SEM: Hitachi, S300N and Jeol, JSM-6360). Optical emission spectrometer (OES) measurements have been done using UV-visible spectrometer (Acton, SpectraPro 2300i) in the wavelength range of 200~800 nm. Mass spectrum has been obtained using quadrupole mass spectrometer (Pfeiffer Vacuum, Prisma™ QMS 200). A cable of optical fibers was used to transfer the optical emission transmitting from the Optopass port (z = 14 cm) to the UV-visible OES, and QMS was connected to other port (z = 14 cm) as shown in **Fig. 5.3**.

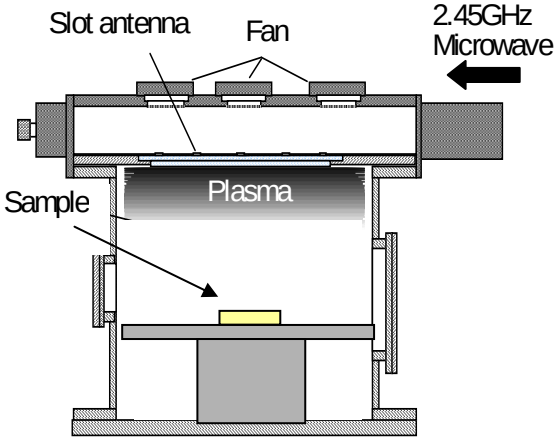

Fig. 5.1 Sample stage in the surface-wave plasma device.

Fig. 5.2 Thermo-label sheets, 5E-50 and 5E-75.

Fig. 5.3 SWP device connected with QMS and OES.

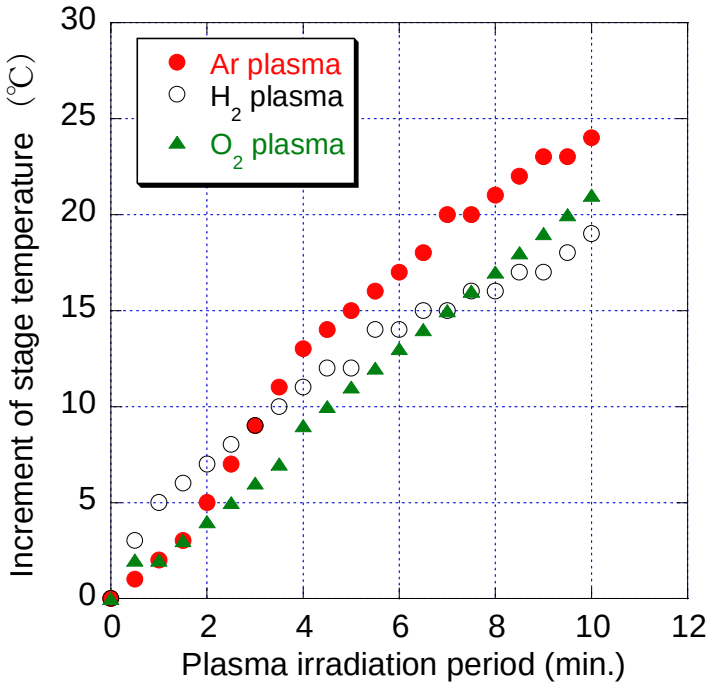

Fig. 5.4 The change in the stage temperature measured with the thermocouple versus the plasma irradiation periods for the different gas species: oxygen, hydrogen and argon. [12]

Figure 5.4 shows the change in the stage (z = 15 cm) temperature as measured using the thermocouple versus the plasma irradiation periods for the different gas species of Ar, H_2 and O_2. After a 10 min plasma discharge, the temperature increased by approximately 25 °C in all cases. Based on the thermo-label measurements, it was also shown that the surface temperature of the Petri dish was less than 55 °C after a 10 min plasma discharge. [12]

5.3 Sterilization effect of SWPs with different gas species

When our group started studying low-temperature microwave excited plasma sterilization, some preliminary experiments that tested sterilization effect with oxygen, argon, hydrogen and nitrogen plasmas were carried out, respectively. Those works have been reported in reference 11 and 12. **Figure 5.5** shows the colony count results of the *G. stearothermophilus* spores irradiated with oxygen, argon and hydrogen plasmas to compare the effect of gas species on sterilization. The discharge conditions were same: A microwave power of 750 W, a pressure of about 75 mTorr, and irradiation duration of 10 min. However, as shown in **Fig. 5.5**, for both the Ar and H_2 plasma discharges, the spores survived even after a 10 min irradiation. From this, that electrons and ions are not the primary agents in this sterilization process was deduced. Consequently, it might be the O_2 plasma that plays a role in killing the spores in this experiment. To study the shape and size of the spores before and after plasma irradiation, SEM analyses were performed. **Figure 5.6(a)** and **5.6(b)** showed the SEM images of the *G. stearothermophilus* spores after 1 min and 4 min O_2 plasma irradiation, respectively. **Figure 5.7** showed the schematic representation of a bacterial spore with its genetic material (DNA) and protecting coats surrounding it, and the changes in the spore size (erosion of the microorgansim) for all discharge durations. It was clearly shown that the length and width of the spores dramatically decreased after only a 4 min plasma irradiation. The ellipsoidal spores with a length of 1.5 μm and a width of 0.9 μm irradiated by O_2 plasma shrank to jellybean-like slender shapes. However, in the case of the Ar or H_2 plasma, it was found that the sizes and shapes of the spores were not affected by a 10 min plasma irradiation. This could be attributed to chemical etching by the oxygen radicals generated in the oxygen plasma.

Pelletier [15] had pointed out that microorganisms are in some ways similar to synthetic polymers – namely, macromolecules composed of the elements C, H, N and O; it is therefore interesting to draw parallels with the abundant literature on plasma treatment and etching of polymers. Many gases and gas mixtures can etch polymers in low-pressure plasma, the common feature being that they convert them into volatile reaction products, which are then removed by the vacuum pump [10]. Lerouge et al. [10] also pointed out that oxygen-containing gases or gas mixtures used for plasma sterilization were chosen on the basis of earlier literature on sterilization and on polymer etching. Especially, oxygen plasma is used widely for the removal of organic materials – for example, for the removal of photoresists after lithographic operations in microelectronics [16] – and the etch rate is strongly correlated to the concentration of

oxygen atoms produced by the dissociation of O_2 [17]. Although hydrogen plasma was also used to etch diamond film and polymers, Lerouge et al. [10] pointed out that H_2 was added on O_2/H_2 (20/80%) to increase the output of vacuum ultraviolet (VUV) radiation by the plasma. Moisan et al. [3] assumed the erosion of the microorganism, atom by atom, through etching stemming from the adsorption of reactive species from the plasma on the microorganism with which they subsequently undergo chemical reactions to form volatile compounds (spontaneous etching). The reactive species can be atomic and molecular radicals, for example, O and O_3, respectively, and excited molecules in a metastable state, for example, the $^1O_2$ singlet state. This chemistry, which occurs under thermodynamic equilibrium conditions, yields small molecules (e.g., CO_2, H_2O) that are the final products of the oxidation process. [15] Such chemical reactions with atomic oxygen free radicals can be found in the literature on plasma etching of polymers [18] as listed below:

$$\text{-C-C- + O:} \rightarrow \text{-}\dot{\text{C}}\text{-C- + }\dot{\text{O}}\text{H} \qquad \text{-C=C- + O:} \rightarrow \text{-}\dot{\text{C}}\text{=C- + }\dot{\text{O}}\text{H}$$

$$\text{RH + }\dot{\text{O}}\text{H} \rightarrow \dot{\text{R}} + \text{H}_2\text{O} \qquad \text{RH + O:} \rightarrow \dot{\text{R}}' + \text{R}''\dot{\text{O}}$$

$$\text{-C=C- + O:} \rightarrow \begin{array}{c}\dot{\text{O}}\\ |\\ \text{-}\dot{\text{C}}\text{-C-}\end{array} \qquad \begin{array}{c}\dot{\text{O}}\\ |\\ \text{-}\dot{\text{C}}\text{-C-}\end{array} \rightarrow \text{-C=O + }\dot{\text{C}}\text{-}$$

Only addition of oxygen to the unsaturated molecule, leading to a saturated radical, results in a weakened C-C bond, therefore, scission processes can occur leading to volatile etch products (such as CO and CO_2) [18].

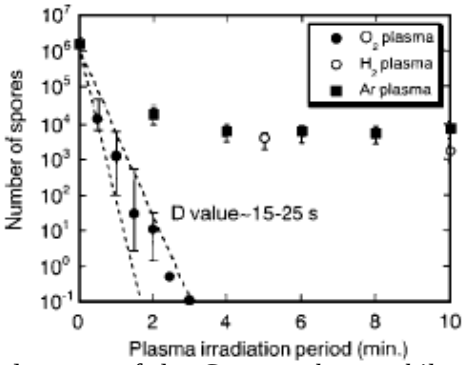

Fig. 5.5 Survival curves of the *G. stearothermophilus* spores irradiated by the oxygen, hydrogen and argon surface-wave plasmas. [12]

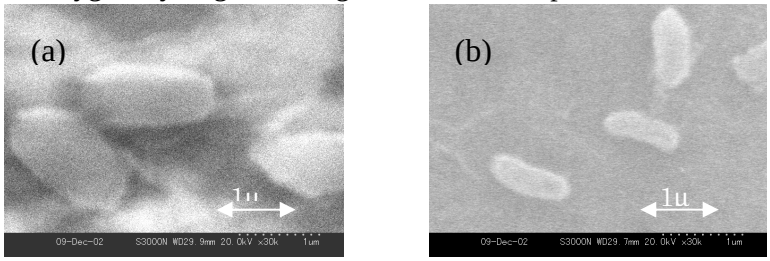

Fig. 5.6 SEM images of *G. stearothermophilus* spores after (a) 1 min and (b) 4 min oxygen plasma irradiation. [11]

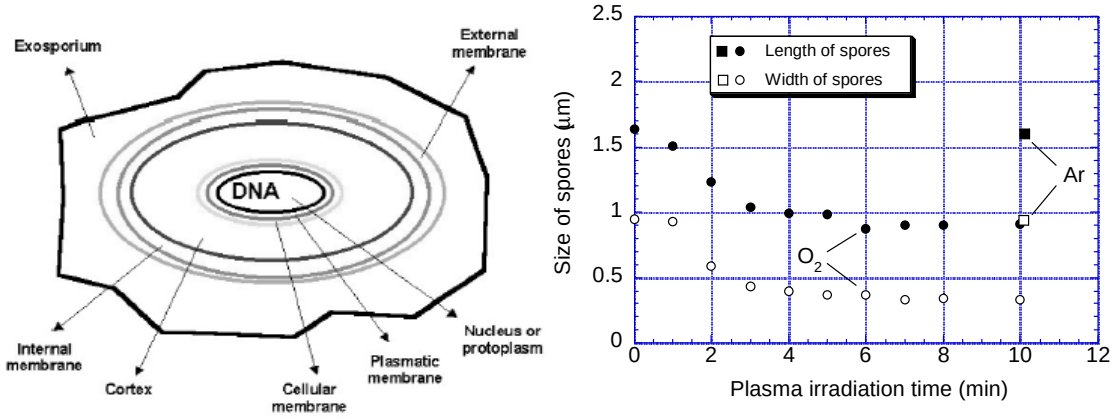

Fig. 5.7 Schematic representation of a bacterial spore with its genetic material (DNA) and protecting coats surrounding it [3]; sizes of spores versus O_2 and Ar plasma irradiation time [11].

In order to examine the effect of the UV radiation emitted from the O_2 plasma, a thin quartz plate with a thickness of 3 mm was placed over the Petri dish to block any charged or neutral particles, while only UV photons with wavelength, λ, greater than 160 nm were able to transmit the quartz plate. However, after a 10 min O_2 plasma discharge, the spores were still viable and had not changed their size or shape. From these results, it would appear that UV radiation is not necessary for this sterilization to be effective in the O_2 plasma experiment. However, it could be the case that, as the radicals approached the Petri dish, UV photons might be generated. The further investigation on the role of UV photons performed using OES will be described in section 5.5.

To examine the effect of oxygen radicals on sterilization, a grounded stainless-steel plate with 4-mm-diameter holes on a stage located 8 cm below the quartz window. Although the electrons and ions were blocked by this punched plate, the neutral radicals could pass through the plate, together with any UV photons that might have a weak effect on sterilization. The survival curve of the *G. stearothermophilus* spores in a Petri dish located 7.5 cm below the punched plate was plotted in **Fig. 5.8**. The number of colony forming units (CFU) for different plasma discharge periods is shown. From the slope of the survival curve, the D value was estimated roughly 30-45 s. The SEM images of the original spores are shown in **Fig. 5.9(a)**, while the images after a 10 min radical irradiation are shown in **Fig. 5.9(b)**, where the changes of spores shape and size are similar with the one as shown in **Fig. 5.6(b)**. Hence, we concluded that the primary sterilization species were the oxygen radicals produced by the surface-wave sustained oxygen plasma. An analogous experiment using nitrogen plasma discharge was performed to study its effect on sterilization. A preliminary result of the colony count was also plotted in **Fig. 5.8**. It was found that the spores were sterilized after a 4

min discharge, where the D value was roughly estimated as 30-40 s.

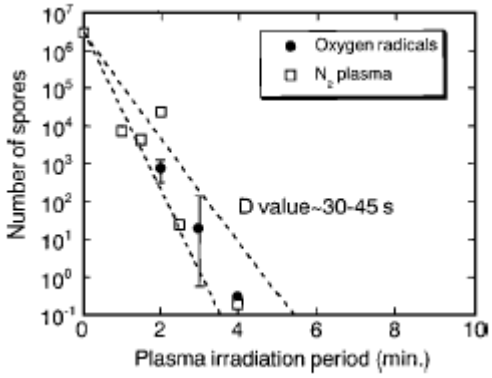

Fig. 5.8 Survival curves of the *G. stearothermophilus* spores irradiated by the oxygen radicals and nitrogen surface-wave plasmas. [12]

Furthermore, it is interesting to note that the spore shapes as shown in **Fig. 5.10(b)** were almost identical to the original ones as shown in **Fig. 5.10(a)** after a 5 min nitrogen plasma irradiation, which differs from the findings with oxygen plasma or oxygen radical irradiation. This result could possibly be caused by UV photons emitted by the nitrogen plasma. Similar experiments have been done by Moisan's group in the microwave plasma with N_2-O_2 gas mixtures and they showed that UV emission ranging from 250 to 320 nm was strongly enhanced by adding 2 % of O_2 gas content into N_2 plasma [2-4]. To confirm the role of UV photons emitted directly from the plasma or those generated when the radicals approach the Petri dish, an examination using UV emission spectroscopy will be presented in section 5.5.

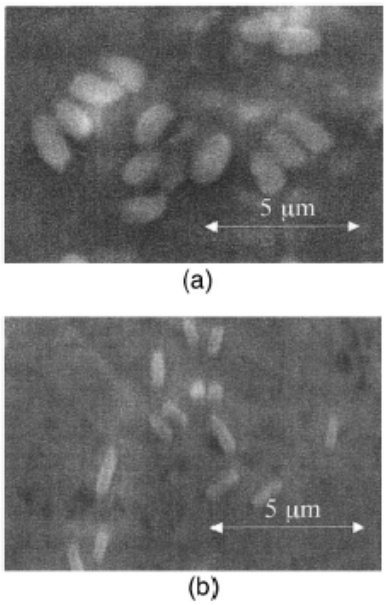

Fig. 5.9 SEM images of *G. stearothermophilus* spores (a) before and (b) after 10 min oxygen radical irradiation. [12]

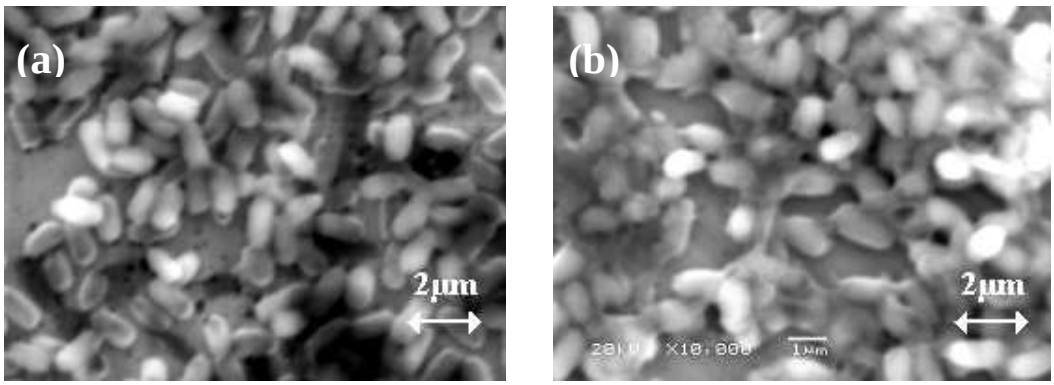

Fig. 5.10 SEM images of *G. stearothermophilus* spores (a) without plasma irradiation and (b) after 5 min nitrogen plasma irradiation.

5.4 Discharge conditions for CW and pulse-modulated oxygen SWPs in low-temperature sterilization

Since that a six-order magnitude reduction of colony forming units (CFU) could be achieved after only a 3 min irradiation with low-pressure oxygen SWP has been reported in reference 10, in this section, the discharge conditions required for low-pressure CW and pulse-modulated oxygen SWPs in low-temperature sterilization have been investigated.

The characteristics of continuous SWP and pulse-modulated SWP [13] have been described in section 2.3. Consequently the survival curves measured using agar-plate based colony-count method will be first presented, then criteria of plasma discharges for CW and pulse-modulated SWP sterilizations will be presented.

5.4.1 Survival curves measured using colony-count method

Here, the BIs used were *G. stearothermophilus* spores with population of 1.5×10^6, which were spread on a small stainless steel disc and placed in a Petri dish set about 15 cm below the quartz window. O_2 discharges were generated at a pressure of 50-60 mTorr with an O_2 gas flow rate of 200 sccm. The survival curves of *G. stearothermophilus* spores (measured with a colony-count technique) for CW and pulsed-microwave plasma discharges are shown in **Figs. 5.11(a)** and **5.11(b)**, respectively. In the case of pulse-modulated microwave plasma discharge, the plasma irradiation period (or total processing period) is the sum of the total microwave on-time and the total microwave off-time. It can be seen that the reduction in spores is almost

linear for both the CW and pulse-modulated SWP sterilizations. For microwave pulses with an instantaneous power of 2.0-2.2 kW and an on- and off-duration of 10 μs, the D value for pulse-modulated SWP sterilization were found to be 21-27 s, similar to those obtained for CW sterilization (a CW power of 750 W, D values of 15-25 s).

Depending upon the instantaneous power, different survival curves were observed and so the criteria for sterilization could be studied by scanning two parameters: the instantaneous power, and the net on-duration of the microwave pulses.

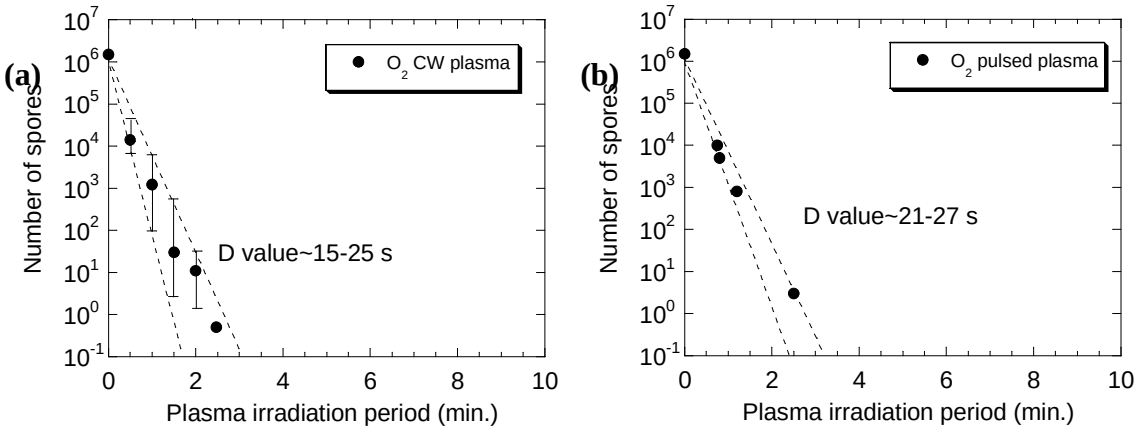

Fig. 5.11 Comparison of survival curves of CW and pulsed microwave plasma sterilization. (a) CW and (b) pulsed microwave.

5.4.2 Criteria of plasma discharges for CW-and pulse-modulated SWP sterilizations

This subsection discusses the experimental results of the CW-SWP sterilization under discharge conditions of a pressure of about 30-70 mTorr and a gas flow rate of 200 sccm. *G. stearothermophilus* spores with a population of 1.5×10^6 were placed on the stage about 15 cm below the quartz window and oxygen plasmas were produced using microwave powers of 500 W, 750 W, 1000 W, 1500 W and 2000 W. Two BI samples were put in the Petri dish on the stage for each plasma irradiation experiment. One sample was to be used for the culture solution color test after incubation and the other was to be used for colony counting.

The temperature of the Petri dish increased from 20 °C at room temperature to 60 °C after 130 s of plasma discharge when excited by a CW power of 1000 W, or 50 s of plasma discharge when excited by a CW power of 1500 W. In **Fig. 5.12**, the temperature in the Petri dish as monitored by the thermo-label sheets for the CW discharge is shown together with the temperature for the pulse-modulated SWPs, under the same microwave power of 900 W-1 kW (average power for CW, while instantaneous power for pulse-modulated SWP).

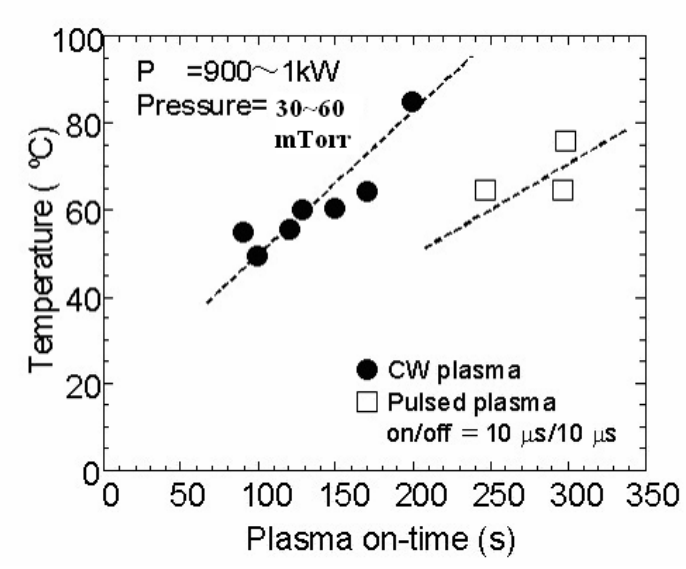

Fig. 5.12 Stage temperature versus net plasma processing time.

The discharge conditions required for CW-SWP sterilization are shown in **Fig. 5.13**. The plasma irradiation period was varied from 30 sec by 10-sec steps, only under the conditions that CW microwave power was kept at 1000 W and 1500 W. Sterilization was confirmed for samples which were irradiated for 50 s or longer with a CW power of 1000 W and for 40 s or longer with a CW power of 1500 W. These results show that the BIs were sterilized using CW oxygen plasma under the following conditions: a) CW power should not be less than 700 W; b) the plasma irradiation period should not be less than 40 sec; c) a total microwave energy of at least 50 kJ is needed.

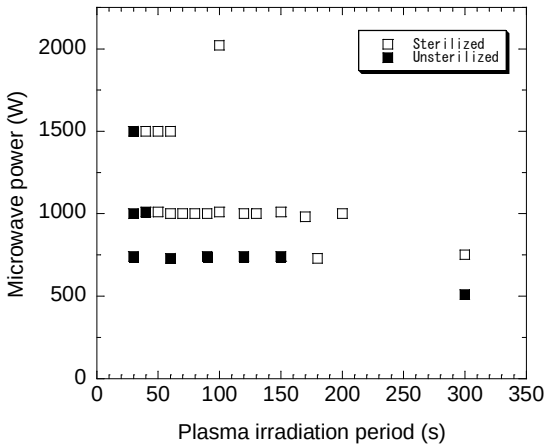

Fig. 5.13 Sterilization criteria of plasma discharge conditions between CW microwave power and total plasma irradiation time.

In reference 11, that BIs could not be sterilized by argon plasma excited by a CW power of 700 W was reported. An interesting experiment was carried out to examine the effects of the oxygen radicals and UV radiation emitted from the oxygen plasma

during sterilization. It was suggested that the spores were mainly killed by chemical reactions with oxygen radicals, as opposed to the UV radiation. Analyses of SWPs with different gas species will be presented in section 5.5 in detailed.

From the irradiation of oxygen plasma excited by pulse-modulated microwave power, we tested several different parameter conditions using this system. The pulsed modulation frequency of the pulsed operation, the microwave on-duration, the instantaneous microwave power and the total microwave on-time were all varied. **Figure 5.14** shows the sterilization effectiveness for a variety of conditions. From these results, it can be concluded that the relationship between the minimum instantaneous microwave power and the total microwave on-time needed for pulse-modulated microwave plasma sterilization can be fitted by a curve which roughly corresponds to a microwave energy of 200 kJ. Qualitatively, it can be understood that the sterilization criteria is related to the discharge conditions, such as the product of radical density and net on-duration, for instance. **Figure 5.14** suggests such a criterion, but a quantitative understanding has not been sufficiently established yet.

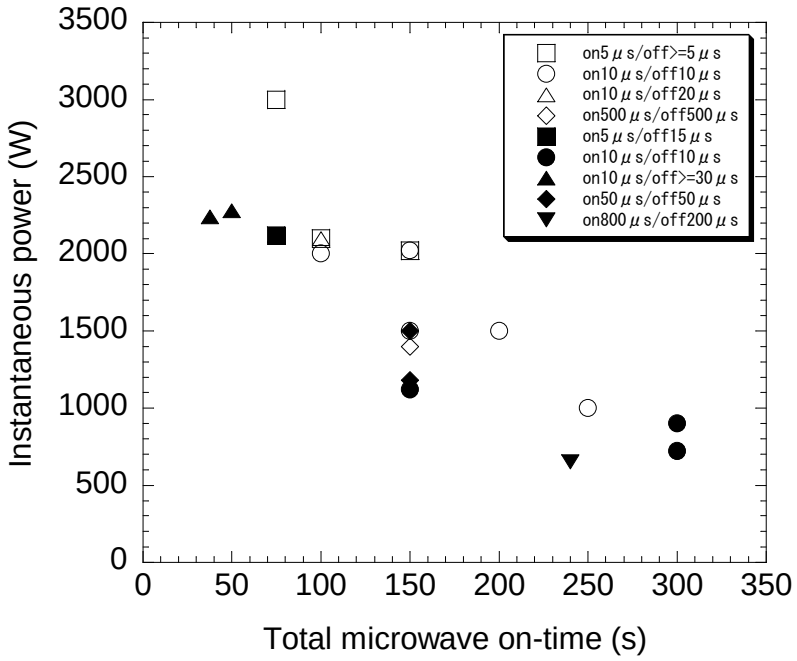

Fig. 5.14 Sterilization criteria of plasma discharge conditions between pulse-modulated microwave instantaneous power and total microwave on-time. Here open symbols indicate sterilized results and solid symbols indicate non-sterilized results.

Figure 5.15 shows a comparison of sterilization results from the relationship between the total on-time of the microwave plasma versus the on-duration of microwave pulses during the pulse-modulated oxygen plasma treatment. The discharge conditions were a pressure of about 120-130 mTorr and a gas flow rate of 200

sccm. *G. stearothermophilus* spores with a population of 3×10^6 were placed on the stage about 23 cm below the quartz window. From this figure, it was found that all the BI samples were sterilized by the pulse-modulated oxygen plasma when the total microwave on-time was longer than 120 s, even when the on-duration per pulse was 10 μs. Based on the thermo-label sheet measurements, it can be shown that the surface temperature of the Petri dish during the 300 s total processing period, that is, the sum of 150 s total microwave on-time and 150 s total microwave off-time, was always less than 70°C. When the total microwave on-time was much shorter than 120 s, we found that a longer on-duration per pulse was required for successful sterilization. The reason for this could be that the total saturating period of ion saturation current increases with on-duration per pulse, when the total microwave on-time is fixed. During a longer saturating period of the ion saturation current, oxygen radicals, which are considered key agents in oxygen plasma sterilization, can be generated.

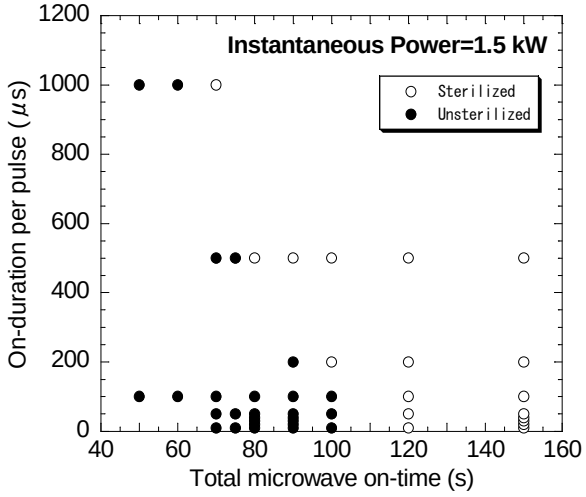

Fig. 5.15 Experimental results of sterilization between on-duration per pulse and total microwave on-time.

5.4.3 Conclusion

This section describes the effects on low-temperature plasma sterilization using CW and pulse-modulated surface-wave excited oxygen plasma. At a discharge pressure of 30~70 mTorr, and a O_2 gas flow rate of 200 sccm, BI samples with 1.5×10^6 *G. stearothermophilus* spores were successfully sterilized when irradiated for 50 s or longer with a CW power of 1000 W, and when irradiated for 40 s with a CW power of 1500 W. When using pulse-modulated oxygen plasma at a discharge pressure of about 120-130 mTorr, and an O_2 gas flow rate of 200 sccm, BI samples with 3×10^6 *G. stearothermophilus* spores were successfully sterilized when the total microwave on

time was longer than 120 s and the instantaneous power was kept at 1500 W.

5.5 Characteristics of SWPs with air-simulated N_2-O_2 mixture gas for low-temperature sterilization

We have studied the discharge conditions required for CW and pulse-modulated oxygen SWPs in low-temperature sterilization. In this section, we aim at investigating the characteristics of low-temperature sterilization using air-simulated gas discharge plasma sustained by the surface-wave. The sterilization mechanisms of SWP with air-simulated gas mixture by using SEM analysis of plasma-irradiated spores, OES and QMS measurements of the plasmas will be discussed. [14]

In the present experiments, we tested pure O_2, pure N_2 and air-simulated mixture gas (N_2 = 80 sccm and O_2 = 20 sccm) in the plasma discharges at a pressure of about 60-70 mTorr with total gas flow rate of 100 sccm. BIs of *G. stearothermophilus* with population of 3×10^6 deposited on an oblong polished stainless steel disc were placed in a Petri dish set on the stage located about z = 23 cm. In the plasma production, the incident microwave power of 750 W was introduced to produce the surface-wave plasma, while the reflected power was minimized to typically 20-30 W.

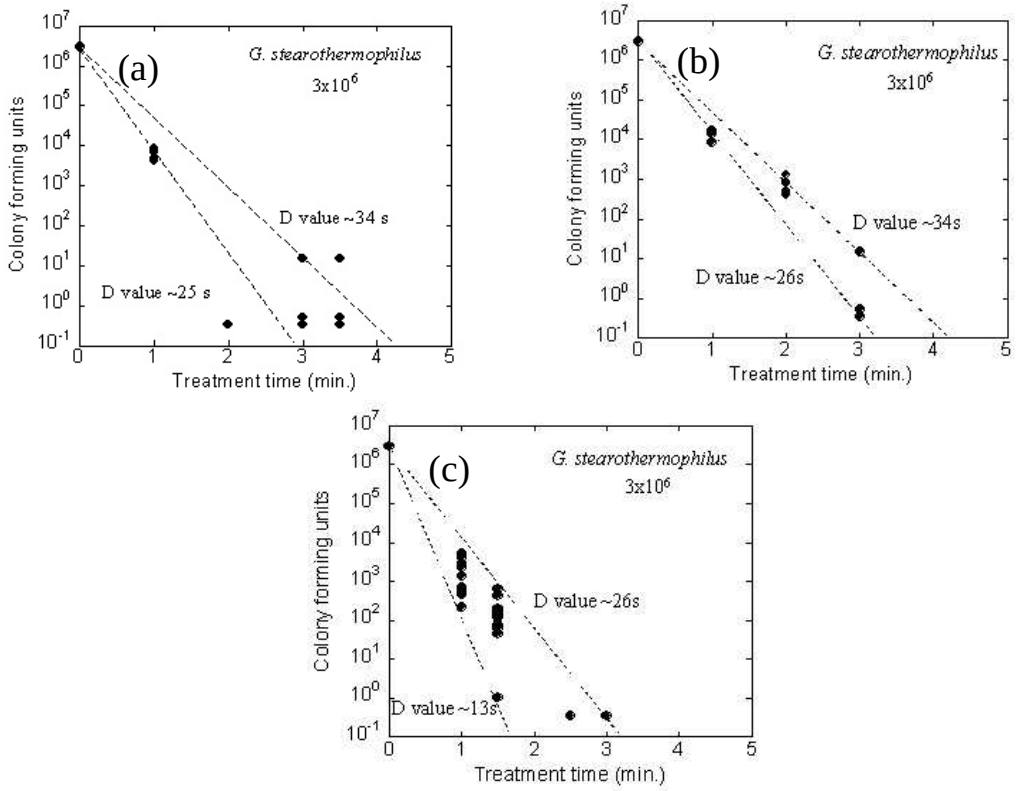

Fig. 5.16 Survival curves measured with the colony counting method in cases of (a) pure O_2, (b) pure N_2 and (c) air-simulated N_2-O_2 mixture gas discharge plasmas.

To study the survival curves of spores with the agar colony-count method, we varied the plasma treatment time from zero to 5 min. During plasma irradiation, the thermo-label sheets were used to measure the environmental temperature of BI samples.

The survival curves measured with the agar colony-count method are shown in **Fig. 5.16** in cases of pure O_2, pure N_2 and air-simulated N_2-O_2 mixture gas discharge plasmas. It was found that the 3.0×10^6 spores were killed after about 4 min plasma discharges with roughly linear slopes for all the cases. Here, we evaluated the D value defined as the time needed to reduce the survival population of spores by one order. From **Fig. 5.16(a)** and **(b)**, we found that D values in the cases of pure O_2 and pure N_2 gas discharges were almost the same and evaluated to be roughly 25-34 s. In each discharge, the thermo-label sheets showed the temperature was around 60-65 °C after 3 min plasma discharge.

In the O_2 plasma, we have concluded that the main mechanism was the chemical etching due to the oxygen radicals because of significant reduction of spore sizes [11, 12]. On the other hand, we speculated that sterilization for the pure N_2 plasma was mainly due to the UV light emission radiated from N_2 plasma, because the killed spores were not changed in size at all. Survival curve in case of the air-simulated N_2-O_2 mixture gas discharge plasma is also shown in **Fig. 5.16(c)**. From its slope, we found that D-value was roughly 13-26 s, which was better than those of pure O_2 and pure N_2 plasma irradiations. Therefore, we believe that the spores can be sterilized using the low-pressure air discharge plasma in the future sterilizer.

Optical emission spectra were measured using the optical emission spectroscopy. In the present measurement, the minimum observable wavelength is 200 nm due to the limitation of monochromator, so that we mainly study in the wavelength between 200-400 nm. **Figure 5.17** shows the spectra in cases of pure O_2, pure N_2 and air-simulated N_2-O_2 mixture gas discharge plasmas. As shown in **Fig. 5.17(b)**, several strong lines at 282.0, 297.7, 313.6, 315.9, 337.1, 357.7 nm were originated from the second positive systems ($C^3\Pi_u \rightarrow B^3\Pi_g$) of N_2 molecules in pure N_2 plasma. As shown in **Fig. 5.17(c)**, there exist strong peaks in the wavelength between 200~280nm in N_2-O_2 mixture gas discharge plasma. Several UV emissions at 214.1, 226.9, 237.0, 247.9, 258.8 nm were considered originated from NO γ system ($A^2\Sigma^+ \rightarrow X^2\Pi$). It has been found that the emission intensity in the UV region is extremely large in pure N_2 and air-simulated N_2-O_2 mixture gas discharge plasmas compared with the pure O_2 plasma. Although we did not measure the absolute intensities of the UV emission, they might play a role in sterilizing the spores in addition to N_2 positive system in the wavelength region of 300-400 nm and the etching process due to oxygen radicals.

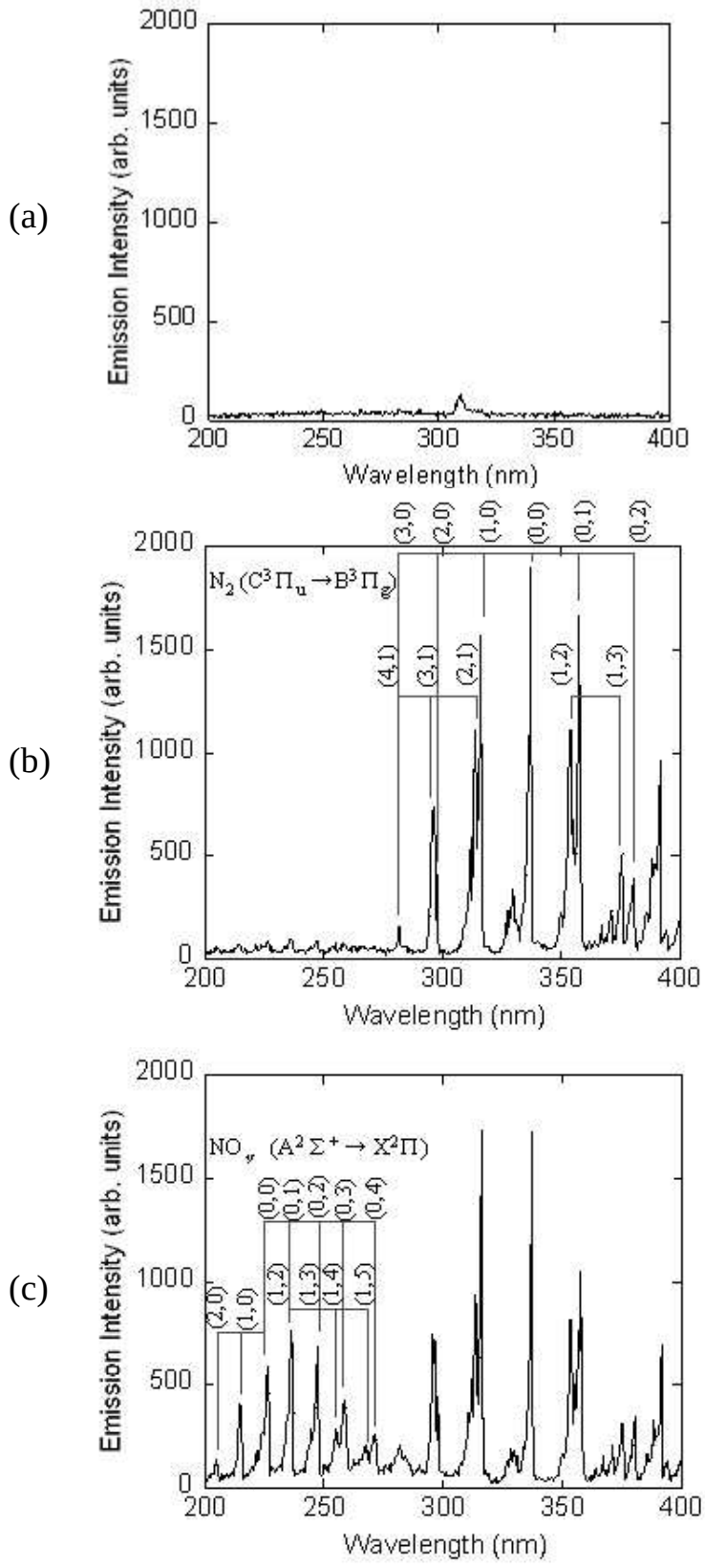

Fig. 5.17 Optical emission spectra in wavelength between 200~400 nm in cases of (a) pure O_2, (b) pure N_2 and (c) air-simulated N_2-O_2 mixture gas discharge plasmas.

Furthermore, we should take into account of the sterilizing effects due to several N atomic (N I) lines in the wavelengths between 113-175 nm and N_2 bands between 140-175 nm [19]. To examine the effect of these emission lines on the sterilization, we carried out the comparison experiment using a LiF plate and a fused quartz plate as optical filters. **Figure 5.18** shows the schematic drawing of the experimental setup to compare the role of UV emission in the wavelength region of shorter than 200 nm. We placed LiF thin plate and quartz thin plate with each thickness of 2 mm on the sample holders for BIs. One sample holder was used without any top plate, so that the all of the UV emission can irradiate the spore sample. The lower limit of wavelength at 50 % transmittance is roughly ~120 nm for LiF plate and ~180 nm for fused quartz plate, respectively. The maximum transmittances of LiF and quartz plate are about 90 % or higher. In the present experiment, we used nitrogen plasma to examine the effect of UV emission of shorter wavelength on sterilization. Plasma discharge conditions were same as the previous experimental conditions, except that the BIs were set inside the metal cylinder (sample holder) with about 10 mm in height. **Figure 5.19** shows the results of survival curves of three samples. Here, it was noted that the slopes of the colony forming units versus treatment time became worse than those shown in **Fig. 5.16(b)**. The D values estimated by the second slope were roughly 2.4-3.7 min, that is to say 144-222 s, as around six times longer than those in **Fig. 5.16(b)**. This might be due to that the samples were set on the bottom inside the metal cylinder, so that the UV emissions were allowed to enter only from the upper open area of cylinder. As seen in **Fig. 5.19**, one can not clearly distinguish among three samples. It suggests that the effect of UV emission in the wavelength shorter than 200 nm might be not so significant in the present sterilization process using surface-wave excited nitrogen plasma.

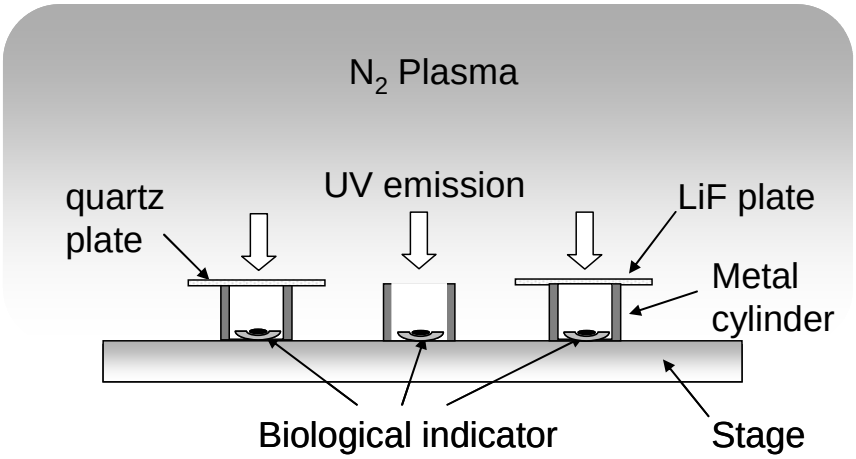

Fig. 5.18 Schematic drawings of three samples: LiF thin plate and quartz thin plate were used as filter on the top, and open without top plate.

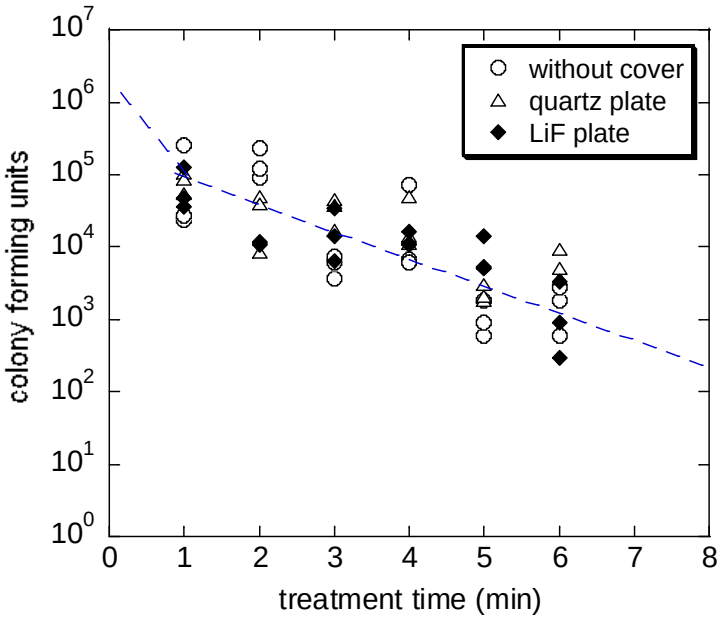

Fig. 5.19 Survival curves measured with the colony counting method in cases of LiF plate, quartz plate and air-simulated N_2-O_2 mixture gas discharge plasmas.

Figure 5.20 show the spectra in cases of different O_2 percentage added to N_2-O_2 mixture gas discharge plasmas as (a) O_2: 10 sccm + N_2: 90 sccm, (b) O_2: 20 sccm + N_2: 80 sccm, (c) O_2: 40 sccm + N_2: 60 sccm and (d) O_2: 60 sccm + N_2: 40 sccm. It has been found that the emission intensity at certain wavelength in the UV region changed with the added O_2 percentage.

To conclude the relations between the changes of emission intensity at certain wavelength and the O_2 percentage as shown in **Fig. 5.20**, the UV intensity at 237.0 nm originated from the NO γ system ($A^2\Sigma^+ \rightarrow X^2\Pi$), at 297.7 nm and 337.1 nm originated from the second positive systems ($C^3\Pi_u \rightarrow B^3\Pi_g$) of N_2 molecules in N_2-O_2 plasma as a function of the O_2 percentage added to N_2-O_2 mixture gas have been investigated as shown in **Fig. 5.21**. **Figure 5.21(a)** showed that the UV intensity at 237.0 nm originated from the NO γ system ($A^2\Sigma^+ \rightarrow X^2\Pi$) achieved its maximum value while at 10~20% O_2. **Figure 5.21(b)** and **(c)** showed that the UV intensity at 297.7 nm and 337.1 nm originated from the second positive systems ($C^3\Pi_u \rightarrow B^3\Pi_g$) of N_2 molecules decreased with the increase of the O_2 percentage. These results suggest that in air the O_2 percentage is optimum for sterilization. So that, we tested low-pressure air discharge plasma sustained by the 2.45 GHz surface-wave and confirmed a rapid sterilization with the actual air discharge after about 4 min irradiation at temperature about 65 °C.

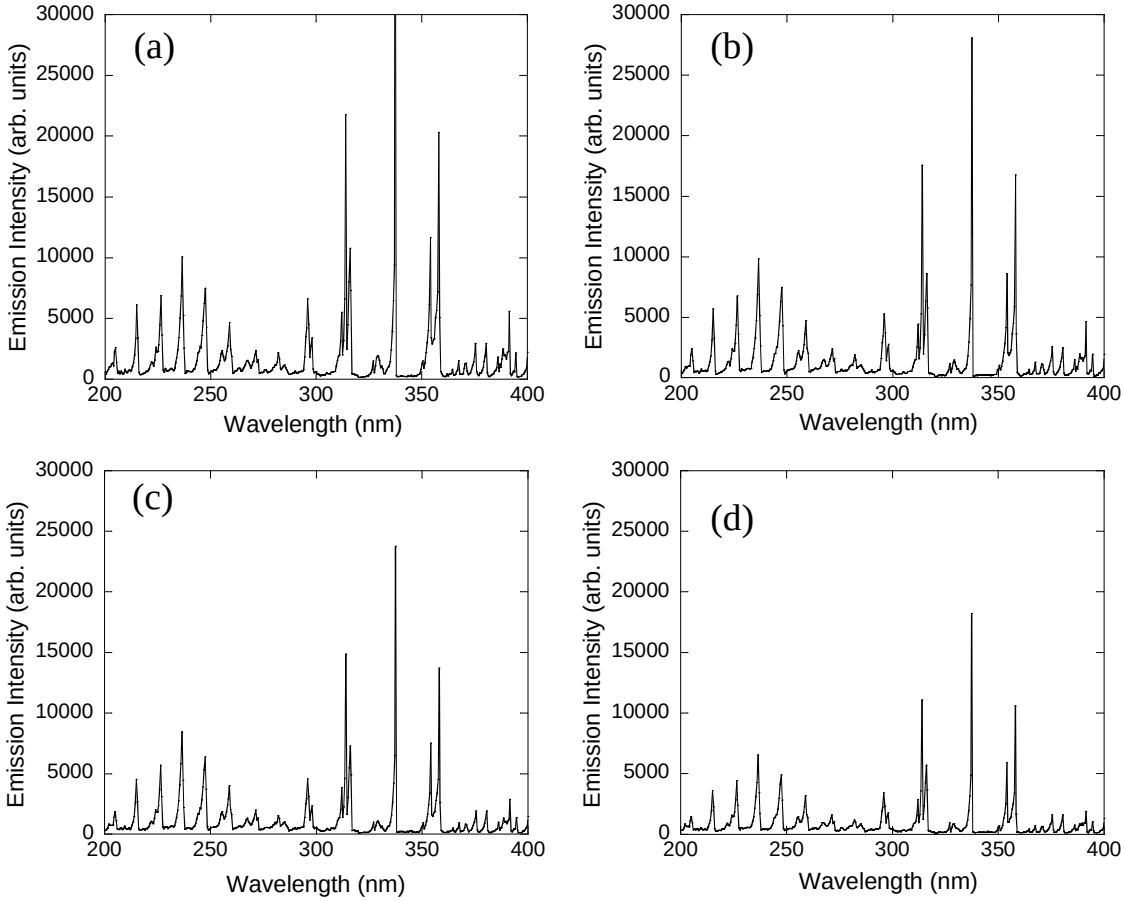

Fig. 5.20 Optical emission spectra in cases of (a) O_2: 10+N_2: 90 sccm, (b) O_2: 20+N_2: 80 sccm, (c) O_2: 40+N_2: 60 sccm and (d) O_2: 60+N_2: 40 sccm in N_2-O_2 mixture gas plasmas.

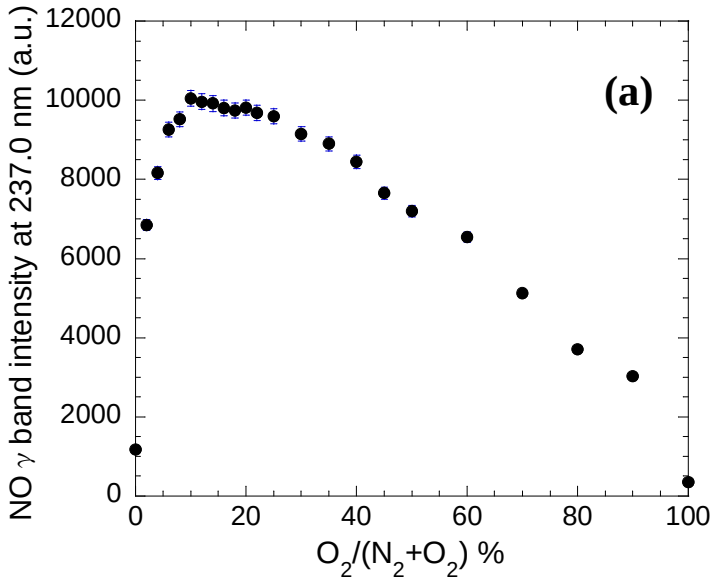

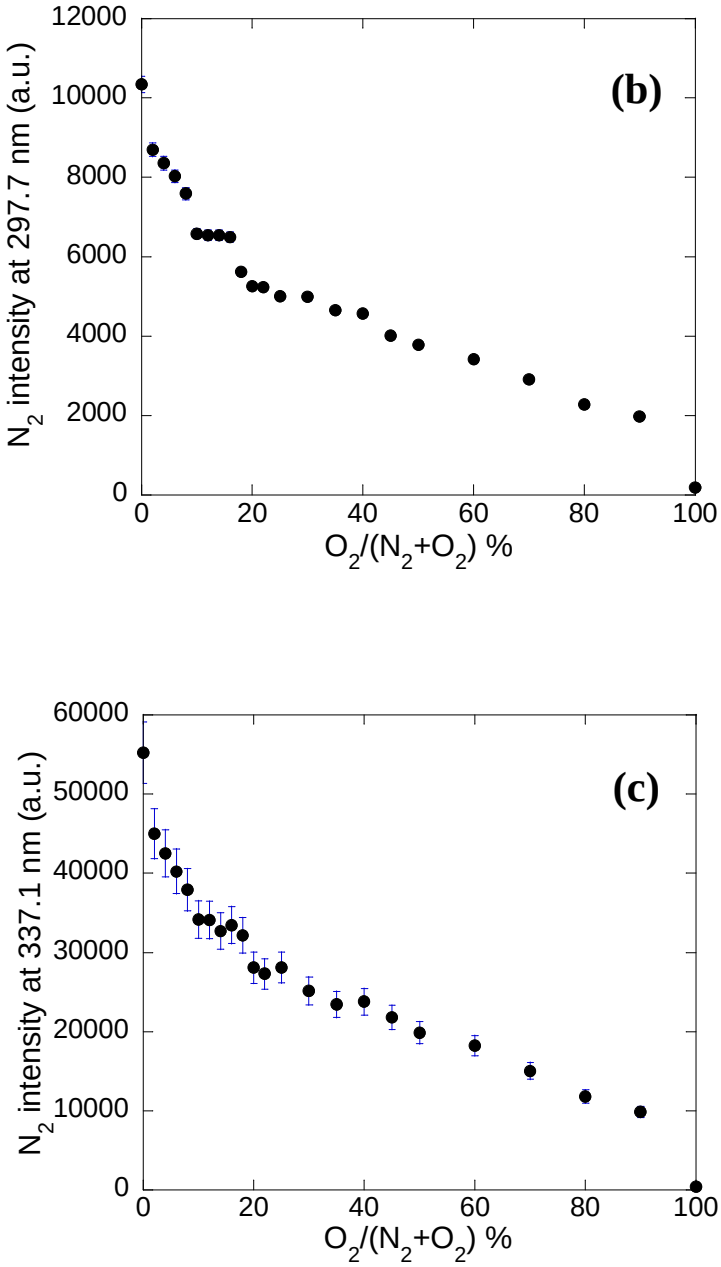

Fig. 5.21 Measured intensity at (a) 237.0 nm, (b) 297.7 nm and (c) 337.1 nm in the N_2-O_2 plasmas as a function of the added O_2 percentage.

To confirm the existence of NO in the N_2-O_2 mixture gas discharge plasmas, quadrupole mass spectrometry (QMS) was also carried out to obtain mass spectrum (mass number between 0-50) of air-simulated N_2-O_2 mixture gas discharge plasmas as shown in **Fig. 5.22**, after the discharge became stable. It proved that NO (mass=30) existed in air-simulated N_2-O_2 mixture gas discharge plasmas.

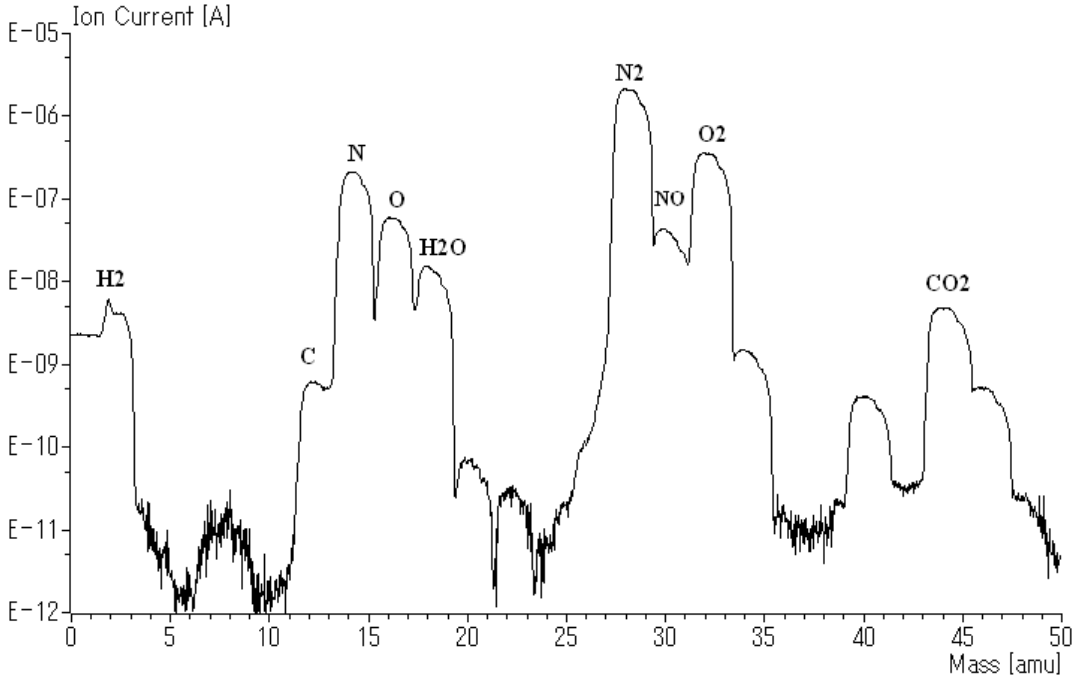

Fig. 5.22 Mass spectrum of air-simulated N_2-O_2 mixture gas discharge plasmas.

5.6 Summary

In this chapter, we have presented an experimental study on low-temperature sterilization with low-pressure large-area surface-wave plasmas.

First, the preliminary experiments that tested sterilization effect with different gas species plasmas were carried out. We presented the experimental results on sterilization using argon, hydrogen, oxygen and nitrogen plasmas excited by surface-waves. It was found that oxygen and nitrogen plasmas were effective for low-temperature sterilization, however, the BIs were not sterilized by argon and hydrogen plasmas.

Next, the discharge conditions for continuous wave (CW) and pulse-modulated oxygen-discharge SWPs in sterilization of 1.5×10^6 and 3×10^6 *G. stearothermophilus* spores as a BI were studied. It was confirmed that using pulse-modulated SWPs serves to reduce the temperature of objects by roughly 10 °C, compared with that of CW

SWPs. At a discharge pressure of 30~70 mTorr, and a O_2 gas flow rate of 200 sccm, BI samples with 1.5×10^6 *G. stearothermophilus* spores were successfully sterilized when irradiated for 50 s or longer with a CW power of 1000 W, and when irradiated for 40 s with a CW power of 1500 W. When using pulse-modulated oxygen plasma at a discharge pressure of about 120-130 mTorr, and an O_2 gas flow rate of 200 sccm, BI samples with 3×10^6 *G. stearothermophilus* spores were successfully sterilized when the total microwave on time was longer than 120 s and the instantaneous power was kept at 1500 W.

Last, some analyses of SWPs with air-simulated N_2-O_2 mixture gas for sterilization of 3×10^6 *G. stearothermophilus* spores as a BI were carried out to make clear the mechanisms of plasma sterilization. It has been found that the main physical mechanisms of air-simulated plasma sterilization are the chemical etching effect due to the oxygen radicals and UV emissions from the N_2 second positive system and NO γ system in the range of 200-400 nm. Low-pressure air discharge plasma sustained by the 2.45 GHz surface-wave was realized and a rapid sterilization with the actual air discharge after about 4 min irradiation was confirmed. The present experimental results supported the feasibility to utilize air as carrier gas in the future environmentally-friendly plasma sterilizer.

References

[1] M. Moisan, J. Barbeau, S. Moreau, J. Pellettier, M. Tabrizian and L'H. Yahia: Int. J. Pharmaceutics **226**, 1-21 (2001).

[2] N. Philip, B. Saoudi, M. C. Crevier, M. Moisan, J. Barbeau and J. Pelletier: IEEE Trans. Plasma Sci. **30**, 1429 (2002).

[3] M. Moisan, J. Barbeau, M. C. Crevier, J. Pelletier, N. Philip, and B. Saoudi: Pure Appl. Chem. **74**, 349-358 (2002).

[4] M. Moisan, B. Saoudi, M. C. Crevier, N. Philip, E. Fafard, J. Barbeau and J. Pelletier: Conf. Proc. Of 5th Int. Workshop Microwave Discharges: Fundamentals and Applications (Greifswald, Germany), pp.210-221 (2003).

[5] J. Feichtinger, A. Schulz, M. Walker, U. Schumacher: Surf. Coat. Technol. **174-175**, 564-569 (2003).

[6] J. Schneider, K. M. Baumgartner, J. Feichtinger, J. Kruger, P. Muranyi, A. Schulz, M. Walker, J. Wunderlich, U. Schumacher: Surf. Coat. Technol. **200**, 929 (2005).

[7] B. J. Park, D. H. Lee, J.-C. Park, I.-S. Lee, K.-Y. Lee, S. O. Hyun, M.-S. Chun,

K.-H. Chung: Phys. Plasma **10**, 4539-4544 (2003).

[8] K.-Y. Lee, B. J. Park, D. H. Lee, I.-S. Lee, S. O. Hyun, K.-H. Chung, J.-C. Park: Surf. Coat. Technol. **193**, 35-38 (2005).

[9] J. Ehlbeck, A. Ohl, M. Maas, U. Krohmann, T. Neumann: Surf. Coat. Technol. **174-175**, 493-497 (2003).

[10] S. Lerouge, M. R. Wertheimer, R. Marchand, M. Tabrizian, L'H. Yahia: J. Biomed. Mater. Res. **51**, 128-135 (2000).

[11] M. Nagatsu, F. Terashita, Y. Koide: Jpn. J. Appl. Phys. **42**, L856-L859 (2003).

[12] M. Nagatsu, F. Terashita, H. Nonaka, L. Xu, T. Nagata, Y. Koide: Appl. Phys. Lett. **86**, 211502 (2005).

[13] L. Xu, F. Terashita, H. Nonaka, A. Ogino, T. Nagata, Y. Koide, S. Nanko, I. Kurawaki and M. Nagatsu: J. Phys. D: Appl. Phys. **39**, 148-152 (2006).

[14] L. Xu, H. Nonaka, H. Y. Zhou, A. Ogino, T. Nagata, Y. Koide, S. Nanko, I. Kurawaki and M. Nagatsu: J. Phys. D: Appl. Phys. **40**, 803-808 (2007).

[15] J. Pelletier: Agressologie **33**, 105-110 (1993).

[16] F. D. Egitto, V. Vukanovic, G. N. Taylor: Plasma deposition, treatments, and etching of polymers, ed. R. d'Agostino, pp. 321-422 (Boston: Academic Press) (1990).

[17] D. L. Flamm, G. K. Herb: Plasma etching: An introduction, ed. D. M. Manos, D. L. Flamm, pp. 91-183 (Boston: Academic Press) (1989).

[18] F. D. Egitto: Pure & Appl. Chem. **62**, 1699-1708 (1990).

[19] M. Masoud, K. Martus and K. Becker: J. Phys. D: Appl. Phys. **38**, 1674-1683 (2005).

6 Low-temperature sterilization with volume-wave plasma source

6.1 Introduction

Low-temperature plasma sterilization using low-pressure surface-wave plasma has been investigated in chapter 5. The problem of the plasma sterilization is essentially on the treatment of the surface only. In order to sterilize inside the medical instruments wrapped with perforated plastic packing, it is required to produce the plasma inside the packing material. [1] To overcome this problem, volume-wave plasma (VWP) is proposed for plasma sterilization, as shown in **Fig. 6.1**.

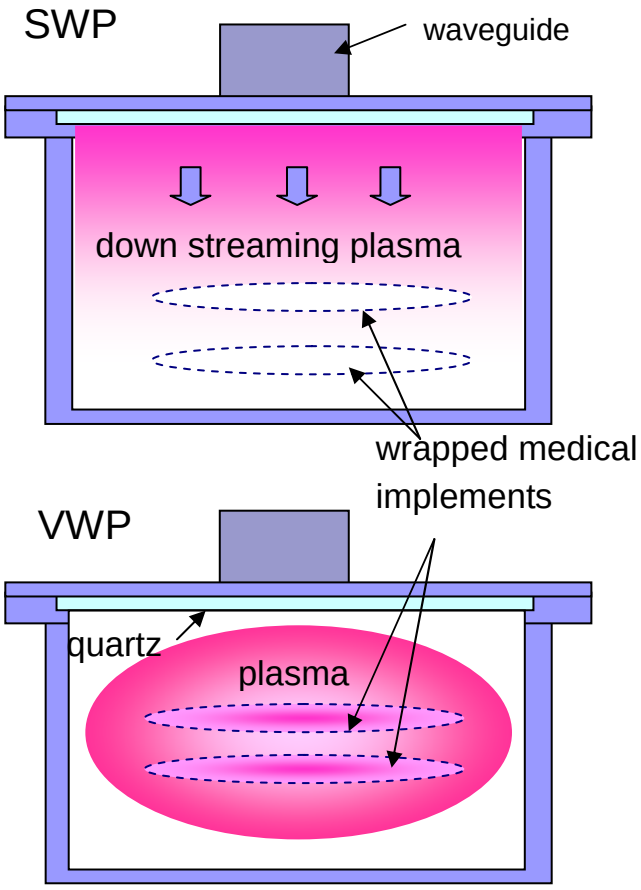

Fig. 6.1 Schematic drawings of (a) surface-wave plasma and (b) volume-wave plasma sterilization techniques.

In this chapter, sterilization experiments of BIs with and without their original package using VWP and SWP in O_2, N_2 and air simulated gas mixture were investigated firstly. Later on, sterilization experiments of polyethylene (PE) film wrapped BIs using different gas species plasma with water vapor addition were investigated.

6.2 Experimental setup

For plasma sterilization, the BI samples used were placed in Petri dishes set on the movable stage with a diameter of 50 cm about 30~45 cm below the quartz vacuum window. During plasma irradiation, the stage temperature was indicated by thermo-label sheets (Nichiyu, Thermo Label 5E-50, 5E-75, 5E-100) attached to the Petri dish and covered by a piece of thin glass. The morphology of the spores after the plasma irradiation has been analyzed with the SEM (Jeol, JSM-6360). OES measurements have been done using UV-visible spectrometer (Acton, SpectraPro 2300i) in the wavelength range of 200~800 nm. Mass spectrum has been obtained using quadrupole mass spectrometer (Pfeiffer Vacuum, Prisma™ QMS 200) connected to the port on left sidewall of the lower section of chamber and time-modulated plasma discharges can be operated with a remote-control on/off timer module as shown in **Fig. 6.2**. A cable of optical fibers was used to transfer the optical emission transmitting from the viewing-port on the front-loading door.

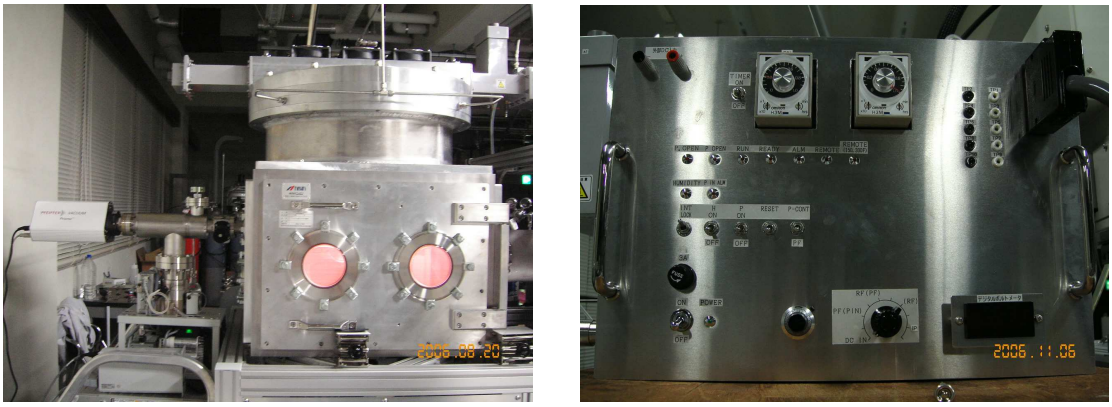

Fig. 6.2 Photographs of the VWP device connected with QMS and the remote-control on/off timer module.

To find the suitable plasma on-time to prevent process part of chamber from high temperature, stage temperature was measured using thermo-label sheets attached to the Petri dish during oxygen plasma irradiation by 2-min step. **Figure 6.3** shows the relationship between substrate stage temperature and plasma on-time when incident microwave power is 2 kW at pressure of 50 mTorr with the movable stage at 40 cm below quartz window. From the figure, we found that stage temperature had already achieved 70 °C only after 5-min plasma irradiation. Therefore, continuous plasma on-time within 5 min and then several minutes off-time for cooling down is recommended. To reduce more temperature, the suitable plasma on-time and off-time

are needed to know as a remote-control timer is used to apply time-modulated plasma discharges. A thermocouple (Custom, CT-700S Digital thermometer; Sensor: Type K -50 ~ +1200 °C) attached to the surface of the metal stage at about 38 cm below the quartz window was used to indicate the temperature. **Figure 6.4** shows the temperature reduction by applying the time-modulated plasma discharges.

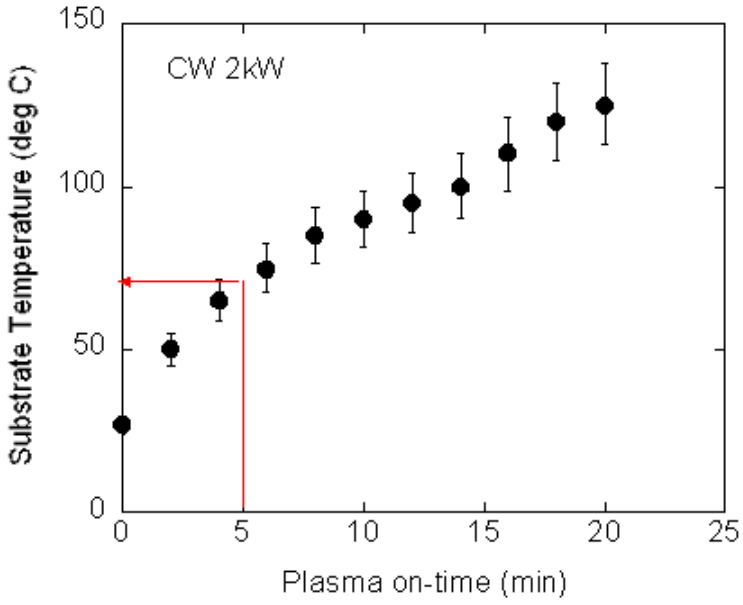

Fig. 6.3 Relationship between stage temperature and plasma on-time.

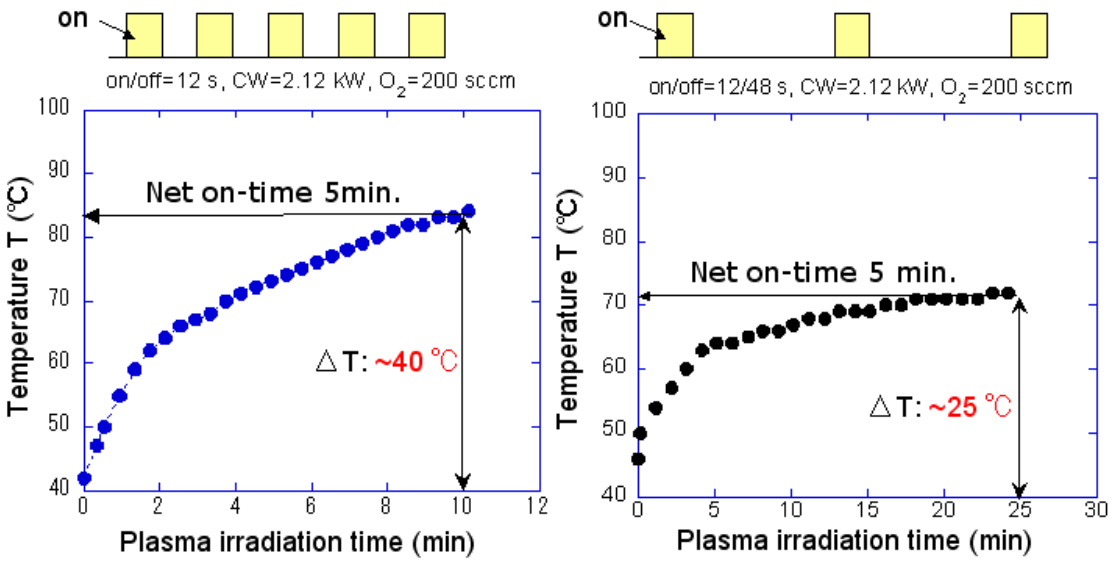

Fig. 6.4 Time reduction using time-modulated microwave plasmas.

6.3 Results and discussion

6.3.1 Sterilization experiments of BIs with and without original package

When we started the sterilization experiments with the volume-wave plasma source, Steri-chart type BIs were chosen since they had not been successfully sterilized with their wrapped glassine paper pouch by the 40-cm-diameter SWP source. The placement of BI samples is as shown in **Fig. 6.5**. As a preliminary test, wrapped steri-chart type BIs with 10^3 and 10^4 *G. stearothermophilus* spores had been successfully sterilized by the VWP source using $Ar/N_2/O_2$ plasma.

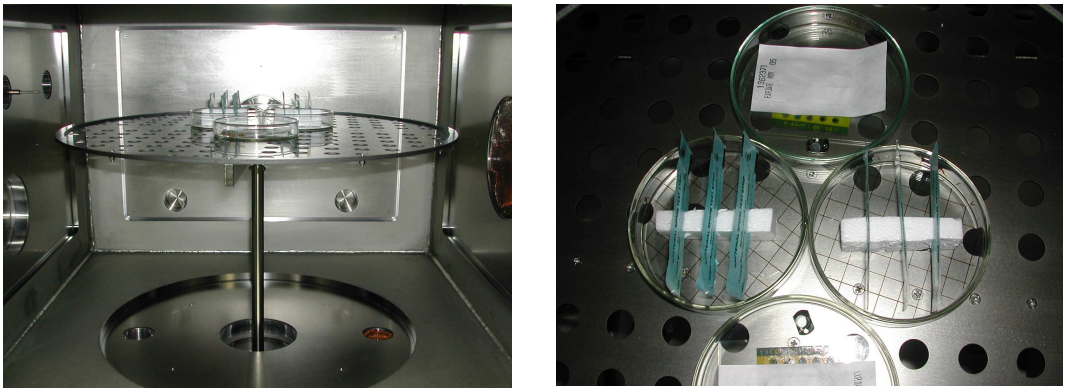

Fig. 6.5 Placement of BI samples from side view and top view.

Then, we investigated the sterilization effect of BIs wrapped with and without their original package by using O_2, N_2 and air-simulated plasmas. [2] First, we show the sterilization results by using oxygen plasma in **Table 6.1**. When CW power was kept 2.5 kW at pressure of 200 mTorr for total 20 min, all the wrapped Steri-chart type *B. atrophaeus* spores with population of 10^4 to 10^8 were sterilized. Moreover, unwrapped SUS type *G. stearothermophilus* spores with population of 10^6 were also sterilized. To decrease temperature of samples during plasma irradiation, we decreased CW power to 2 kW at pressure of 50 mTorr and set the stage 10 cm lower than previous position. Only wrapped Steri-chart type *B. atrophaeus* spores with population of 10^4 to 10^6 and unwrapped SUS type *G. stearothermophilus* spores with population of 10^6 were sterilized. When CW power was decreased to 1.5 kW at pressure of 50 mTorr, if the plasma irradiation period was long enough, even the SUS type *G. stearothermophilus* spores wrapped with Tyvek®/poly pouch was sterilized. We noticed that from the discharge transition curve shown in **Fig. 3.8(b)**, the first two cases were SWP sterilization, only the last case was VWP sterilization. Since the glassine paper pouch

of Steri-chart type BIs has many minor holes on it, thus, parts of high density down streaming SWP can still sterilize the spores embedded in the cellulose strip. However, the Tyvek® pouch of SUS type BI can only let discharge gas penetrate it, which makes us owe the internal sterilization effect to VWP produced inside the Tyvek® pouch. To achieve lower temperature during plasma irradiation, plasma on-time during one cycle was decreased to less than 1 min.

Discharge condition	**Stage Location**	**Irrad. periods**	**Temp.**	**Sterilization results**						
				B. atrophaeus **wrapped** *(B. subtilis)* Steri-chart					*G. stearothermophilus* SUS	
				10^4	10^5	10^6	10^7	10^8	$2.5x10^6$	
CW=2.5kW O_2::200sccm	30cm	5min x 4times	~95°C	○	○	○	○	○	unwrapped	○
CW= 2 kW O_2::200sccm	40cm	2min x10times	<90°C	○	○	○	×	×	unwrapped	○
CW=1.5 kW O_2::200sccm		2min x30times	~90°C	○	○	○	---	---	unwrapped	○
									wrapped	○

Table 6.1 Results of sterilization experiment using CW oxygen plasma.

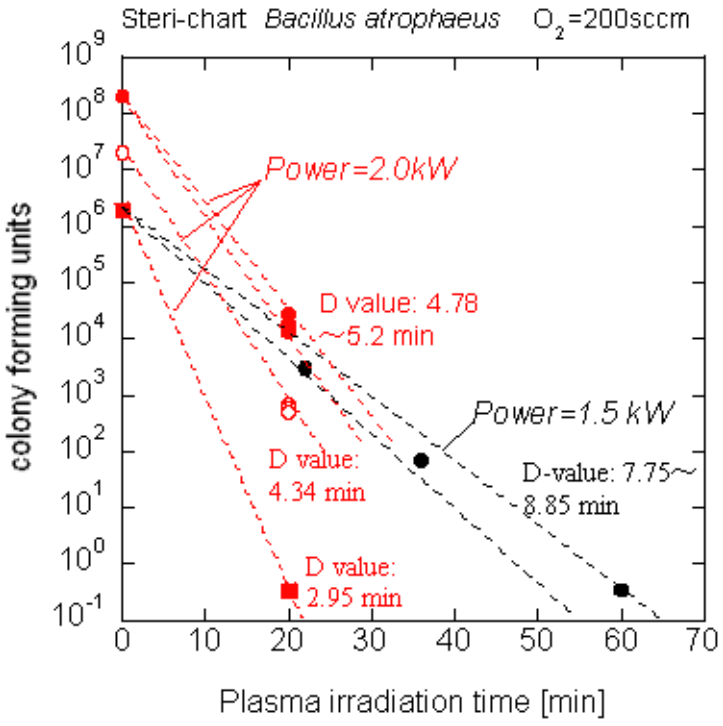

Fig. 6.6 Survival curves of the *B. atrophaeus* spores irradiated by oxygen plasma.

By agar-plate based colony-count method, we can calculate D value to know the sterilization effect relying on plasma irradiation time. **Figure 6.6** shows the survival curves of the wrapped Steri-chart type *B. atrophaeus* spores irradiated by oxygen plasma. The D value estimated by the plotted data for SWP sterilization (power = 2 kW, pressure = 50 mTorr) was roughly 2.95-5.2 min, while for VWP sterilization (power = 1.5 kW, pressure = 50 mTorr) was roughly 7.75-8.85 min.

Next, we show the sterilization results by using nitrogen plasma and air-simulated plasma in **Table 6.2**. For the nitrogen plasma case, when CW power was kept 2 kW at pressure of 50 mTorr for total 20 min, unwrapped *G. stearothermophilus* spores with population of 10^4 to 10^6 were sterilized. Moreover, unwrapped *B. atrophaeus* spores with population of 10^6 were also sterilized. Since we applied time-modulated microwave with cycles of on-time of 30 sec and off-time of 60 sec, it made the temperature at about 70 °C. For the air-simulated plasma case, to decrease temperature of samples during plasma irradiation, we adjusted time-modulated microwave with cycles of on-time of 12 sec and off-time of 48 sec. Unwrapped *G. stearothermophilus* spores with population of 10^4 and 10^5 were sterilized. The temperature after total 20 min plasma irradiation was less than 55 °C.

Discharge condition	**Stage Location z (cm)**	**Irrad. periods**	**Temp.**	**Sterilization results**					
				B. atrophaeus (B. subtilis) **unwrapped**	*G. stearothermophilus* **unwrapped**				
				10^6	10^4	10^5	10^6	10^7	10^6 SUS
CW= 2kW N_2::200sccm	35cm	30 sec x 40 times	~70°C	○	○	○	○	×	○
CW=2.3 kW N_2/O_2:: 200/50sccm	37cm	12 sec x100 times	<55°C	---	○	○	×	×	×

Table 6.2 Results of sterilization experiment using CW nitrogen plasma and air-simulated plasma.

We also show the sterilization results by using pulse-modulated microwave excited air-simulated N_2-O_2 plasma in **Table 6.3**. On-duration and off-duration of modulation signal were both 500 μs. When instantaneous microwave power was kept 4 kW for 15 min, wrapped Steri-chart type *B. atrophaeus* spores with population of 10^4 and 10^5 were sterilized. Unwrapped SUS type *B. atrophaeus* spores and *G. stearothermophilus* spores with population of 2.5×10^6 were also sterilized. If we lengthened 5 min, with the addition of wrapped Steri-chart type *B. atrophaeus* spores with population of 10^6 and 10^7 could be sterilized. Since the maximum instantaneous power of 4 kW leads to too high temperature to destroy the original package of BIs, such as Tyvek®/poly pouch or glassine paper pouch, there is no sense in studying low-temperature plasma sterilization using such kind of pulse-modulated microwave excited plasmas.

Discharge condition	**Stage location z (cm)**	**Irrad. periods**	**Temp.**	**Sterilization results**						
				Steri-chart *B. atrophaeus* **wrapped**					SUS 10^6 **unwrapped**	
				10^4	10^5	10^6	10^7	10^8	*B. atrophaeus*	*G. stearothermophilus*
Instant power 4 kW 500/500 μs $N_2$200/$O_2$50 sccm	30 cm	**5 min x 4 times**	>95℃	○	○	○	○	×	○	○
		5 min x 3 times		○	○	×	×	×	○	○

Table 6.3 Results of sterilization experiment using pulse-modulated air-simulated plasma.

6.3.2 Sterilization experiments of PE film wrapped BIs

From the sterilization results described in last subsection, in spite of the good result that internal sterilization of Tyvek®/poly pouch wrapped BI was only achieved by VWP, we still expected much better internal sterilization effect, which made us start the sterilization experiments attempting to achieve internal sterilization of polyethylene film wrapped BIs.

Polyethylene is a thermoplastic commodity heavily used in consumer products (over 60 million tons are produced worldwide every year). In the polymer industry the name

is sometimes shortened to PE. The PE films have been widely used as fresh-keeping wrap, a layer cling to the paper in the paper package for drink, etc.. Therefore, we think it is useful for food packaging industry to use such internal plasma sterilization technique for PE film wrapped materials. The very thin PE film (whose melt temperature is only higher than 60 °C) used in the present work and the placement of the BI samples are as shown in **Fig. 6.7**.

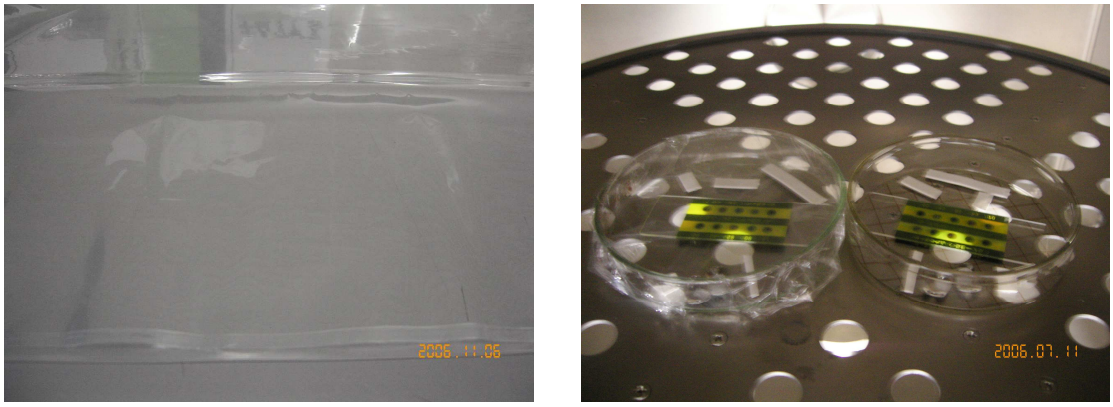

Fig. 6.7 Photographs of PE film cling to a protective film and the placement of BI samples with and without PE film wrap.

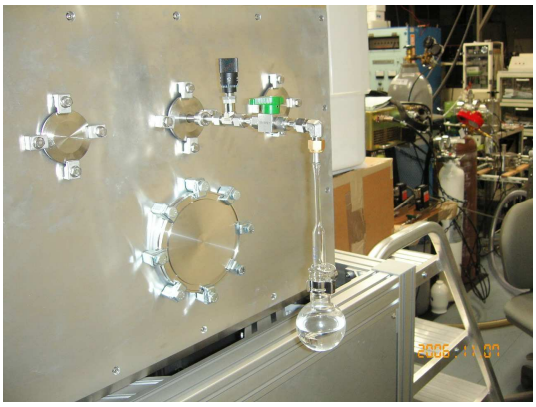

Fig. 6.8 Photograph of the matrass supplying water vapor via a small needle valve.

We show the sterilization results of PE film wrapped BIs (Steri-chart type *G. stearothermophilus* spores) in **Table 6.4**. As CW power was 2 kW at pressure of 50 mTorr in air-simulated plasma (VWP mode), when modulated on/off time was kept as 12/48 s per cycle, sterilization of BI with spores population of 10^3 and 10^4 were successful with temperature at about 60 ℃. When on/off time was modified to 12/60 s and stage was set 5 cm lower, sterilization of PE film wrapped BI with spore population of 10^3 and 10^4 were successful with temperature lower than 55 ℃. Recently

Hayashi et al. [3] carried out a sterilization experiment using radicals produced by oxygen/water vapor RF plasma. We also found if water vapor was supplied directly into the chamber from a matrass filled with pure water via a small needle valve (**Fig. 6.8**) addition on the air-simulated plasma, even stage was 40 cm below quartz window, sterilization were successful for all the spores with population of 10^3-10^6 with and without PE film wrap.

Gas	On/Off (s)	On-time	Temp.	Spore Population *G. stearothermophilus*			
				10^3	10^4	10^5	10^6
N_2/O_2:: 200/50 sccm	12/48	20 min Z=35cm	~60℃ Without PE film	○	○	×	×
	12/60	20 min Z=40cm	<55℃ with PE film	○	○	×	×
N_2/O_2:: 200/50 sccm + H_2O:: 500 ppm	12/60	20 min Z=40cm	<55℃ With & without PE film	○	○	○	○

Table 6.4 Sterilization results of PE film wrapped BIs using air-simulated plasma.

Optical emission analyses of the plasma have been firstly carried out by the discharge image, then by OES. **Figure 6.9** show the discharge images of **(a)** air-simulated plasma emitting orange light while **(b)** water vapor added air-simulated plasma emitting pink light. There might be some new products, which are useful for sterilization.

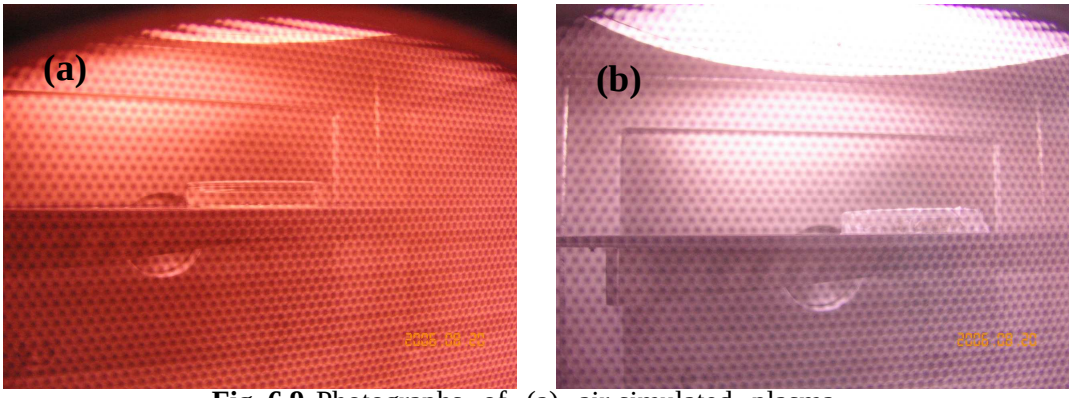

Fig. 6.9 Photographs of (a) air-simulated plasma and (b) water vapor added air-simulated plasma.

Figure 6.10(a) shows the optical emission spectrum in cases of water vapor addition on air-simulated plasmas with and without PE film wrap. We find the only difference between them is emission intensity. **Figure 6.10(b)** shows the optical emission spectrum in case of air-simulated plasmas with and without water vapor addition, the difference is also emission intensity. It means that optical emission during UV range can transmit through PE film, and is almost not affected by water vapor addition. It has been found that the emission intensity in the UV region is extremely large and the strong lines are originated from the second positive system of N_2 molecules, however, no obvious UV emission are originated from NO, which is different with the optical emission spectrum obtained in the SWP source with air-simulated plasma.

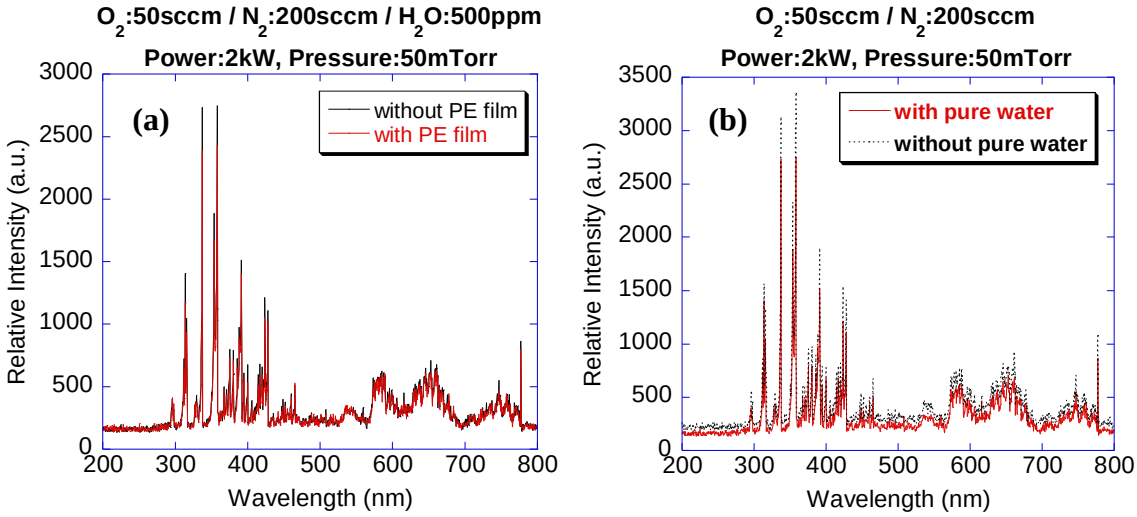

Fig. 6.10 Optical emission spectra in case of (a) water vapor addition on air-simulated plasma and (b) air-simulated plasma.

Since the water vapor addition on the air-simulated plasma greatly improved the sterilization effect, we carried out sterilization experiments with SUS type BIs (*G. stearothermophilus* spores and *B. atrophaeus* spores with population of 2.5×10^6) with and without PE film wrap, using O_2 (200 sccm), N_2 (200 sccm), air-simulated N_2-O_2 plasma (N_2: 200 + O_2: 50 sccm) with and without water vapor addition (2000 ppm). In all the experiments, discharge conditions are same as: CW microwave power = 2kW, time-modulated on/off timer = 12/60 s, pressure = 50 mTorr. These experiments also prepared the samples for SEM analyses and agar-plate based colony-count analyses. **Table 6.5(a)** lists the sterilization results of *G. stearothermophilus* spores relying on plasma irradiation period. **Table 6.5(b)** lists the sterilization results of *B. atrophaeus* spores relying on plasma irradiation period.

(a) *G. stearothermophilus* spores (SUS type)	Sterilization results relying on plasma irradiation period			
Experimental conditions:	10 min	20 min	30 min	40 min
N_2+O_2	×	○	○	○
N_2+O_2+water	×	○	○	○
PE film: N_2+O_2	×	×	×	×
PE film: N_2+O_2+water	×	×	○	○
O_2	×	○	○	—
O_2+water	×	○	○	—
PE film: O_2	—	—	—	—
PE film: O_2+water	×	×	×	—
N_2	×	×	○	—
N_2 +water	×	×	○	—
PE film: N_2	—	—	—	—
PE film: N_2 +water	×	×	×	—

(b) *B. atrophaeus* spores (SUS type)	Sterilization results relying on plasma irradiation period		
Experimental conditions:	10 min	20 min	30 min
N_2+O_2	×	○	○
N_2+O_2+water	×	○	○
PE film: N_2+O_2	—	—	—
PE film: N_2+O_2+water	×	×	×
O_2	×	○	○
O_2+water	×	○	○
PE film: O_2	—	—	—
PE film: O_2+water	×	×	×
N_2	×	×	×
N_2 +water	×	×	×
PE film: N_2	—	—	—
PE film: N_2 +water	×	×	×

Table 6.5 Sterilization results relying on plasma irradiation period in case of (a) *G. stearothermophilus* spores and (b) *B. atrophaeus* spores with population of 2.5×10^6.

SEM analyses were performed to study the shape and size of the spores before and after plasma irradiation. For spores sterilized by nitrogen plasma (**Fig. 6.11(b)**), spores

have no change compared with the control (**Fig. 6.11(a)**). We considered the spores were inactivated by UV radiation. For spores sterilized by water vapor added nitrogen plasma (**Fig. 6.11(c)**), spore appearance changed and looked like the spores sterilized by ozone [4]. Therefore, we considered the spores were oxidized by some strong oxidizers, in addition to inactivation by UV radiation.

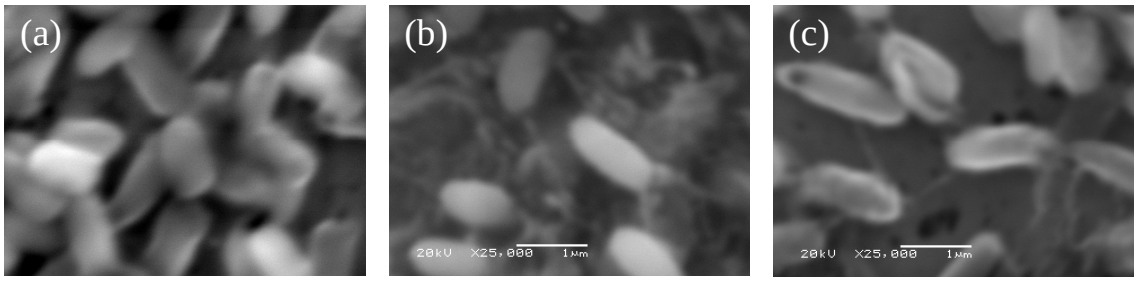

Fig. 6.11 SEM images of *G. stearothermophilus* spores (a) without plasma irradiation, (b) after 30 min nitrogen plasma irradiation and (c) after 30 min water vapor added nitrogen plasma irradiation.

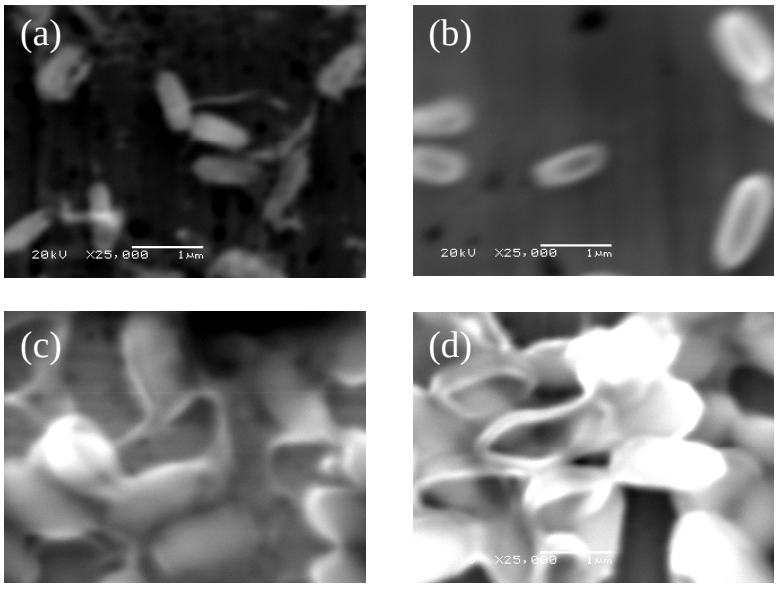

Fig. 6.12 SEM images of *G. stearothermophilus* spores (a) after 30 min air-simulated plasma irradiation, (b) after 30 min water vapor added air-simulated plasma irradiation, (c) with PE film wrap after 40 min air-simulated plasma irradiation and (d) with PE film wrap after 30 min water vapor added air-simulated plasma irradiation.

For spores sterilized by air-simulated plasma (**Fig. 6.12(a)**), spore size and shape changed. We considered the spores were etched by oxygen radicals in addition to

inactivation by UV radiation. For spores sterilized by water vapor added air-simulated plasma (**Fig. 6.12(b)**), spore size, shape and appearance changed. We considered additional oxidation reaction to spores happened. For spores with PE film wrap irradiated by air-simulated plasma (**Fig. 6.12(c)**), spores have no change compared with the control (**Fig. 6.11(a)**). For spores with PE film wrap sterilized by water vapor added air-simulated plasma (**Fig. 6.12(d)**), only spore appearance changed. We considered the spores were oxidized by some strong oxidizers, in addition to inactivation by UV radiation.

Effort on finding out the specie of the strong oxidizers produced by water vapor added air-simulated plasma was done by using QMS. Three mass spectra (mass number between 0-50) of air-simulated N_2-O_2 mixture gas discharge plasmas with no water vapor addition (**Fig. 6.13(a)**), with water vapor addition of 2000 ppm (**Fig. 6.13(b)**) and 5000 ppm (**Fig. 6.13(c)**) were obtained. By comparing the three mass spectra we found that the value of H_2 (mass=2), OH (mass=17) and H_2O (mass=18) distinctly increased as the value of added water vapor increased. The value of H_2O_2 (mass=34) and NO (mass=30) also had a minor but not distinct increase as the value of added water vapor increased. These results suggested that hydrogen peroxide (H_2O_2) vapor might be the strong oxidizer produced by water-vapor added air-simulated plasma because of the existence of OH radical. Moreover, it suggests that more water vapor is helpful for producing useful agents on sterilization, such as OH, H_2O_2 and NO.

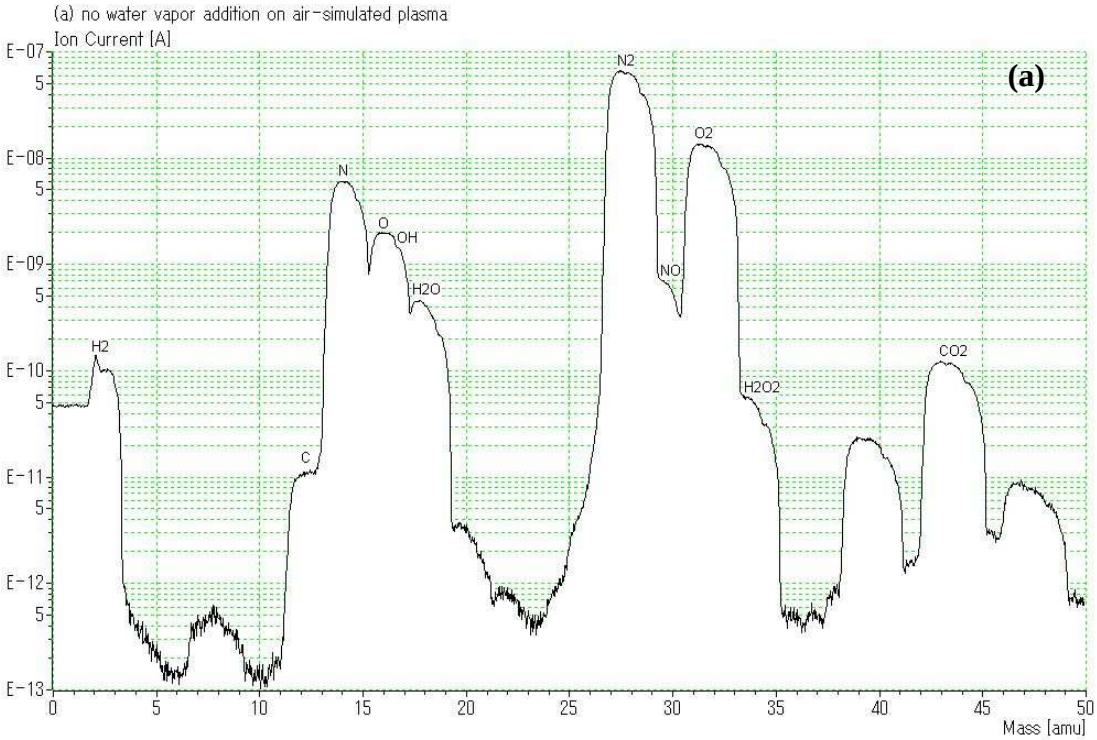

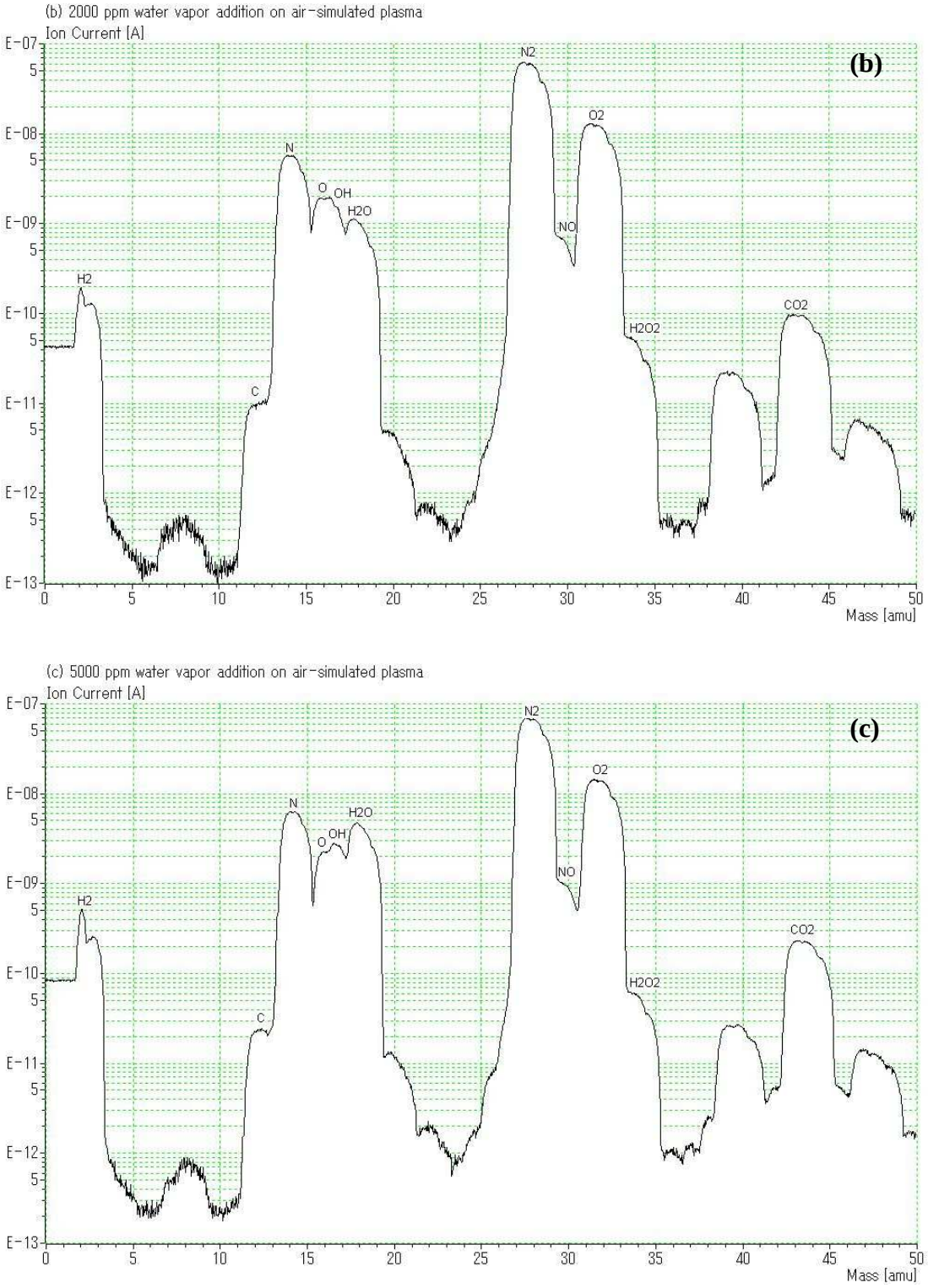

Fig. 6.13 Mass spectra of air-simulated N_2-O_2 mixture gas discharge plasmas (a) with no water vapor addition, with water vapor addition of (b) 2000 ppm and (c) 5000 ppm.

By agar-plate based colony-count method, we can calculate D value to know the sterilization effect relying on plasma irradiation time. **Figure 6.14** show the survival curves of the SUS type *G. stearothermophilus* spores irradiated by water vapor added oxygen plasma and water vapor added nitrogen plasma. The D value estimated by the plotted data was roughly 2.8-4.4 min for water vapor added oxygen plasma, while roughly 3.5-4.4 min for water vapor added nitrogen plasma. This result suggests that oxygen radicals have more effectiveness on the inactivation of spores than UV photons.

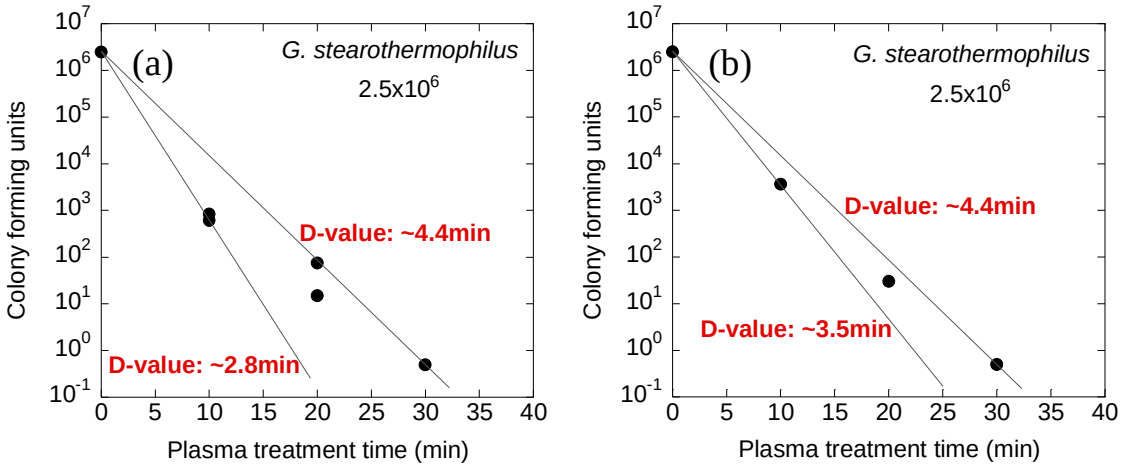

Fig. 6.14 Survival curves measured with colony-count method in cases of (a) water vapor added O_2 plasma and (b) water vapor added N_2 plasma.

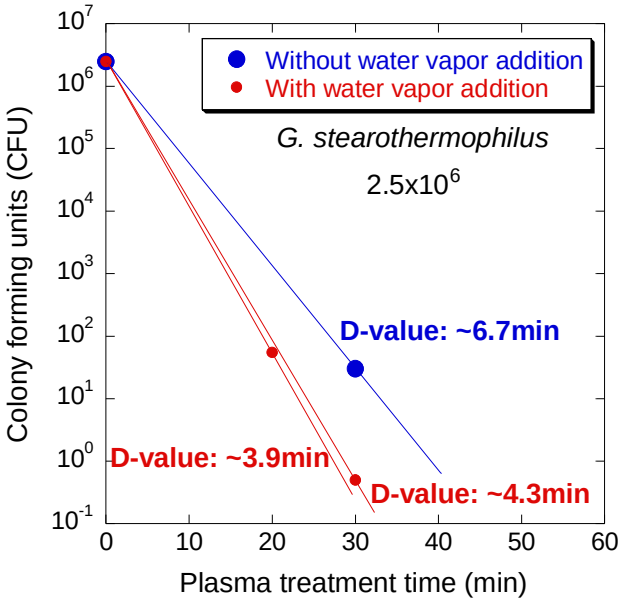

Fig. 6.15 Survival curves measured with colony-count method in cases of PE film wrapped BIs irradiated by air-simulated plasma with and without water vapor addition.

Colony-count results of PE film wrapped SUS type *G. stearothermophilus* spores were plotted in the **Fig. 6.15**. In air-simulated plasma case, the 4-order magnitude of cfu reduction during 20 min was found and it just matched the sterilization results presented in **Table 6.4**. After water vapor was added into air-simulated plasma, successful sterilization was achieved after 30 min plasma irradiation. The D value estimated by the plotted data was roughly 3.9-4.3 min for PE film wrapped SUS type *G. stearothermophilus* spores irradiated by water vapor added air-simulated plasma. It was not so bad compared with the D value for water vapor added oxygen or nitrogen plasma without PE film wrap. This result suggests that water vapor added plasmas are easy to achieve internal sterilization effect.

6.4 Summary

In this chapter, we investigated the internal sterilization technique using VWP and SWP for application to the sterilization of the wrapped medical materials. Water vapor addition on different gas species plasma has been found have a great improvement on sterilization effect, especially on internal sterilization effect.

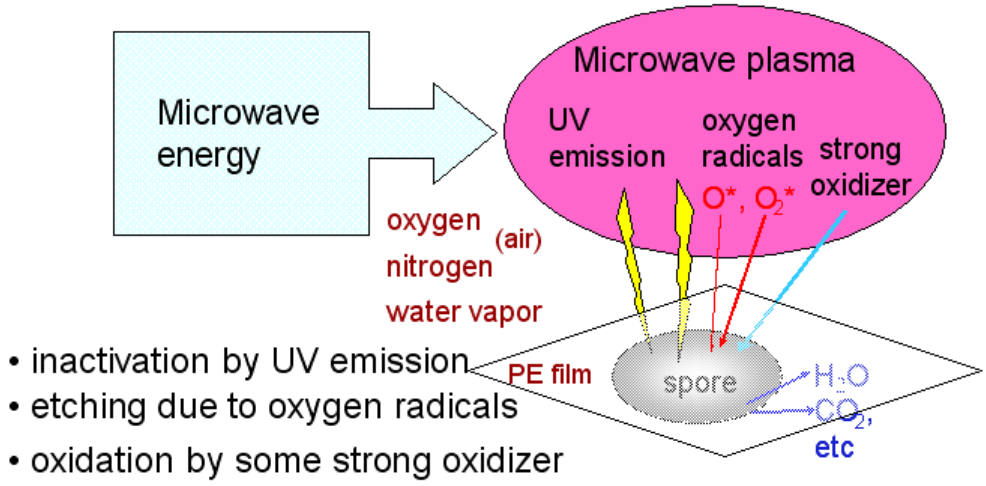

Fig. 6.16 Possible sterilization mechanisms in the present work.

In the end, I would like to summarize the possible sterilization mechanisms in the present work as shown in **Fig. 6.16**. When microwave energy was induced to a chamber filled with oxygen, nitrogen and pure water, microwave plasma was excited, then UV radiation, oxygen radicals and some strong oxidizer would be produced. Consequently, spores will be inactivated by UV radiation, be etched by oxygen radicals,

be oxidized by some strong oxidizer. If spores were wrapped by PE film, oxygen radicals would loose energy while contacting PE film, therefore, oxygen radicals would be shut down by PE film.

References

[1] M. Nagatsu, F. Terashita, L. Xu, H. Nonaka, K. Ninomiya, T. Nagata, Y. Koide, S. Nanko and I. Kurawaki: Abstracts and full-papers CD of 17th Int. Symp. Plasma Chemistry (Toronto, Canada), pp. 1100-1101 (2005).

[2] L. Xu, H. Y. Zhou, A. Ogino, Y. Koide and M. Nagatsu: Conf. Proc. 6th Int. Workshop on Microwave Discharges: Fundamentals and Applications (Zvenigorod, Russia), pp. 321-326 (2006).

[3] N. Hayashi, W. M. Guan, S. Tsutsui, T. Tomari and Y. Hanada: Jpn. J. Appl. Phys. **45**, 8358-8363 (2006).

[4] H. Etoh, Y. Ohno, A. Ogino and M. Nagatsu: Oral presentation at 67th JSAP autumn meeting (The Japan Society of Applied Physics, Kusatsu, 2006).

7 Low-temperature sterilization with atmospheric pressure plasma sources

7.1 Introduction

In the previous chapters, we concentrated on the study of low-temperature plasma sterilization using low-pressure microwave plasma. The characteristics of low-pressure microwave excited air plasma and air-simulated N_2-O_2 mixture gas discharge plasma for low-temperature sterilization were investigated. On the other hand, atmospheric pressure discharges have been widely investigated in recent years because of a variety of advantages they offer, such as low-cost equipment, no vacuum operation and the discharge reactivity. To enrich the study of low-temperature plasma sterilization, the low-temperature sterilization applications with recently popular atmospheric pressure plasma sources in addition to the low-temperature sterilization applications with microwave plasma sources are necessary to this thesis. Therefore, I would like to present some previous work in sterilization application using atmospheric pressure plasma in air circumstance in this chapter. A recent result and OES diagnostics of atmospheric pressure air plasma will also be briefly mentioned.

Atmospheric pressure plasma, such as the arc, torch produced by arc discharge have also been investigated and applied to a number of industrial fields. However its application is limited yet, because these plasma sources are thermal plasma sources having high gas temperature that leads to indiscriminate “burning” rather than selective chemical reactions. A discharge generated at or upon a dielectric surface can generate highly active non-equilibrium plasma at atmospheric pressure and even at room temperature. Roth et al. [1], H. Koinuma group [2-6] and J. Park group [7-9] have developed kinds of non-equilibrium atmospheric pressure plasma sources, such as symmetric pectinate electrodes panel driven by audio-frequency power and plasma jet source driven by 13.56 MHz RF power, respectively. Those atmospheric pressure plasma sources can be used for environmental protections, deposition of thin films, etching materials, and surface treatment of materials. Roth et al. used a one atmosphere uniform glow discharge plasma (OAUGDP) in killing microorganisms [1].

In this work, we firstly studied atmospheric pressure surface barrier discharge (APSBD) in air using kinds of pectinate electrodes panels driven by audio-frequency power and experimentally proved such APSBD plasma was a very simple, effective and innocuous tool for inactivation of *Escherichia coli* bacteria [10]. There are several merits of this kind of discharge plasma: the temperature is low which avoids the

shortcomings occurring in the high-temperature method; the plasma is innocuous and persons can stay near the discharge without any precautionary measures; the process can be carried out in any conditions with only a portable high-voltage apply. We also discuss the mechanism of killing.

Later, we found if we offered a gas flow to blow out the APSBD plasma and concentrated the highly active non-equilibrium plasma into one line, we could obtain atmospheric pressure plasma jet driven by audio-frequency power. Therefore, we developed two structure types of atmospheric pressure plasma jet sources named PJ-1 and PJ-2, which are driven by easily generated audio-frequency power variable range from 5 kHz to 20 kHz. Using PJ-1 or PJ-2, we can obtain a stable, near homogeneous, arc-free dielectric barrier discharge (DBD) with argon at atmospheric pressure, without water-cooling device. [11]

7.2 Experimental setup

7.2.1 Symmetric pectinate electrodes covered dielectric panel scheme

Figure 7.1 schematically shows the experimental setup for the sterilization. A sinusoidal voltage up to several tens of kilovolt peak-to-peak was applied to the electrodes, and the source frequency was varied in the range of 1-20 kHz. Experiment was carried out at room-temperature in air, pectinate electrodes generated heat to some degree after 10 min, but the surface of *E. coli* sample which was 20 mm away from the plasma panel maintained room-temperature. The area of *E. coli* was about 28 cm^2 while the rectangle area of pectinate electrodes was about 9 cm^2. The gas species were diagnosed by a mass spectrometer (LZL-203D). The current and voltage waveforms were recorded in a digital oscilloscope (Tektronics, TDS220) using the measurement circuit as shown in the next subsection (**Fig. 7.5**).

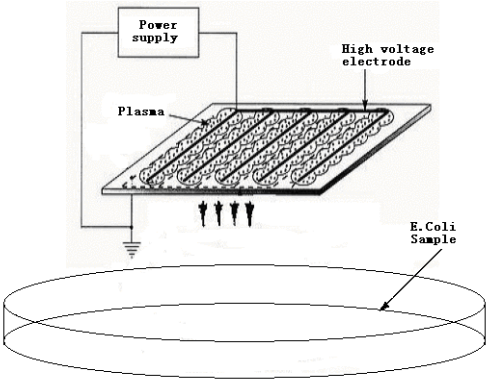

Fig. 7.1 Experimental setup for sterilization.

The dielectric panels used is 55 mm × 55 mm copper-clad plate whose dielectric constant is 2.6; the thickness is 1.0 mm. Electrodes are made of red copper, coved with lead-tin foil. The high voltage electrode consists of seven interconnected electrode strips 1-mm-wide, 10-μm-thick, 33-mm-long with a strip-to-strip distance of 4 mm, and the grounded electrode consists of the same pectinate electrodes on the lower surface (**Fig. 7.2**). The construction can be regarded as several capacitances connected in parallel and the constant capacitance of the dielectric panel and the electrodes between the high voltage electrodes and the grounded electrodes can be calculated as 5.4 pF. The impedance of the set of capacitances can also be estimated as about 300 Ω while the frequency of applied voltage is 10 kHz.

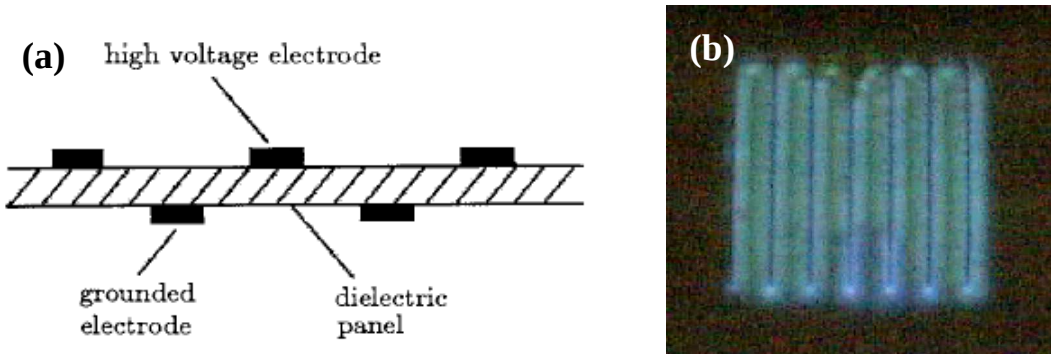

Fig. 7.2 (a) Schematic of dielectric panel and pectinate electrode, (b) image of discharge.

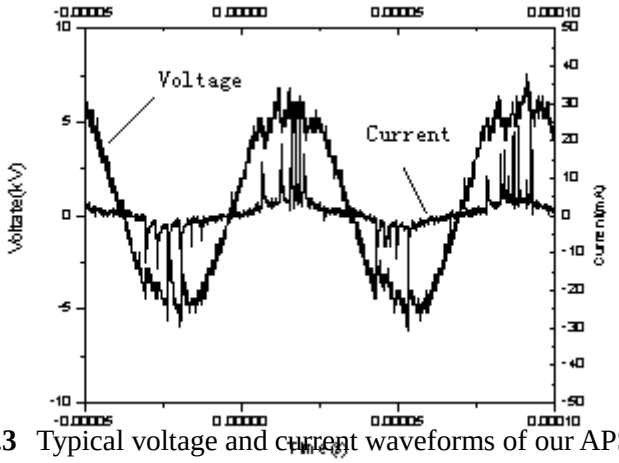

Fig. 7.3 Typical voltage and current waveforms of our APSBD.

Figure 7.3 shows the typical voltage and current waveforms of our APSBD. We can see that the current waveform consists of a sinusoidal wave with many current peaks. It indicates that this kind of discharge is not glow discharge, whose current is characterized by only one narrow peak every half cycle of the applied voltage [12], but

a dielectric barrier discharge (DBD). In the common DBD waveforms, current is 90 ° ahead of voltage. However, in our case, we can not find the phase difference. The reason might be that in our current measurement circuit the resistor used (2 kΩ) has much larger impedance than the electrodes covered dielectric panel (300 Ω while frequency = 10 kHz), which made the phase difference between current and voltage mainly dependent on not the capacitive electrodes covered dielectric panel scheme but the resistor. If we chose a resistor that had much less impedance than the electrodes covered dielectric panel, we should obtain the common DBD waveforms.

7.2.2 Plasma jet scheme

A schematic drawing of the experimental setup is shown in **Fig. 7.4**. The common ground of main structure of PJ-1 and PJ-2 is that they both consist of two concentric electrodes. The outer electrode is coupled to an audio-frequency power supply at variable frequency range from 5 kHz to 20 kHz, and the inner one is grounded with the discharge gas such as argon or helium passing it through. The key differences between these two structure types of plasma jet source are the surfaces of inner electrode and the shapes of outer electrode. For PJ-1, the grounded inner electrode is a stainless steel pipe closing on one end and only opening the other end as gas inlet. There are several holes used as spray nozzle of gas along a circular helix on the wall of the inner electrode having 8 mm inner diameter. The outer electrode of PJ-1 is a metal pipe (inner diameter 15 mm) covered with both sides insulating coat. For PJ-2, there are no holes on the wall of the inner electrode, except one nozzle at each side of the grounded inner stainless steel pipe. The outer electrode of PJ-2 is just a coil around an insulating pipe.

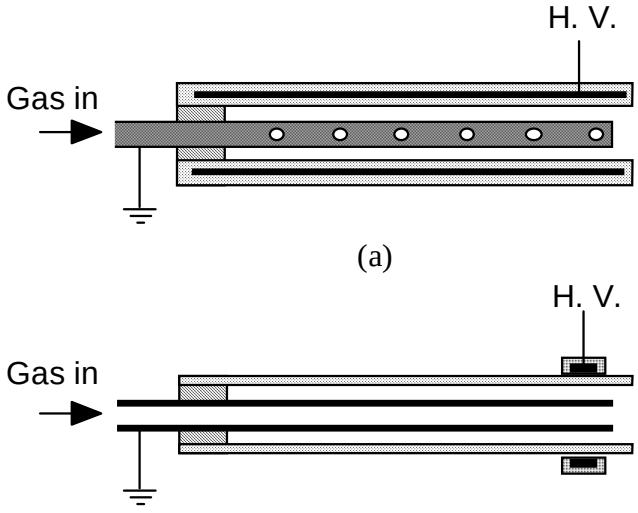

Fig. 7.4 Schematic drawing of the atmospheric pressure plasma jet sources (a) PJ-1 and (b) PJ-2.

The gas flow rate was measured by a mass flow meter. **Figure 7.5** shows the electrical circuit of audio-frequency power-driven atmospheric pressure plasma jet source. A sinusoidal voltage up to several tens of kilovolts peak-to-peak was applied to the outer electrodes, and the source frequency was varied in the range from 5 kHz to 20 kHz. The current and voltage waveforms below were recorded by using a digital oscilloscope (Tektronics, TDS220).

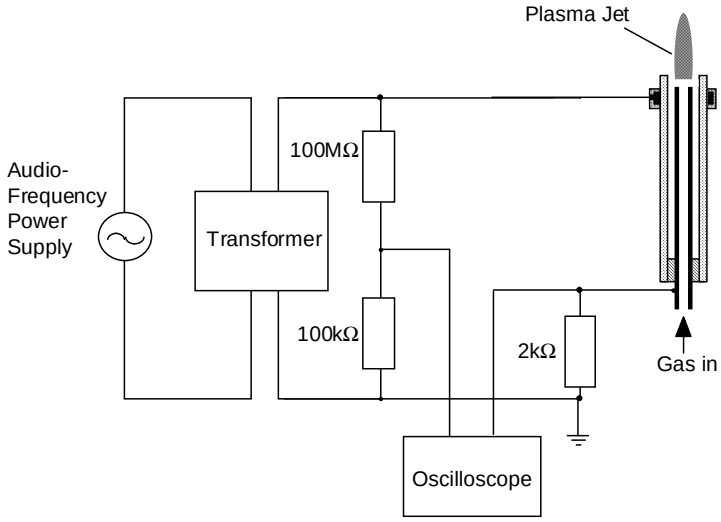

Fig. 7.5 Audio-frequency power-driven atmospheric pressure plasma jet source.

7.3 Results and discussion

7.3.1 Symmetric pectinate electrodes covered dielectric panel scheme

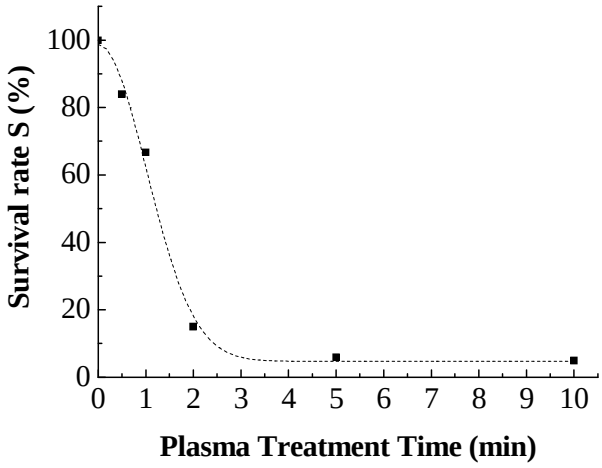

Fig. 7.6 Survival curve of *E. coli*; the sample was exposed directly to APSBD plasma in air.

Figure 7.6 shows a survival curve of *E. coli* treated by the discharge plasma when the voltage peak to peak of 40 kV is applied and the treatment durations are 30 s, 1, 2, 5 and 10 min respectively. We can see that APSBD is very effective for bacterial inactivation: at the beginning, 0-2 min, the curve drops rapidly and a quick killing process is going along. The curve drops slowly after 2 min.

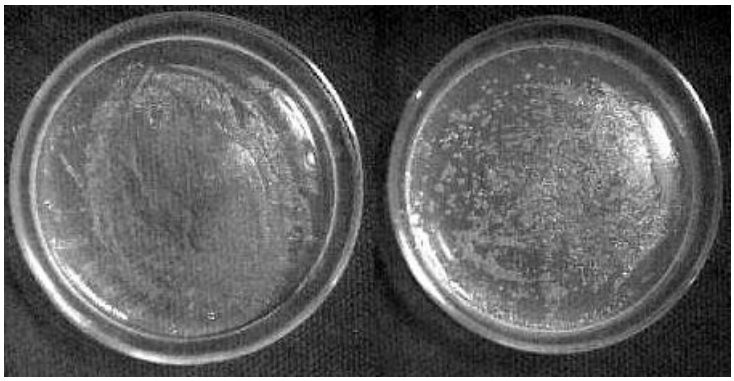

(a)

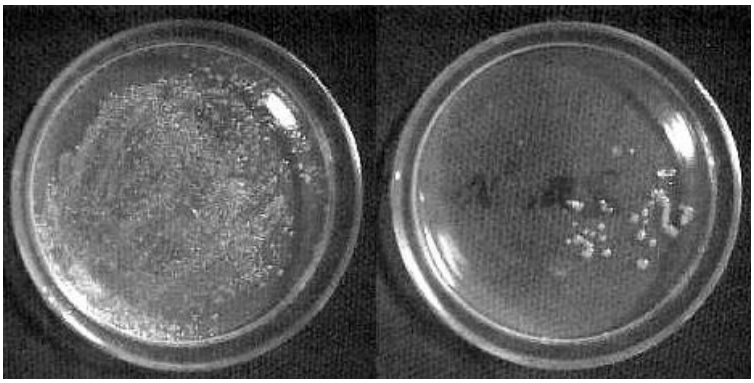

(b)

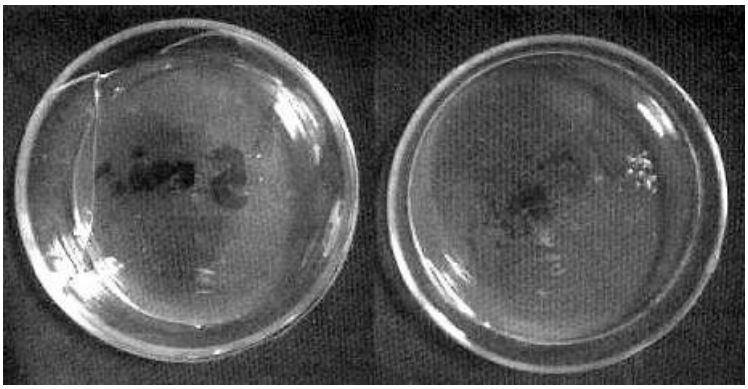

(c)

Fig. 7.7 Samples of *E. coli* incubated after treatment by air plasma for different durations. (a) Untreated (left) and treated for 30 s (right), (b) treated for 1 min (left) and treated for 2 min (right), (c) treated for 5 min (left) and treated for 10 min (right).

Figure 7.7 illustrates the photos of samples of *E. coli* that were incubated in an incubator for 14 h. One of them is the sample that had not been treated by APSBD plasma, while the other five samples were treated for 30 s, 1, 2, 5 and 10 min respectively. We can see that there is almost no bacterial colony in the sample after being treated for 2 min.

The mechanism of sterilization was one important thing we are concerned with. In order to know which species plays major role in this process, we used a mass spectrometer to investigate the discharge plasma. The result is that molecular oxygen and monatomic oxygen increase with time, nitric oxide NO also increases but its content is much smaller compared with molecular oxygen and monatomic oxygen (**Fig. 7.8**), while other species, such as NO_2, OH, HO_2, H_2O_2, have not been found.

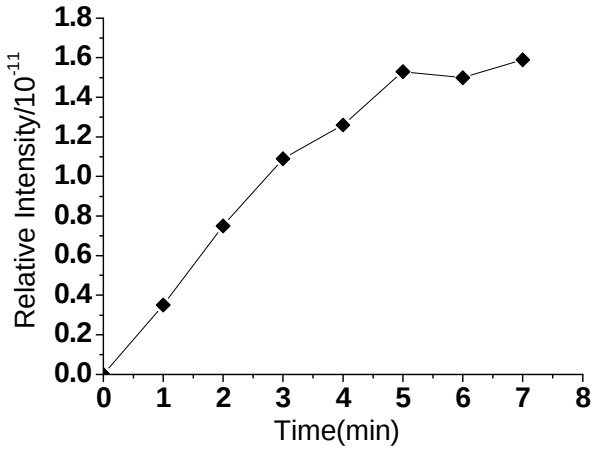

(a)

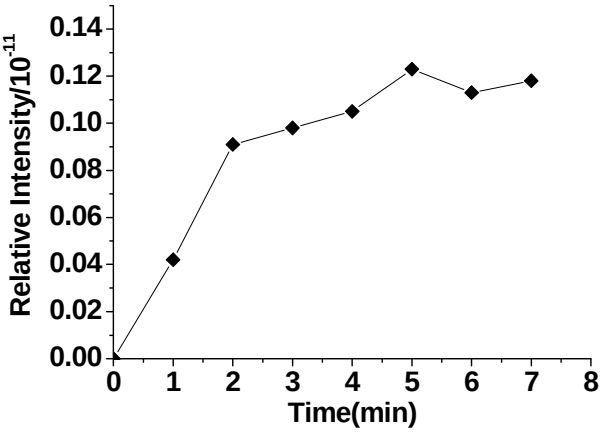

(b)

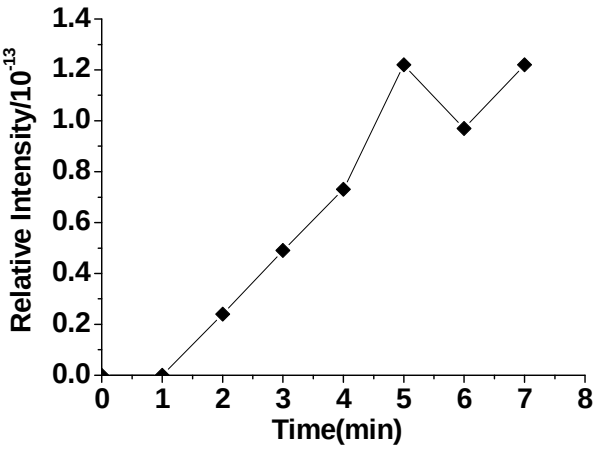

(c)

Fig. 7.8 Intensity of several active species produced by APSBD: (a) O_2, (b) O and (c) NO.

Strangely, the most common product of DBD, ozone, could not be found in the mass spectrometer, but we could smell the characteristic odour of ozone even far from the discharge. The reason may be that ozone is unstable and when it enters the mass spectrometer, it decomposes very quickly,

$$O_3 + e \rightarrow O_2 + O + e\,, \tag{1}$$

$$O + O_3 + M \rightarrow 2O_2 + M\,, \tag{2}$$

The discharge generates ozone due to the reactions

$$O_2 + e \rightarrow O + O + e\,, \tag{3}$$

$$O_2 + e \rightarrow O + O^+ + 2e\,, \tag{4}$$

$$O + O_2 + M \rightarrow O_3 + M\,, \tag{5}$$

where M can be N_2, O_2 or O, and excitation and dissociation of nitrogen molecules lead to a number of additional reaction paths such as

$$N + O_2 \rightarrow NO + O\,, \tag{6}$$

$$N + NO \rightarrow N_2 + O\,, \tag{7}$$

These reactions can produce additional oxygen atoms for ozone generation.

Ozone is a kind of strong oxidant, it can kill bacteria in different forms: it can decompose enzyme that is desirable in synthesizing glucose in bacteria; react with bacteria and virus directly and destroy cell wall, DNA and RNA of them; permeate the pericellular membrane and invade into the cell, destroy lipoprotein and lipopolysaccharide. The disinfectant process is from cell wall, pericellular membrane to cytoplasm and chromatin body, so the killing is very exhaustive. Ozone will

degrade into molecular oxygen and monatomic oxygen, and the latter is another oxidant and some of the monatomic oxygen will combine into molecular oxygen, so they leave no harmful by-products at the end. Ozone, as a kind of gas, can pervade to the whole space and leaves no dead angle.

Of course APSBD in air may generate other reactive oxygen species, such as O_2^- [13]

$$O_2 + e^- \rightarrow O_2^- . \tag{8}$$

O_2^- is a highly toxic material and can destroy important high polymer and membrane of anaerobic bacteria's cell, but superoxide dismutase in the aerobic bacteria will turn it into H_2O_2, which then degrades into H_2O, so it does little harm to persons.

Since the ozone and monatomic oxygen are the main antimicrobial products of APSBD, we can infer that this kind of discharge can be useful not only in killing *E. coli*, but also in killing a variety of microorganisms [14]. The wide application of APSBD is very promising.

7.3.2 Plasma jet scheme

First, we present the results of PJ-1 source. When argon gas flow rate was kept at 200 L/h and the applied voltage increases up 13.1 kV_{pp} at frequency 15 kHz, a soft blue glow was produced between the concentric outer and inner electrode, which then exited the narrow space through the nozzle of outer pipe electrode, namely, the nozzle of PJ-1. At 1.5 cm from that nozzle, the gas temperature was kept at 47 ºC. A photograph of atmospheric pressure discharge of PJ-1 with argon is shown in **Fig. 7.9(a)**. Visual inspection of the discharge at the nozzle seems like a uniform glow with no apparent arcing. In **Fig. 7.9(b)**, we show the typical waveforms of DBD current and voltage in PJ-1 source, where the discharge gas stream comes out from several holes along the circular helix of the grounded inner electrode. Although it does not appear to revolve flow of discharge gas like some condition under the arc discharge jet, the PJ-1 structure results in the inconsistent direction of discharge gas slowly spraying at the nozzle of outer electrode.

In order to clearly know the discharge status between the inner electrode and the outer electrode, we modified the outer electrode of PJ-1 by using a quartz tube as an insulating medium with spiral wire over it as outer electrode. The image of plasma discharge is shown in **Fig. 7.10(a)**, where visual inspection of the discharges between the electrodes at each hole along the inner electrode is revealed obviously. **Figure 7.10(b)** shows the waveforms of current and voltage waveforms in the modified PJ-1 source. Even though the structure is slightly different from PJ-1, we can see from **Fig.**

7.10(a) that the discharge plasma appears around the inner electrode nearly at the same time when gas streams sprayed out from several holes along the circular helix of the grounded inner electrode. As shown in **Fig. 7.9(a)**, the plasma spray at the nozzle of PJ-1 looks like a flame and not straight. For applications such as etching, deposition, surface modification and sterilization, however, the present plasma shape is not satisfactory to achieve a rapid material processing. Hence, we designed PJ-2 to improve the characteristics of plasma spray at the nozzle.

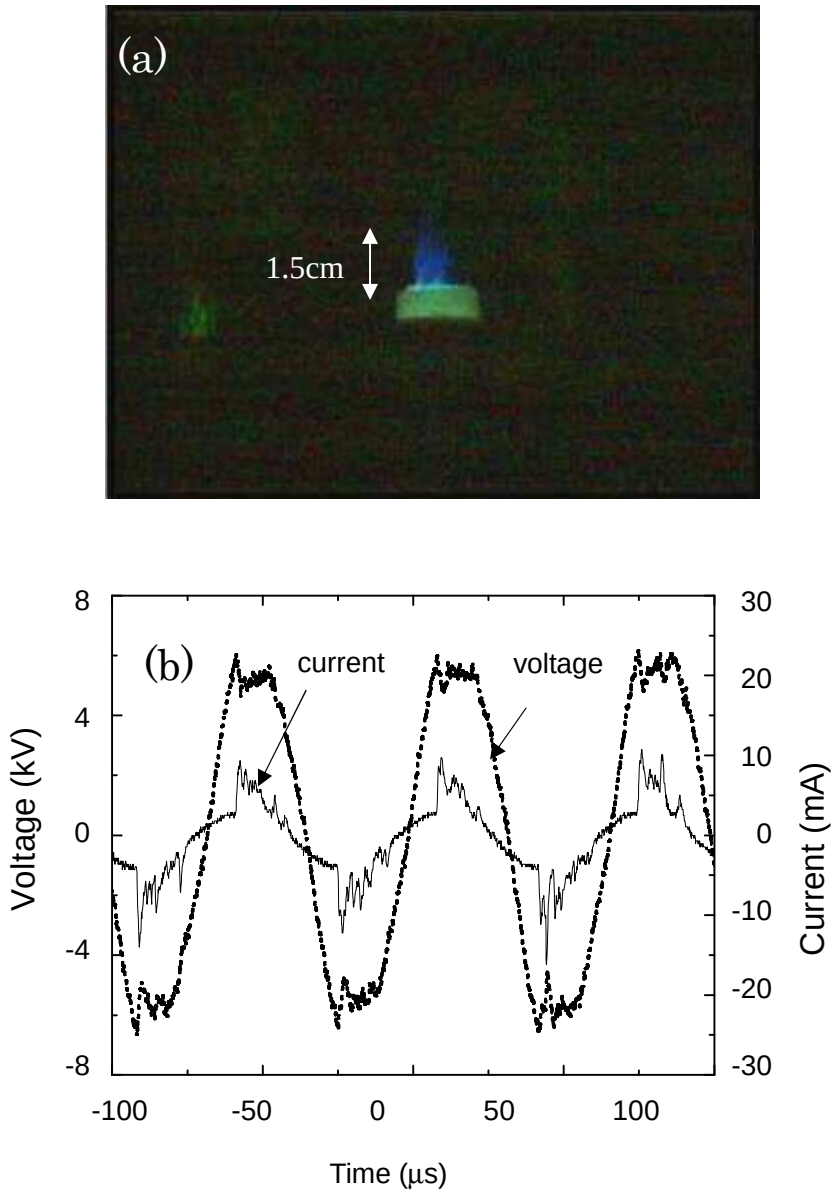

Fig. 7.9 (a) Image of discharge of PJ-1 and (b) time-depending current and voltage waveforms.

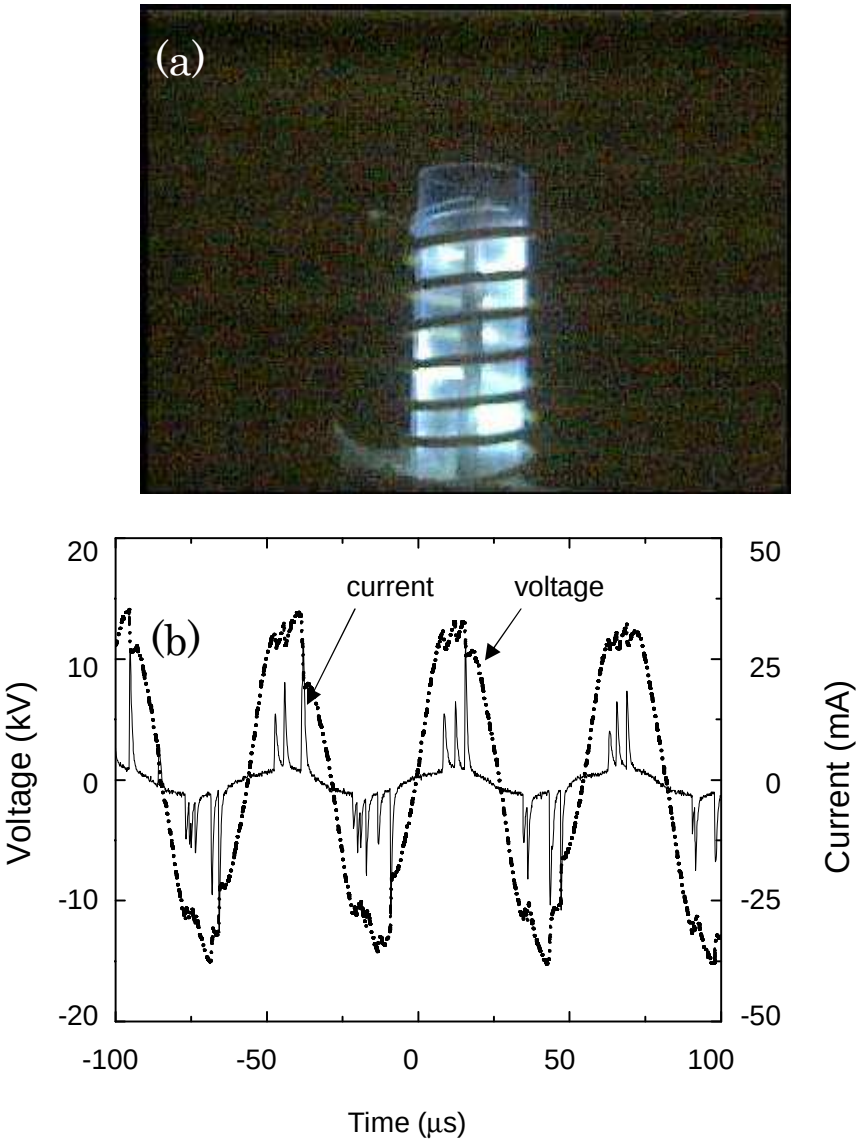

Fig. 7.10 (a) Image of discharge, and (b) time-depending current and voltage waveforms.

In the case of PJ-2 source, argon gas flow rate was kept at 200 L/h and the applied voltage was increased up 49.3 kV_{pp} at frequency 15.9 kHz. As shown in **Fig. 7.11(a)**, a bright white glow was produced at the nozzle of the grounded inner electrode and spraying outside the nozzle of PJ-2 for almost 2 cm long. At 1.5 cm from the nozzle, the gas temperature was kept at 38 ºC. **Figure 7.11(b)** shows typical current and voltage waveforms of the PJ-2 source.

Although the atmospheric pressure plasma jet has wide applications, in the present work, we studied the sterilizing characteristics as one of its applications. Since the highest temperature for living *E. coli* is 47.5 ºC, we tested the sterilization effect to *E.*

coli using plasma jet of PJ-2 at 1.5 cm away from the nozzle, so as to keep gas temperature at 38 ºC.

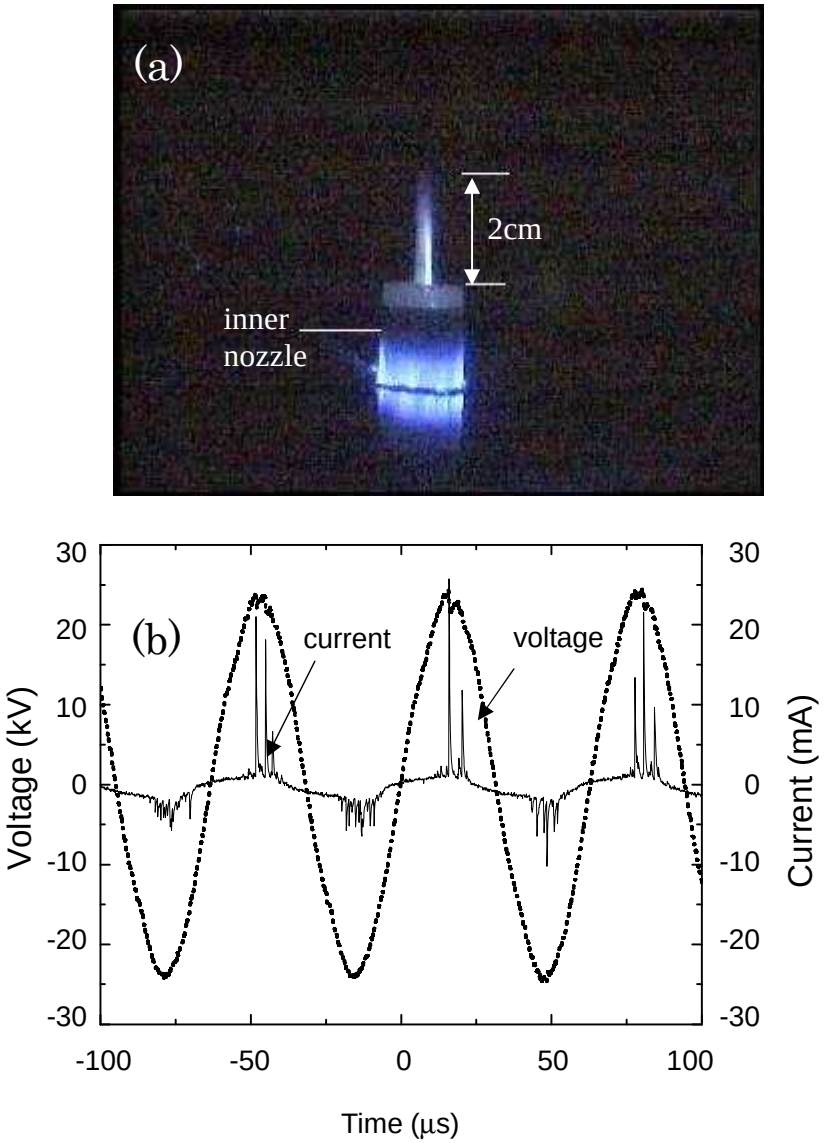

Fig. 7.11 (a) Image of discharge of PJ-2 and (b) time-depending current and voltage waveforms.

Figure 7.12 shows the experimental setup of sterilizing application. We placed the culture mediums into which *E. coli* was implanted beforehand, at 1.5 cm from the nozzle of PJ-2. After the plasma processing, the culture mediums were then kept at 37 ºC for 14 h for the incubation. By contrast with untreated culture medium growing *E. coli*, we plotted the relative area ratio *S* of colonies versus plasma treatment times in **Fig. 7.13**. It is obviously found from **Fig. 7.13** that such a plasma jet source as PJ-2 is very effective in the disruption of *E. coli*.

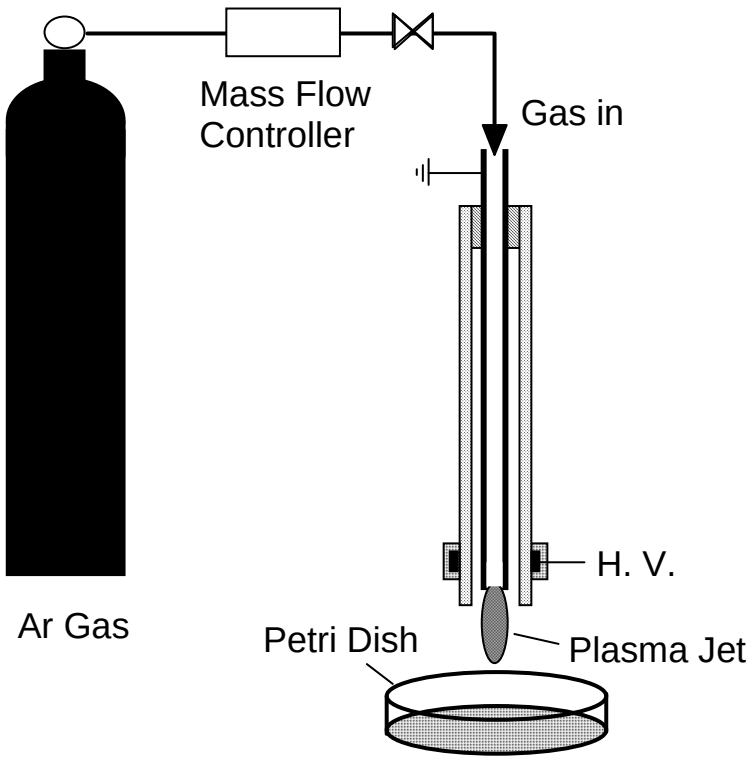

Fig. 7.12 Schematic setup of sterilization.

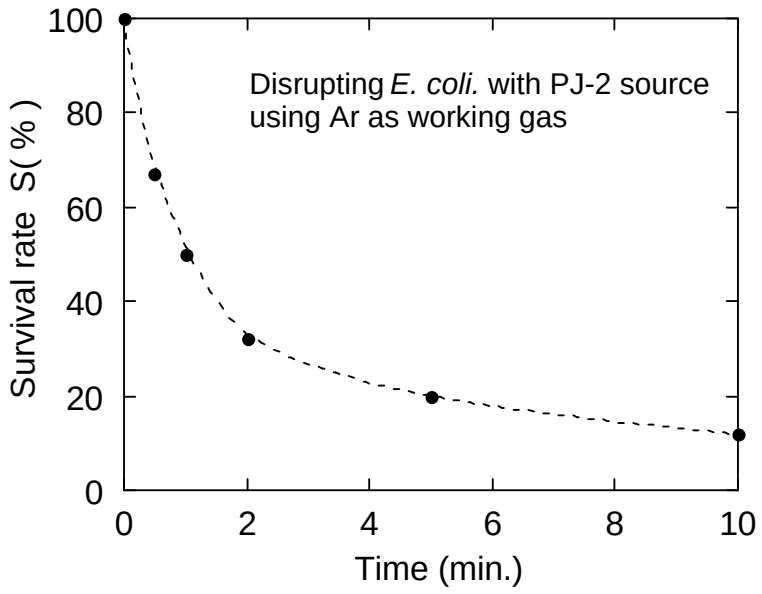

Fig. 7.13 Relation between survival rate S and plasma treatment time.

In the case of PJ-2, we could produce higher density plasma jet compared with that in the case of PJ-1, because we could apply higher voltage and current in the case of PJ-2 under lower gas temperature, such as 38 ºC. Such lower temperature in the PJ-2 was realized due to strong gas flow from one exit of the inner pipe differently from the case of PJ-1, where gas flow through each hole in the inner pipe was weak because of several gas through-holes.

In the present sterilization experiment, we consider that one of the possible sterilization mechanisms is ozone generated by the Ar plasma jet under the air circumstance at atmospheric pressure. The production yield of ozone in the case of PJ-2 may be stronger than that in the case of PJ-1. Therefore, PJ-2 is more effective in the sterilizing *E. coli* compared with PJ-1.

Although we have also carried out the mass spectroscopic measurement to study the by-products by the Ar plasma jet, we could not detect the ozone directly because of their unstable characteristics. However, it was no doubt that the ozone was produced under the present atmospheric plasma jet, since we could recognize their existence from the strong smell of ozone. It might be that the sprayed Ar plasma offered free electrons for oxygen in air circumstance to generate ozone due to the reactions of Equation (3)-(5) as presented in subsection 7.3.1.

7.3.3 Line-shaped dielectric barrier discharge plasma scheme

Recently, a line-shaped DBD plasma source has been developed in our group. Since the experiment was also carried out at room-temperature in air, which is very similar to the case of symmetric pectinate electrodes covered dielectric panel scheme, I would like to only mention a result of optical emission spectroscopy (OES) measurement to enrich the analyses of sterilization mechanism as presented in subsection 7.3.1.

Figure 7.14 shows optical emission spectra of the line-shaped dielectric barrier discharge in air (**Fig. 7.14(a)** for spectrum in the wavelength between 200-400 nm, while **Fig. 7.14(b)** for spectrum in the wavelength between 200-800 nm). As shown in **Fig. 7.14(a)**, it has been found that the emission intensity in the UV region is extremely large and the strong lines are originated from the second positive system of N_2 molecules, however, no obvious UV emission are originated from NO. On the other hand, in **Fig. 7.14(b)**, we can not find the strong O atomic (O I) line at 777.7 nm. These spectra are not similar to the spectrum of low-pressure air-simulated surface-wave plasma, but similar to the spectrum of low-pressure nitrogen surface-wave plasma as

presented in chapter 5. The reason might be owing to the short lifetime of NO, O atoms at atmospheric pressure and the energy difference because of different plasma excitation methods.

Relating the results of mass spectroscopy measurement in APSBD as presented in subsection 7.3.1, the increase of molecular oxygen and monatomic oxygen can be considered as the evidence of that ozone is decomposed by the mass spectrometer itself, because no O atomic (O I) line is measured by OES. We reached a conclusion that ozone and monatomic oxygen are the main antimicrobial products of APSBD, however, with the OES results, ozone and the UV emission originated from the second positive system of N_2 molecules should be considered as the main antimicrobial products of APSBD.

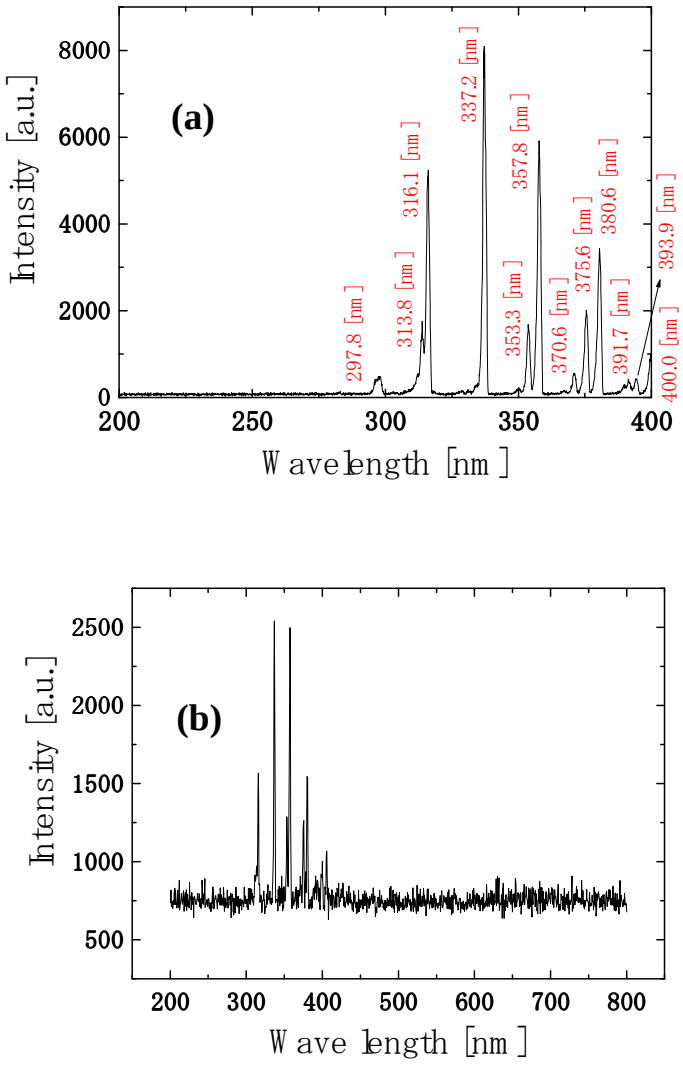

Fig. 7.14 Optical emission spectra in wavelength between (a) 200-400 nm and (b) 200-800 nm.

7.4 Summary

In this chapter, the effects of low-temperature plasma sterilization of audio-frequency-excited APSBD plasma in air and atmospheric pressure plasma jet (APPJ) using argon have been investigated. Experimental results suggested that the *E. coli* could be completely killed by irradiating with low-temperature air APSBD plasma for more than 10 min. We consider that one possible reason why APPJ using argon as discharge gas has the effect on disrupting *E. coli* is the sprayed Ar plasma offered free electrons for oxygen in air circumstance to generate ozone due to the reactions of Equation (3)-(5) as presented in subsection 7.3.1.

References

[1] R. B. Gadri, J. R. Roth, T. C. Montie, K. K.-Wintenberg, P. P.-Y. Tsai, D. J. Helfritch, P. Feldman, D. M. Sherman, F. Karakaya, Z. Chen: Surf. Coat. Technol. **131**, 528 (2000).

[2] H. Koinuma, H. Ohkubo, T. Hashimoto, K. Inomata, T. Shiraishi, A. Miyanaga and S. Hayashi: Appl. Phys. Lett. **60**, 816 (1992).

[3] K. Inomata, H. Ha, K. A. Chaudhary and H. Koinuma: Appl. Phys. Lett. **64**, 46 (1994).

[4] K. Inomata, H. Koinuma, Y. Oikawa and T. Shiraishi: Appl. Phys. Lett. **66**, 2188 (1995).

[5] H. Ha, M. Yoshimoto, H. Koinuma, B. Moon and H. Ishiwara: Appl. Phys. Lett. **68**, 2965 (1996).

[6] B. Lee, Y. Kusano, N. Kato, K. Naito, T. Horiuchi, and H. Koinuma, Jpn. J. Appl. Phys. **36**, 2888 (1997).

[7] J. Y. Jeong, S. E. Babayan, V. J. Tu, J. Park, I. Henins, R. F. Hicks and G. S. Selwyn: Plasma Sour. Sci. Technol. **7**, 282 (1998).

[8] S. E. Babayan, J. Y. Jeong, V. J. Tu, J. Park, G. S. Selwyn and R. F. Hicks: Plasma Sour. Sci. Technol. **7**, 286 (1998).

[9] Andreas Schutze, James Y. Jeong, Steven E. Babayan, Jaeyoung Park, Gary S. Selwyn and Robert F. Hicks: IEEE Trans. Plasma Sci. **26**, 1685 (1998).

[10] L. Xu, R. Zhang, P. Liu, L. L. Ding and R. J. Zhan: Chin. Phys. **13**, 913-917 (2004).

[11] L. Xu, P. Liu, R. J. Zhan, X. H. Wen, L. L. Ding, M. Nagatsu: Thin Solid Films **506-507**, 400-403 (2006).

[12] F. Massines, A. Rabehi, P. Decomps, R. B. Gadri, P. Segur and C. Mayoux: J. Appl. Phys. **83,** 2950~2957 (1998).

[13] D. Q. Zhou: Tutorial to Microbiology (in Chinese), (Beijing: Higher Education Publishers), (1993).

[14] S. Masuda, S. Hosokawa, X. L. Tu, K. Sakakibara, S. Kitoh and S. Sakai: IEEE Trans. Indust. Appl. **29**, 781 (1993).

8 Summary and outlook

In this thesis, the low-temperature plasma sterilization using low-pressure large-area surface-wave-produced and volume-wave-produced discharges and atmospheric pressure dielectric barrier discharge (DBD) have been studied. The experiments were performed in two slot antennae large-area microwave planar plasma sources and two self-made atmospheric pressure dielectric barrier discharge plasma sources. Surface sterilization effect and internal sterilization effect realized by low-temperature plasma were investigated in detail.

Characteristics of low-pressure pulse-modulated surface-wave plasma (SWP) in a 40-cm-diameter SWP device and characteristics of low-pressure SWP and volume-wave plasma (VWP) in a new 55-cm-diameter microwave plasma device were studied in chapter 2 and chapter 3, respectively. That was helpful for us to apply microwave excited plasmas in suitable mode for surface or internal sterilization. In chapter 5, the discharge conditions for CW and pulse-modulated SWPs in low-temperature sterilization, and the mechanisms of plasma sterilization with different gas species were investigated in the 40-cm-diameter SWP device. To achieve and improve internal sterilization effect, in chapter 6, the new large-area low-pressure planar microwave source, in which SWP and VWP are able to be controlled, was used for plasma sterilization. By adding water vapor into different gas species plasma, great improvement of internal sterilization effect was noticed. Accordingly, kinds of analyses of the plasma and the spores as biological indicator were carried out to clarify the mechanisms of plasma internal sterilization effect.

In chapter 7, some previous works about atmospheric pressure plasma sterilization using scheme of symmetric pectinate electrodes covered dielectric panel and plasma jet scheme were presented. Relating with the optical emission spectra obtained by the new line-shaped DBD plasma source, the mechanisms of atmospheric pressure air plasma sterilization were analyzed.

This thesis contributes to not only the development of a high-speed low-temperature surface plasma sterilization technique and a low-temperature internal plasma sterilization technique for medical application, but also clarifying the mechanisms of kinds of low-temperature plasmas.

Although much work has been done, there are still some tasks need to do, such as: accurate measurement of oxygen and OH radicals as the effective agents on sterilization

by OES, QMS and other available methods; efforts on reducing temperature and treatment time for internal plasma sterilization technique; also, to catch the latest trend in plasma application, making portable plasma sterilizer for clinic or dental surgeon using atmospheric pressure plasma is expected.

My goal in the study of low-temperature plasma sterilization is to develop a commercial plasma sterilizer for medical application. I think though there is still a long way from the goal, I am already on the way.

Acknowledgements

I would like to express my gratitude to all the people who helped me complete this dissertation.

First of all, I am deeply indebted to my supervisor Prof. Masaaki Nagatsu for his help, invaluable guidance and advice. Thank him for offering me the opportunity to perform research at his laboratory. I also want to thank Prof. Masashi Kando for his kind help of introducing my previous research work to Prof. Nagatsu, which made me thus get a chance to skip master course to directly enter the doctoral course, and then got the MEXT scholarship. Thank my previous supervisor Prof. Ru-Juan Zhan in USTC for recommending me to Prof. Nagatsu, which made me have the chance writing acknowledgements for doctoral thesis here. I am very grateful to all the members of our laboratory for their help, especially, to Dr. Akihisa Ogino for his help in kinds of experiments.

I wish to thank the members of my committee – Prof. M. Kando, Prof. T. Sugiura, Prof. A. Fukuda and Prof. M. Nagatsu. I know it is not easy for them to make time to examine the hundred-page-thesis from their tight schedule.

Thanks must be given to Prof. Yukio Koide, Prof. Toshi Nagata and Dr. Masato Uchijima at the Microbiology Laboratory in Hamamatsu University School of Medicine for their cooperation in teaching me how to carry out agar-plate based colony-count method and offering our laboratory some bacteria for plasma sterilization experiment.

The present work has been partly supported by a Grant-in-Aid for Scientific Research from the Japan Society for the Promotion of Science (JSPS), new regional consortium projects from the Ministry of Economy, Trade and Industry (METI) and a grant from the Regional Science Promotion (RSP) program of the Shizuoka Organization from the Creation of Industries. Nissin Inc. is appreciated for providing the microwave oscillator systems.

I would like to acknowledge the financial support of my study and research in Japan by the MEXT scholarship offered by the Ministry of Education, Culture, Sports, Science and Technology of Japanese Government.

In the end, I would like to thank my family back in China, especially my parents, for their endless support, love and understanding. I would like to thank all my friends for their support and help.

List of publications

Journal

[1] Sterilization of *E. coli* bacterium with an atmospheric pressure surface barrier discharge

Xu Lei, Zhang Rui, Liu Peng, Ding Li-Li, and Zhan Ru-Juan

Chinese Physics, Vol. 13, No. 6 (2004) pp. 913-917

Related chapter: 7

[2] Experimental study on low-temperature plasma sterilization

Lei Xu, Peng Liu, Ru-Juan Zhan, Xiao-Hui Wen, Li-Li Ding, Masaaki Nagatsu

Annual report of Graduate School of Electronic Science and Technology, Shizuoka University, Vol. 26 (2005) pp. 85-91

Related chapter: 5, 7

[3] Effects of oxygen radicals in low-pressure surface-wave plasma on sterilization

Masaaki Nagatsu, Fumie Terashita, Hiroyuki Nonaka, Lei Xu, Toshi Nagata and Yukio Koide

Applied Physics Letters, Vol. 86 (2005) 211502

Related chapter: 5

[4] Discharge conditions for CW and pulse-modulated surface-wave plasmas in low-temperature sterilization

L. Xu, F. Terashita, H. Nonak, A. Ogino, T. Nagata, Y. Koide, S. Nanko, I. Kurawaki and M. Nagatsu

Journal of Physics D: Applied Physics, Vol. 39 (2006) pp. 148-152

Related chapter: 2, 5

[5] Experimental study and sterilizing application of atmospheric pressure plasmas

L. Xu, P. Liu, R. J. Zhan, X. H. Wen, L. L. Ding, M. Nagatsu

Thin Solid Films, Vol. 506-507 (2006) pp. 400-403

Related chapter: 7

[6] Characteristics of surface-wave plasma with air-simulated N_2-O_2 gas mixture for low-temperature sterilization

L. Xu, H. Nonak, H. Y. Zhou, A. Ogino, T. Nagata, Y. Koide, S. Nanko, I. Kurawaki and M. Nagatsu

Journal of Physics D: Applied Physics, Vol. 40 (2007) pp. 803-808

Related chapter: 5

International Conference

[1] Experimental study and sterilizing application of atmospheric pressure plasmas

L. Xu, P. Liu, R. J. Zhan, X. H. Wen, L. L. Ding, M. Nagatsu

Abstracts of 7th Asia-Pacific Conference on Plasma Science and Technology & 17th Symposium on Plasma Science for Materials (7th APCPST & SPSM-17), Fukuoka, Japan (June 29-July 2, 2004) pp. 414

Related chapter: 7

[2] Study of time-modulated microwave plasmas for low temperature sterilization

Lei Xu, Fumie Terashita, Hiroyuki Nonaka, Shohei Nanko, Akira Kubota, Toshi Nagata, Yukio Koide and Masaaki Nagatsu

Proc. of 4th International Symposium on Microwave Science and Its Application to Related Fields (Microwave 2004), Takamatsu, Japan (July 27-30, 2004) pp. 533-534

Related chapter: 5

[3] Low-temperature sterilization technique using surface-wave or volume-wave excited microwave plasmas at 2.45 GHz

Masaaki Nagatsu, Fumie Terashita, Hiroyuki Nonaka, Lei Xu, Shohei Nanko, Akira Kubota, Toshi Nagata and Yukio Koide

Proc. of 4th International Symposium on Microwave Science and Its Application to Related Fields (Microwave 2004), Takamatsu, Japan (July 27-30, 2004) pp. 360-361

Related chapter: 5, 6

[4] Effect of oxygen radicals on plasma sterilization using low-pressure surface-wave plasmas

M. Nagatsu, F. Terashita, L. Xu, H. Nonaka, T. Nagata and Y. Koide

Proc. of Inter-Academia 2004, Budapest, Hungary (September 6-9, 2004) pp. 443-449

Related chapter: 5

[5] Low temperature sterilization using CW and pulse-modulated surface-wave plasma

Lei Xu, Hiroyuki Nonaka, Kouji Kondo, Fumie Terashita, Toshi Nagata, Yukio Koide, Shohei Nanko, Ichiro Kurawaki and Masaaki Nagatsu

Proc. of 8th Joint International Conference on Advanced Science and Technology (JICAST 2004), Hangzhou, China (December 23-26, 2004) pp. 27-30

Related chapter: 2, 5

[6] Sterilization characteristics of pulse-modulated microwave plasma and effects of oxygen radicals

Lei Xu, Hiroyuki Nonaka, Fumie Terashita, Kouji Kondo, Toshi Nagata, Yukio Koide, Shohei Nanko, Ichiro Kurawaki and Masaaki Nagatsu

Proc. of Plasma Science Symposium 2005 & 22nd Symposium on Plasma Processing (PSS-2005/SPP-22), Nagoya, Japan (January 26-28, 2005) pp. 689-690

Related chapter: 5

[7] Effect of nitrogen addition on sterilization using microwave excited oxygen plasma

Hiroyuki Nonaka, Lei Xu, Fumie Terashita, Kouji Kondo, Toshi Nagata, Yukio Koide, Shohei Nanko, Ichiro Kurawaki and Masaaki Nagatsu

Proc. of Plasma Science Symposium 2005 & 22nd Symposium on Plasma Processing (PSS-2005/SPP-22), Nagoya, Japan (January 26-28, 2005) pp. 685-686

Related chapter: 5

[8] Application of microwave plasma to medical sterilization

Masaaki Nagatsu, Fumie Terashita, Hiroyuki Nonaka, Lei Xu, Toshi Nagata, Yukio Koide, Shohei Nanko and Ichiro Kurawaki

Proc. of Plasma Science Symposium 2005 & 22nd Symposium on Plasma Processing (PSS-2005/SPP-22), Nagoya, Japan (January 26-28, 2005) pp. 197-198

Related chapter: 5, 6

[9] Effect of time modulation of microwave on surface-wave plasma sterilization

Lei Xu, Hiroyuki Nonaka, Akihisa Ogino, Yukio Koide, Shouhei Nanko, Ichiro Kurawaki and Masaaki Nagatsu

Abstracts of 18th Symposium on Plasma Science for Materials (SPSM-18), Tokyo, Japan (June 28-29, 2005) pp. 51

Related chapter: 2, 5

[10] Low-temperature sterilization using surface-wave sustained air plasma

Hiroyuki Nonaka, Lei Xu, Akihisa Ogino, Toshi Nagata, Yukio Koide, Shouhei Nanko, Ichiro Kurawaki and Masaaki Nagatsu

Abstracts of 18th Symposium on Plasma Science for Materials (SPSM-18), Tokyo, Japan (June 28-29, 2005) pp. 108

Related chapter: 5

[11] Development of low-temperature sterilizer using large-volume microwave plasma

Masaaki Nagatsu, Hiroyuki Nonaka, Lei Xu, Akihisa Ogino, Toshi Nagata, Yukio

Koide, Shouhei Nanko and Ichiro Kurawaki

Abstracts of 18th Symposium on Plasma Science for Materials (SPSM-18), Tokyo, Japan (June 28-29, 2005) pp. 107

Related chapter: 6

[12] Low temperature sterilization using CW and pulsed surface-wave plasmas

L. Xu, F. Terashita, H. Nonaka, K. Kondo, T. Nagata, Y. Koide, S. Nanko, I. Kurawaki and M. Nagatsu

Abstracts and full-papers CD of 17th International Symposium on Plasma Chemistry (ISPC-17), Toronto, Canada (August 7-12, 2005) pp. 1094-1095

Related chapter: 2, 5

[13] Novel plasma sterilization technique using volume wave plasma excited by 2.45 GHz microwaves

M. Nagatsu, F. Terashita, L. Xu, H. Nonaka, K. Ninomiya, T. Nagata, Y. Koide, S. Nanko and I. Kurawaki

Abstracts and full-papers CD of 17th International Symposium on Plasma Chemistry (ISPC-17), Toronto, Canada (August 7-12, 2005) pp. 1100-1101

Related chapter: 6

[14] Sterilization characteristics of low-pressure CW and pulse-modulated surface-wave plasmas with oxygen and nitrogen gases

L. Xu, H. Nonaka, A. Ogino, T. Nagata, Y. Koide, S. Nanko, I. Kurawaki and M. Nagatsu

Proc. of Inter-Academia 2005, Wuppertal, Germany (September 19-22, 2005), Vol. 2, pp. 347-356

Related chapter: 2, 5

[15] Development of large-volume microwave plasma device for low-temperature medical sterilization

M. Nagatsu, L. Xu, H. Nonaka, K. Ninomiya, A. Ogino, T. Nagata, Y. Koide, S. Nanko, and I. Kurawaki

Proc. of Inter-Academia 2005, Wuppertal, Germany (September 19-22, 2005), Vol. 1, pp. 217-225

Related chapter: 3, 6

[16] Optical emission spectroscopy and mass spectroscopy in pulse-modulated microwave plasma for sterilization

Lei Xu, Haiyang Zhou, Hiroyuki Nonaka, Akihisa Ogino, Toshi Nagata, Yukio Koide, Shohei Nanko, Ichiro Kurawaki, Masaaki Nagatsu

Proc. of 5th Symposium on Microwave Science and Its Application to Related Fields,

Tsukuba, Japan (November 2-4, 2005) pp. 108-109

Related chapter: 5

[17] Development of medical sterilizer using large-volume microwave plasma

Masaaki Nagatsu, Lei Xu, Haiyang Zhou, Hiroyuki Nonaka, Keigo Ninomiya, Akihisa Ogino, Toshi Nagata, Yukio Koide, Shohei Nanko and Ichiro Kurawaki

Proc. of 5th Symposium on Microwave Science and Its Application to Related Fields, Tsukuba, Japan (November 2-4, 2005) pp. 106-107

Related chapter: 3, 6

[18] Effect of hydroxyl group addition on sterilization performance of microwave plasma with dry air

Hiroyuki Nonaka, Tatsuya Yamashita, Lei Xu, Akihisa Ogino, Toshi Nagata, Yukio Koide, Shohei Nanko, Ichiro Kurawaki and Masaaki Nagatsu

Proc. of 5th Symposium on Microwave Science and Its Application to Related Fields, Tsukuba, Japan (November 2-4, 2005) pp. 210-211

Related chapter: 5

[19] Diagnostics of pulse-modulated microwave plasmas for medical sterilization using optical emission and quadrupole mass spectrometry

Lei Xu, Hiroyuki Nonaka, Haiyang Zhou, Akihisa Ogino, Toshi Nagata, Yukio Koide, Shohei Nanko, Ichiro Kurawaki and Masaaki Nagatsu

Proc. of 6th International Conference on Reactive Plasma & 23rd Symposium on Plasma Processing (ICRP-6/SPP-23), Matsushima, Japan (January 24-27, 2006) pp. 559-560

Related chapter: 2, 5

[20] Internal sterilization of wrapped medical implement using pulse-modulated, volume-wave excited air plasma

Masaaki Nagatsu, Lei Xu, Hiroyuki Nonaka, Haiyang Zhou, Akihisa Ogino, Toshi Nagata, Yukio Koide, Shohei Nanko and Ichiro Kurawaki

Proc. of 6th International Conference on Reactive Plasma & 23rd Symposium on Plasma Processing (ICRP-6/SPP-23), Matsushima, Japan (January 24-27, 2006) pp. 557-558

Related chapter: 3, 6

[21] Effect of Hydroxyl-group addition on low-temperature sterilization using surface-wave sustained air plasma

Hiroyuki Nonaka, Tatsuya Yamashita, Lei Xu, Akihisa Ogino, Toshi Nagata, Yukio Koide, Shohei Nanko, Ichiro Kurawaki and Masaaki Nagatsu

Proc. of 6th International Conference on Reactive Plasma & 23rd Symposium on

Plasma Processing (ICRP-6/SPP-23), Matsushima, Japan (January 24-27, 2006) pp. 561-562

Related chapter: 5

[22] Internal sterilization of wrapped medical implements using volume-wave plasma

L. Xu, H. Y. Zhou, A. Ogino, Y. Koide and M. Nagatsu

Proc. of VIth International Workshop on Microwave Discharge, Zvenigorod, Russia (September 11-15, 2006) pp. 321-326

Related chapter: 3, 6

[23] Effect of hydrogen peroxide produced in surface-wave excited air/H_2O plasma on sterilization

Lei Xu, Yoshihito Ohno, Akihisa Ogino and Masaaki Nagatsu

Proc. of 24th Symposium on Plasma Processing (SPP-24), Osaka, Japan (January 29-31, 2007) pp. 299-300

Related chapter: 3, 6

[24] Ozone sterilization of wrapped medical instruments using flexible dielectric barrier discharge

Hiroyuki Eto, Yoshihito Ohno, Lei Xu, Akihisa Ogino and Masaaki Nagatsu

Proc. of 24th Symposium on Plasma Processing (SPP-24), Osaka, Japan (January 29-31, 2007) pp. 301-302

Related chapter: 7

Local Conference

[1] Experimental study on audio-frequency atmospheric pressure plasma jet

Lei Xu, Peng Liu, Ru-Juan Zhan, Xiao-Hui Wen, Li-Li Ding and Masaaki Nagatsu

2004 年秋季第 65 回応用物理学会学術講演会（東北学院大学、2004 年 9 月 1－4 日）、講演予稿集第 1 分冊 pp.130、講演番号 3a-S-25

Related chapter: 7

[2] 表面波励起酸素プラズマを用いた低温滅菌特性－パルス変調の効果－

野中　雄之，徐　蕾，寺下　文恵，永田　年，小出　幸夫，南光　正平，久保田　彰，永津　雅章

2004 年秋季第 65 回応用物理学会学術講演会（東北学院大学、2004 年 9 月 1－4 日）、講演予稿集第 1 分冊 pp.130、講演番号 3a-S-26

Related chapter: 2, 5

[3] Effect of pulse-modulation in plasma sterilization experiment using

surface-wave excited oxygen plasma

Lei Xu, Hiroyuki Nonaka, Fumie Terashita, Toshi Nagata, Yukio Koide, Shohei Nanko, Akira Kubota, Masaaki Nagatsu

平成 16 年度電気関係学会東海支部連合大会（名古屋工業大学、2004 年 9 月 27－28 日）、講演番号 O-045

Related chapter: 2, 5

[4] 表面波プラズマ滅菌におけるマイクロ波パワーと照射時間の関係

野中　雄之，徐　蕾，寺下　文恵，永田　年，小出　幸夫，南光　正平，久保田　彰，永津　雅章

平成 16 年度電気関係学会東海支部連合大会（名古屋工業大学、2004 年 9 月 27－28 日）、講演番号 O-044

Related chapter: 2, 5

[5] Effect of oxygen radicals in pulse-modulated surface-wave plasma sterilization

Lei Xu, Hiroyuki Nonaka, Fumie Terashita, Kouji Kondo, Toshi Nagata, Yukio Koide, Shohei Nanko, Akira Kubota, Masaaki Nagatsu

プラズマ・核融合学会第 21 回年会（静岡県コンベンションアーツセンター、2004 年 11 月 23－26 日）、予稿集 pp.158、講演番号 24aB18P

Related chapter: 2, 5

[6] 低圧力表面波プラズマを用いた低温滅菌実験における投入パワーとガス種の効果

野中　雄之，徐　蕾，寺下　文恵，近藤　浩司，永田　年，小出　幸夫，南光　正平，倉脇　一郎，永津　雅章

プラズマ・核融合学会第 21 回年会（静岡県コンベンションアーツセンター、2004 年 11 月 23－26 日）、予稿集 pp.158、講演番号 24aB17P

Related chapter: 5

[7] Characteristics of plasma sterilization using pulse-modulated microwave discharges

Lei Xu, Hiroyuki Nonaka, Fumie Terashita, Akihisa Ogino, Toshi Nagata, Yukio Koide, Shohei Nanko, Ichiro Kurawaki, Masaaki Nagatsu

2005 年春季第 52 回応用物理学関係連合講演会（埼玉大学、2005 年 3 月 29 日－4 月 1 日）、講演予稿集第 1 分冊 pp.203、講演番号 31a-D-9

Related chapter: 2, 5

[8] 表面波プラズマ滅菌実験における UV 光放射の効果

野中　雄之，徐　蕾，寺下　文恵，荻野　明久，永田　年，小出　幸夫，南光　正平，倉脇　一郎，永津　雅章

2005 年春季第 52 回応用物理学関係連合講演会（埼玉大学、2005 年 3 月 29

日－4 月 1 日）、講演予稿集第 1 分冊 pp.202、講演番号 31a-D-8
Related chapter: 5

[9] Discharge conditions for sterilization using pulse-modulated surface-wave plasmas

Lei Xu, Hiroyuki Nonaka, Akihisa Ogino, Toshi Nagata, Yukio Koide, Shohei Nanko, Ichiro Kurawaki, Masaaki Nagatsu

2005 年秋季第 66 回応用物理学会学術講演会（徳島大学、2005 年 9 月 7－11 日）、講演予稿集第 1 分冊 pp.128、講演番号 10p-ZH-2
Related chapter: 2, 3, 5, 6

[10]空気を放電ガスとして用いる表面波プラズマの低温滅菌特性

野中　雄之，徐　蕾，荻野　明久，永田　年，小出　幸夫，南光　正平，倉脇　一郎，永津　雅章

2005 年秋季第 66 回応用物理学会学術講演会（徳島大学、2005 年 9 月 7－11 日）、講演予稿集第 1 分冊 pp.128、講演番号 10p-ZH-3
Related chapter: 5

[11]表面波励起空気放電プラズマを用いた低温滅菌実験

野中　雄之，徐　蕾，荻野　明久，永田　年，小出　幸夫，南光　正平，倉脇　一郎，永津　雅章

平成 17 年度電気関係学会東海支部連合大会（名城大学、2005 年 9 月 15－16 日）、講演番号 O-040
Related chapter: 5

[12]Mass spectroscopy measurement in pulse-modulated microwave plasma for medical sterilization

Lei Xu, Hiroyuki Nonaka, Haiyang Zhou, Akihisa Ogino, Toshi Nagata, Yukio Koide, Shohei Nanko, Ichiro Kurawaki, Masaaki Nagatsu

プラズマ・核融合学会第 22 回年会（東京都タワーホール船堀、2005 年 11 月 29－12 月 2 日）、予稿集 pp.245、講演番号 02aB03P
Related chapter: 2, 5

[13]マイクロ波プラズマ滅菌における OH 基添加の効果

野中　雄之，山下　達也，徐　蕾，荻野　明久，永田　年，小出　幸夫，南光　正平，倉脇　一郎，永津　雅章

プラズマ・核融合学会第 22 回年会（東京都タワーホール船堀、2005 年 11 月 29－12 月 2 日）、予稿集 pp.244、講演番号 02aB02P
Related chapter: 5

[14]Development of medical sterilizer using large-volume microwave plasma

Lei Xu, Haiyang Zhou, Akihisa Ogino, Toshi Nagata, Yukio Koide, Shohei Nanko,

Ichiro Kurawaki, Masaaki Nagatsu
2006 年春季第 53 回応用物理学関係連合講演会（武蔵工業大学、2006 年 3 月 22－26 日）、講演予稿集第 1 分冊 pp.166、講演番号 25a-ZC-I1
Related chapter: 3, 6

[15]マイクロ波プラズマを用いた低温滅菌装置の開発－滅菌メカニズムと処理後の安全性－
永津　雅章，徐　蕾，野中　雄之，周　海洋，荻野　明久，永田　年，小出　幸夫，南光　正平，倉脇　一郎
2006 年春季第 53 回応用物理学関係連合講演会（武蔵工業大学、2006 年 3 月 22－26 日）、講演予稿集第 1 分冊 pp.167、講演番号 25a-ZC-I2
Related chapter: 5

[16]Low temperature sterilization of PE film-wrapped material using microwave plasma
Lei Xu, Yoshihito Ohno, Akihisa Ogino, Yukio Koide, Masaaki Nagatsu
2006 年秋季第 67 回応用物理学会学術講演会（立命館大学、2005 年 8 月 29 日－9 月 1 日）、講演予稿集第 1 分冊 pp.173、講演番号 1a-Q-2、第 21 回（2006 年秋季）応用物理学会「講演奨励賞」受賞
Related chapter: 3, 6

[17]Effect of pure water addition on low-temperature sterilization using microwave excited air-simulated plasma
Lei Xu, Akihisa Ogino, Yukio Koide, Masaaki Nagatsu
平成 18 年度電気関係学会東海支部連合大会（岐阜大学、2006 年 9 月 28－29 日）、講演番号 O-272
Related chapter: 3, 6

[18]Effect of water vapor addition on low-temperature sterilization using microwave excited air plasma
Lei Xu, Yoshihito Ohno, Akihisa Ogino, Masaaki Nagatsu
プラズマ・核融合学会第 23 回年会（筑波大学大学会館、2006 年 11 月 28－12 月 1 日）、予稿集 pp.127、講演番号 29aA14P
Related chapter: 3, 6